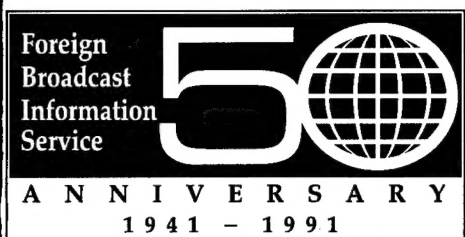


19 JUNE 1991



JPRS Report

Science & Technology

USSR: Engineering & Equipment

INDUSTRIAL ROBOTICS

19980116 223

DTIC QUALITY INSPECTED 2

REPRODUCED BY
U.S. DEPARTMENT OF COMMERCE
NATIONAL TECHNICAL INFORMATION SERVICE
SPRINGFIELD, VA. 22161

DISTRIBUTION STATEMENT A

Approved for public release;
Distribution Unlimited

JPRS-UEQ-91-007
19 JUNE 1991

SCIENCE & TECHNOLOGY
USSR: ENGINEERING & EQUIPMENT
INDUSTRIAL ROBOTICS

91FE0203A Leningrad IZVESTIYA VYSSHIKH UCHEBNYKH ZAVEDENIY: PRIBOROSTROYENIYE
in Russian No 10, 1990 (manuscript received 9 Jul 90) pp 3-91

CONTENTS

Industrial Robotics: Status and Some Trends of Development [A. M. Petrina, A. S. Yushchenko].....	1
Morphological Analysis of Flexible Manufacturing Systems [O. M. Kalin].....	8
Modified Net Methods in Problems of Control and Automated Simulation of Assembly Manufacturing Systems [A. V. Borusan, A. A. Lavrov, et al.].....	19
Implementation of Contour Control in NP Systems of Multilink Articulated Manipulators [S. V. Goryachev, M. Ya. Ostrovskiy].....	23
Program-Adaptive Algorithms for Positional and Contour Control of Robot [A. V. Timofeyev, A. B. Godun].....	30
Self-Adjusting Two-Way System With Adjustment by Variable Parameters of Manipulator [V. F. Filaretov, A. F. Polyanskiy].....	40

Experimental Adaptive Robotic Complex [S. A. Vorotnikov, A. Yu. Korneyev, et al.].....	51
Force Sensitization System of Deburring Robot [A. Yu. Sumich].....	57
Recognition System of Industrial Robots [Yu. D. Zhabotinskiy, V. A. Malyshev].....	64
Mathematical Model of Pointer Strobe Television System Under Noisy Conditions [V. M. Artemyev, K. V. Glagolev].....	75
Segmentation of Multigradation Images Using Odd Linguistic Variables [V. I. Solntsev].....	88
Use of Associative Principles for Processing and Representation of Visual Information [V. I. Volkov, R. M. Zharkoy].....	94
Optical Robotic Vision Television System for Checking Shape of Semiconductor Crystals [V. I. Syryamkin, V. S. Titov, et. al.].....	100
Controlled Model of Fiber Sorption Electronic Muscles [S. G. Agranovskiy, Yu. N. Yegorov, et al.].....	105
Multioutput Actuating Modules for Robots and Robotic Complexes [P. F. Khasanov, Kh. N. Nazarov, et al.].....	118

UDC 621.865.8

INDUSTRIAL ROBOTICS: STATUS AND SOME TRENDS OF DEVELOPMENT

917F0203A Leningrad IZVESTIYA VYSSHIKH UCHEBNYKH ZAVEDENIY:
PRIBOROSTROYENIYE in Russian No 10, 1990 (manuscript received 9 Jul 90)
pp 3-8

[Article by A. M. Petrina and A. S. Yushchenko, Moscow State Technical University imeni N. E. Bauman]

[Text] A survey of the current status of industrial robotics in the USSR and abroad and also analysis of some trends of its development is presented.

The use of robotics today is one of the main methods of increasing the volume of the products of industrial production, of increasing their quality and, which is especially important, of a flexible response to the variable requirements of the market. Industrial robots play a key role in the designs of future plants--automated plants--being developed today. Robotics has been transformed into a major sector of industry in the developed capitalist countries. Such well known corporations as Fanuk, Fujitsu (Japan), General Electric and IBM (United States), Olivetti (Italy), Volkswagen (West Germany), ASEA (Sweden) and also many medium and small enterprises are involved in research, development, production and marketing of robotics. More than 700 companies, including approximately 400 companies in Japan, 50 companies in the United States, and 250 companies in Western Europe, are engaged in manufacture of industrial robots (PR) in the overall complexity of capitalist countries. A significant part of research in robotics is performed at the leading technical universities. Departments on robotics have been created, for example, at the Massachusetts Institute of Technology, and Carnegie-Mellon and Stanford Universities. The research is financed mainly by industrial enterprises, interested in introduction of new technology into manufacturing. However, significant funds for development of robotics are also allocated from the state budget of the leading capitalist governments. All this leads to steady growth of both the number of industrial robots used in industry and to an increase of the quality characteristics of robotic systems. According to data of the French Federation on Robotics, there were 44,000 industrial robots in Western Europe, 38,000 in the United States, and 210,000 in Japan by the end of 1989 [1]. One should bear in mind

the conditional nature of these figures, related to different definitions of industrial robots in different countries. However, the trend of development of industrial robots can be established. According to forecasts of the early 1980's, the manufacture and introduction of robotic devices should be performed on a considerably greater scale and should have a significant influence on their rate of employment in industrial production. Thus, according to data of the Institute of Robotics of Carnegie-Mellon University, industrial robots should free 7 million workers from production in the United States. According to the forecast of the second half the 1980's, compiled by the American economists V. Leontyev and F. Dachin, no fewer than 2 million workers will be freed due to robotics by the year 2000. Other forecasts are also subject to correction toward a decrease. This variation of the prospects is mainly related to the difficulties in introduction of the manufactured product. The new forecasts proceed from the fact that the rates of growth of the worldwide capitalist market of industrial robots have stabilized and comprise 15-20 percent annually. A period of euphoria has been replaced by a more sober attitude toward the aspects of the application of robotics.

The forecasts concerning the structure of robotic systems and their areas of application have been largely confirmed. As one would assume, second-generation robots, which have external information sensors that permit them to correct their motions to some extent, comprised a significant part of the industrial robot stock by the mid-1980's. These are mainly robotic vision systems and force-moment sensitization. The main sphere of application of industrial robots still remains machine building, primarily, the automotive industry, and electronics and electrical engineering enterprises. However, the demand for robotic systems, designed for automation of operations in nonmachine-building sectors, has now increased sharply. These are construction, transport, the coal-mining industry, light industry and agriculture. According to data of the Japanese Association on Industrial Robots, which conducted research on the needs of industry for second-generation industrial robots, the main part of these industrial robots in machine building should be engaged in assembly operations (20.9 percent). At the same time, 32.2 percent of industrial robots are required for automation of operations in extreme environments, 8.3 percent are required for automation of transport operations, 12.4 percent are required for repair and preventive maintenance, and 6.1 percent are required for use in emergency situations [2].

The output of industrial robots in the USSR during the 12th Five-Year Plan should comprise 100,000 units [3], which is double the data for the 10th Five-Year Plan. Thus, there is the tendency to maintain the high rates of growth of the industrial robot stock. Considerable experience in robotization of the automotive industry, machine tool building and instrument building has been accumulated. A total of 28 percent of industrial robots is now involved in welding operations, 30 percent service stamping machines and presses, and 22 percent service machine tools. The operations are mainly automated due to first-generation

robots, i.e., rigidly programmed robots, 69 percent of them have cyclic control and 28 percent have position control. A total of 3 percent comprise robots with contour control that use microprocessors [4]. At the same time, this figure now comprises 31 percent for the industrial robots used in the West and in Japan. Thus, there is some lag in the structure of the industrial robot stock; second-generation robots have not yet found broad introduction in industry. One of the causes of this is the low reliability of industrial robots, manufactured at some enterprises. According to the technical assignment, it usually comprises approximately 2,000 hr of mean times between failure, whereas this figure is equal to 10,000 for Western industrial robots. In practice, the mean times between failure is rarely less. Another problem is the high cost of robotics. The cost of loading-transport industrial robots now comprises 11,000-15,000 rubles, while that of production industrial robots comprises 35,000- 95,000 rubles. The level of prices for robotics increases by 30-40 percent annually. Because of this, the level of the economic impact of the use of industrial robots in the USSR remains very low. In the opinion of industrial workers, transition to new management conditions may result in a significant decrease of plans for introduction of robotics at enterprises. To avoid this, a serious change of the structure of robotic systems manufactured by industry toward an increase of second-generation industrial robots, improvement of the reliability of industrial robots, and of their efficiency are required. Estimates show that the necessary efficiency will be achieved with an increase of the number of realistically freed workers of three-fivefold per industrial robot.

The worldwide trend, related to expansion of the traditional sphere of application of robotics in the nonmachine-building sector of the national economy, has also been manifested in Soviet robotics [5]. This direction is of important social significance, since the percentage of unskilled heavy manual labor is very high in the USSR, compared to the other industrially developed countries. This is primarily true of the coal and mining industry, ferrous and nonferrous metallurgy, construction, agriculture, and the light and food industry. The importance of using robotics in these sectors is determined by the fact that a large part of the country's labor resources is engaged in them, while the degree of automation is lower than that in machine building. Studies are being conducted intensively in this sector and the first models of similar robots are beginning to be introduced in the national economy.

Let us present several examples in order for the reader to gain an idea of the technical capabilities of modern industrial robots [6, 7]. The M5030 Hitachi welding robot (Japan) with five degrees of freedom and with capacity of 3 kg performs welding at a rate of 2.4 m/min and with accuracy of ± 0.2 mm. The IRB 2000 ASEA industrial arc-welding robot (Sweden) with capacity of 10 kg has a maximum speed of 3 m/s and a positioning error of ± 0.1 mm, and also a control system for 12 variables simultaneously (6 are related to the robot and 6 are related to external devices). The KUKA robot (West Germany) with capacity of 150 kg, which

has seven degrees of freedom, is used for spot welding in the automotive industry. An example of a modern industrial robot for loading machine tools and pallets is the IBM 3000 industrial robot with capacity of 30 kg, with positioning error of ± 0.4 mm, with a speed of 1.5 m/s, and with working zone radius of 1.95 m. Among second-generation robots designed for welding, one can note the SCARA AR-i 270 Stenzel (West Germany) industrial robot, distinguished by special accuracy, with capacity of 2 kg, with speed of 4.1 m/s, and with positioning error of ± 0.05 mm. The Sony Corporation (Japan) has delivered to the market two-armed assembly robots with length of the arms of 250 and 350 mm, capacity of 1 and 5 kg, respectively, and with speed of 5.3 m/s.

Intel-8086, Intel-80186, and Motorola 68000 microprocessors are used as the control systems of these robots. Programming is in high-level VAL, VAL II, AL, AML, HELP, JARS, and MSL languages, and also in universal C, Fortran, and Basic programming languages.

The MP-9S and MP-11 (Minavtoprom [USSR Ministry of the Automotive Industry]), the RF-202, RF-204, Granat-2.5 and Granat-10 (USSR Ministry of the Radio Industry]), Elektronika-NTsTM-0.1 and also the M20P40.01 industrial robots produced by MSPO [Moscow Union of Consumers Society] Krasnyy proletariy among the industrial robots, manufactured in the USSR and having characteristics corresponding to the worldwide level can be named; a number of robots is manufactured in the USSR by licenses purchased from foreign companies, including KUKA and Fanuc.

The control systems of Soviet industrial robots are implemented on 16-bit K1810 and K586 microprocessors and one-chip KM1816 computers. The main computer is the NTs80-01DN microcomputer, constructed on KR1801NM2 microprocessors; K580 microprocessors are used to control the drives. A new fourth-generation control system IS.02, which is a combination of standardized modules and which is designed for group and autonomous position-contour control of manipulators in a flexible manufacturing system, has been developed. This system considerably exceeds Soviet analogues (MPSU and Sfera-36) in speed, capacity of the control program (526 kbytes), the number of digital inputs-outputs and reliability. Its mean times between failure is 10,000 hr.

The tendency toward an increase of the role of the electric drive has been noted in the field of industrial robot drives, which has begun to be used not only for small- and medium-capacity robots (10-25 kg), but for large-capacity industrial robots (160-200 kg), i.e., for industrial robots which were earlier constructed on the basis of electrohydraulic drives [8]. Electric drives have been developed in the USSR, which are not inferior to foreign analogues in their parameters. These are the EPB-2 drive with transistor converter and DVU and 2DVU synchronous electric motors, and also the Razmer 2M electric drive with transistor converter and with asynchronous motors of the AI series. The most promising for industrial robots are drives based on contactless electric motors (DC, three-phase asynchronous motors), which have a longer service life than the DC motors previously used here. Reducerless

("direct action") drives based on high-torque contactless motors must be developed to realize high-performance industrial robots, operating at speeds up to 10 m/s. These studies are being conducted both in the USSR and abroad. The specifics of a reducerless drive consists in the need to construct an industrial robot control system with regard to the dynamics of the manipulator mechanism, which in turn requires construction of high-performance computers and real-time operating systems. Difficulties arise in design of a drive for assembly robots, since in this case the industrial robot should reproduce the given laws of variation of forces, along with reproduction of the given laws of motion.

Robotic vision systems and force-moment sensitization are mainly used in industrial robot sensitization systems.

The robotic vision systems (STZ), used under production conditions, ordinarily operate with images of 256×256 or 512×512 elements, the brightness of each of which is encoded by 6 or 8 bits. An essential parameter of robotic vision systems is their speed. A large volume of data on the image (up to 256 kbytes), rigid time restrictions on the permissible time of processing one image impose their own imprint on the architecture of the hardware and on the structure of the software of robotic vision systems. The apparatus of a robotic vision system usually consists of several modules, operating synchronously or in parallel, performing the main volume of image processing with equivalent speed of 10 million image elements per second. Examples of these systems may be the SERIA 150/151 of Imaging Technology, Inc. (United States) and the DT 2861, DT 2858, and DT 7020 modules of Data Translation, Inc. (United States).

The indicated modules perform all the preliminary data processing, related to viewing large files of points, using point image algorithms, realized at the hardware level, filtration, calculation of brightness gradients and histograms, contour description, computation of convolution and so on. The final image description operation in some database and decision-making base is performed on a personal computer or on a specialized controller.

Among the robotic vision systems manufactured in the USSR, one should mention the Videosens, MB-196 and Vedoskan systems, which, although somewhat inferior to the above mentioned microprocessor robotic vision systems in their parameters, process an image within 1-2 seconds at considerably lower cost.

The force-moment sensitization systems of industrial robots, manufactured in the USSR and abroad are completely functional high-class instruments, which measure six projections of the force vector and force moment, conversion of analog data to digital form, processing and transmission of it to the robot controller or to other equipment through a serial interface channel.

Examples of force-moment systems may be: the Dinasens-200 NTs Robototekhnika (USSR) and the FS6-120A of the Astek, Inc. Company (United States).

It should be noted that the use of real-time sensory systems (for example, during assembly, requires development of special control algorithms and an increase of the requirements on the characteristics of the controllers.

Among other problems that require scientific studies, one should mention those of increasing the speeds of industrial robots to 10-15 m/s, increasing the capacity to natural mass ratio of industrial robots, and reducing energy consumption and materials consumption. Systematic study of the technological and economic feasibility of using robotics in modern industrial production is necessary to improve the effectiveness of introducing industrial robots.

The authors are grateful to corresponding member of the USSR Academy of Sciences Ye. P. Popov, and also to colleagues of the Scientific Training Center Robototekhnika G. V. Pismennyy and V. A. Pol'skiy for assistance in compilation of this survey.

Bibliography

1. Robotique, I. V. "La France on 5-eme rang mondial," TECHN. ET EQUIP. PROD., 1990.
2. Nakano, E. "Vvedeniye v robototekhniku" [Introduction to Robotics], Moscow, Izdatelstvo "Mir", 1988.
3. Serebrennikov, I. V. "Analysis of Trends in Development of Industrial Robots in the USSR," "Tezisy dokladov Vsesoyuznogo soveshchaniya 'Zadachi i perspektivy nauchno-tehnicheskogo sotrudничества stran-chlenov SEV'" [Report Topics of All-Union Conference "Problems and Prospects of Scientific and Technical Cooperation of CEMA Members"], Moscow, 1988.
4. Serebrennikov, I. V. "Analysis of the Effectiveness of Robotization of USSR Industry," "Problemy ekonomicheskogo prognozirovaniya razvitiya nauki i tekhnologii" [Problems of Economic Forecasting of the Development of Science and Technology], Moscow, 1989.
5. Melnikov, V. M. "Status and Prospects of Development of Robotics in Nonmachine-Building," "Materialy seminara 'Promyshlennyye roboty i opyt ikh primeneniya v narodnom khozyaystve'" [Proceedings of a Seminar "Industrial Robots and Experience of Using Them in the National Economy"], Leningrad, LDNTP, 1988.
6. "Hannover-Messe Industrie'89 in Zeithen der Automatisierung," TECHNICA, Vol 38, No 12, 1989.

7. Rogots: a retenir de l'exposition. Exporobot, MACH. PROD., No 513, 1989.

8. Poznikov, O. I., Matison, A. G. "Basic Directions of Development of the Electric Drive of Industrial robots," "Materialy seminara 'Promyshlennyye roboty i optyt ikh primeneniya v narodnom khozyaystve'" [Proceedings of a Seminar "Industrial Robots and Experience of Using Them in the National Economy"], Leningrad, LDNTP, 1988.

COPYRIGHT: "IZVESTIYA VUZOV SSSR - PRIBOROSTROYENIYE", 1990

UDC 658.527.011.56-11

MORPHOLOGICAL ANALYSIS OF FLEXIBLE MANUFACTURING SYSTEMS

917F0203A Leningrad IZVESTIYA VYSSHIKH UCHEBNYKH ZAVEDENIY:
PRIBOROSTROYENIYE in Russian No 10, 1990 (manuscript received 28 Feb 90)
pp 9-16

[Article by O. M. Kalin, Kiev Polytechnical Institute]

[Text] Analysis of the structural-configuration layouts of flexible manufacturing systems, based on the use of morphological Zvicky analysis, is considered. Classification features of structural-configuration layouts of flexible manufacturing systems are determined.

The subjective, empirical approach now predominates in design of structural-configuration layouts of flexible manufacturing systems (GPS), which reduces their effectiveness due to constriction of the area of searching for possible solutions. Therefore, the problem of studying processes of objective, formal structurization of manufacturing systems based on morphological methods is timely.

Analysis of the structural-configuration layouts of flexible manufacturing systems, based on the use of morphological Zvicky analysis [2] and further development of it in [3, 5]. Two qualitatively different steps--morphological analysis and morphological synthesis--are distinguished in the morphological method. The step of morphological analysis consists in many-sided consideration of the technical system and description of it in some space of features. The main problem of this step is careful study of the design principles of the system, of the structural components and different forms of their interaction in the system. The purpose of morphological analysis is development of morphological classifiers, which encompasses all the possible structural solutions of the technical system. The step of morphological synthesis consists in analysis and selection of a set of possible solutions of those which correspond to the advanced requirements. The purpose of morphological synthesis is working out optimization algorithms that permit one to orient oneself in the space of possible solutions.

The most acceptable is the method of the morphological Zwicky box among the known morphological methods for problems of formulating the structural-configuration layouts of flexible manufacturing systems. According to this method, the technical system is studied by distinguishing a number of typical features, to which formal variables x_i correspond and on which the structural solution is dependent. Gradations are found for each feature, i.e., mutually exclusive values of the same variable. The qualitative state of the structural component is reflected by an ordinal number of the i -th variable, the number of which varies from 1 to k_i . Each of the possible j -th realizations, corresponding to the i -th value of the variable, is selected for formation of the structural solution.

Graphically, the process of formation of structural solutions can be represented in the following manner. Data on the features of variables and of their gradations are represented in the form of a morphological table:

x_1^1	x_1^2	$x_1^3 \dots x_1^{k_1}$	
x_2^1	x_2^2	$x_2^3 \dots x_2^{k_2}$	
x_3^1	x_3^2	$x_3^3 \dots x_3^{k_3}$	
x_n^1	x_n^2	$x_n^3 \dots x_n^{k_n}$	

Structural solutions are formulated by interrogating the gradations of all features and of including them alternately in discrete sets that characterize one or another variants of the structural designs of the system. For example,

$$\langle x_1^1, x_2^3, x_3^2, \dots, x_n^{k_n} \rangle.$$

It is obvious that a complete structural solution will be formulated only if each feature is represented by one of its gradations. The dimensionality of a specific set of possible structural solutions is generally determined by

$$N = \prod_{i=1}^n k_i,$$

where n is the number of features and k_i is the number of gradations in the i -th feature.

Construction of the morphological classifier is a subjective procedure and is entirely dependent on the qualifications of the compiler. This process can be based on analysis of the structural-configuration layouts of existing flexible manufacturing systems and those operated in industry. Conducting this analysis means objective determination of the main structural design principles of the flexible manufacturing system by the expert method and determination of their quantitative analysis in the form of the applicability factor, which characterizes the fraction of the flexible manufacturing system with given structural feature in the total set of those studied. This approach guarantees determination of all the structural features of the flexible manufacturing system and provides a panorama of their use in practice.

The production design characteristics of manufacturing objects affect to a considerable degree the selection of one or another principle structural-configuration layout of a flexible manufacturing system. Specifically, the design, overall dimensions and shape of objects affect the selection of the automated transport-warehousing system of the flexible manufacturing system. Taking this characteristic into account, the entire combination of studied flexible manufacturing systems must be divided into two groups upon morphological analysis: flexible manufacturing systems, designed to manufacture objects of prismatic shape (housing parts)--GPS(Pr)--and flexible manufacturing systems, designed to manufacture parts of the body of revolution type--GPS(Tv). The applicability of the structural solutions f_{IP} and f_{TB} , respectively, is determined within the limits of each of the groups.

The following classification features are determined as a result of the structural-configuration solutions of more than 200 flexible manufacturing systems, data on which are presented in [1, 7, 8]: x_1 --the type of flow scheme of blanks, x_2 --the principle of organization of accumulation of production objects, x_3 --the principle of arrangement of the main production equipment with respect to the flow of production objects, x_4 --the principle of organization of the automatic checking system, x_5 --the principle of organization of the automated tool support system, and x_6 --the principle of organization of the automated waste removal system.

The given classification features fully characterize the technological system of a flexible manufacturing system, which includes, according to GOST [State Standard] 26228-85, an automated transport-warehousing system, automatic checking system, tool support system and waste removal system. The problem subsequently reduces to study of the set of structural-configuration layouts of the flexible manufacturing system according to the adopted classification features, determination of the gradations of these features, and also according to the quantitative

analysis of the applicability of structural solutions by coefficient $f_{\Pi p}$ and f_{TB} .

The results of the analysis are presented in Tables 1-6. It must be noted that analysis of the principles of organization of automated tool support system (Table 5) and of a waste removal system (Table 6) showed that the class of manufacturing objects does not affect the organization of these systems; therefore, the analysis was performed for a general combination of flexible manufacturing systems without separation into GPS(Pr) and GPS(Tv).

The analysis permitted us to formulate a morphological table of the principal structural-configuration layouts of a flexible manufacturing system, which includes the entire set of the possible structural-configuration layouts of flexible manufacturing systems. Performing alternate interrogation of the gradations of all the structural features, one can find the set of variants of the structural design of the system

$$W = \{\omega_i\}$$

(where $i = \overline{1, N}$), each of which is a sample of the gradations of the features of variables, for example,

$$\omega_r = \{x_1^3, x_2^2, x_3^3, x_4^2, x_5^3, x_6^2\}.$$

This structural solution is characterized by: the use of a rectilinear broken type of blank flow, by centralized separate arrangement of blanks and of machined parts, by location of the main production equipment under the main transport path (overhead transport is used), by implementation of automatic checking, by organization of developmental support based on the main transport system of the flexible manufacturing system with the flow of tools from a central tool warehouse (TsIS) directly to the machine tool without intermediate storage on a separate section (IU), and removal of wastes on the basis of the main automated transport-warehouse system of the flexible manufacturing system.

Table 1. Types of Blank Flow Layouts

Тип схемы (1)	x_1	$f_{\text{тв}}$	$f_{\text{пп}}$	Изображение (2)
(3) Линейный	(4) Прямолиней- ный	x_1^1	0,11	0,06
	(5) Реверсивный	x_1^2	0,09	0,17
	(6) Прямолиней- ный ломаный	x_1^3	0,04	0,02
(7) Замкнутый	(8) Кольцевой	x_1^4	0,07	0,10
	(9) Кольцевой разветвленный	x_1^5	0,02	0,09
	(10) Кольцевой матричный	x_1^6	0,24	0,19
(11) Многорядный	(12) Матричный прямолиней- ный	x_1^7	0,04	0,04
	(13) Матричный реверсивный	x_1^8	0,13	0,05
	(14) Сетевой	x_1^9	0,11	0,21
(15) Радиальный	x_1^{10}	0,14	0,08	

(Key on following page)

KEY:

- | | |
|-----------------------|------------------------|
| 1. Type of layout | 9 Circular branched |
| 2. Representation | 10. Circular matrix |
| 3. Linear | 11. Multirow |
| 4. Rectilinear | 12. Matrix rectilinear |
| 5. Reversible | 13. Matrix reversible |
| 6. Rectilinear broken | 14. Network |
| 7. Closed | 15. Radial |
| 8. Circular | |

The problem of morphological analysis terminates in design of a morphological classifier. The problem of morphological synthesis can generally be formally described as [5].

The specific function $f(\omega_i)$ is determined on set W , i.e., an algorithm for calculating this function $f(\omega_i)$ for any $\omega_i \in W$ is constructed.

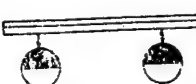
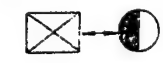
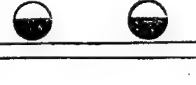
Generally $f(\omega_i) = \{f_k(\omega_i), k = \overline{1, m}\}$ is a set of criteria, part of which is minimized, and part of which is maximized. The problem of morphological synthesis consists in removal of

$$f_0\{\omega_i\} \rightarrow \text{opt}/\omega_i \in W; \\ f_j(\omega_i) \geq 0, f_p(\omega_i) \leq 0,$$

where f_0 is the optimal value of the criterion of quality, $f_j(\omega_i)$ and $f_p(\omega_i)$ are restrictions, and $j = \overline{1, k}$, $p = k + 1, m$.

The following methods can be used to solve the problem of morphological synthesis with the vector criterion of quality: sequential analysis and elimination of variants of design solutions [4], competing points [6], and filtration for tree-like design [5].

Table 2. Principles of Accumulation of Blanks and Parts

(1) Принцип накопления и размещения		x_2	f_{Tb}	f_{Pr}	(2) Изображение
(3) Централизованный	(4) Общее	x_2^1	0,45	0,44	
	(5) Раздельное	x_2^2	0,10	0,05	
(6) Децентрализованный	Общее(4) x_2^3	0,08	0,10		
	Раздельное(5) x_2^4	0,10	0,06		
(7) Комбинированный	Общее (4) x_2^5	0,07	0,08		
	Раздельное(5) x_2^6	0,06	0,04		
Накопление на транспортной системе	(8)	x_2^7	0,14	0,23	
(9) Примечание.					



(10)
— автоматизированная рабочая позиция



(11)

— автоматизированный склад



(12)
— накопительное устройство общее для заготовок и деталей



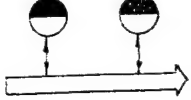
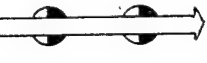
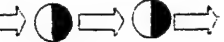
(13)
— накопительные устройства раздельные для заготовок и деталей

(Key on following page)

KEY:

- | | |
|---|--|
| 1. Principle of accumulation and location | 8. Accumulation on transport system |
| 2. Representation | 9. Note |
| 3. Centralized | 10. Automated work position |
| 4. Common | 11. Automated storage |
| 5. Separate | 12. Storage device common for blanks and parts |
| 6. Decentralized | 13. Storage device separate for blanks and parts |
| 7. Combination | |

Table 3. Principles of Arrangement of Production Equipment With Respect to Blank Flow

Принцип (1) расположения	x_3	f_{TB}	f_{Π_B}	(2) Изображение
(3) Рабочие позиции расположены в стороне от основного транспортного пути	(4) С общим ответвлением для ввода и выдачи заготовок и деталей	x_5^1	0,44	0,46 
	(5) С раздельным ответвлением для ввода заготовок и выдачи деталей	x_5^2	0,11	0,07 
Рабочие позиции расположены: (6) под основным транспортным путем (7)	x_5^3	0,21	0,03 	
на основном транспортном пути (8)	x_5^4	0,24	0,04 	

KEY:

1. Principle of arrangement
2. Representation
3. Work positions arranged in direction from main transport path
4. With common branching for input and output of blanks and parts
5. With separate branching for input of blanks and output of parts
6. Work positions are located
7. Under main transport path
8. On main transport path

Table 4. Principles of Organization of Automatic Checking System of Flexible Manufacturing System

(1) Принцип организации САК	x_4	i_{TE}	$f_{\text{ПР}}$	(2) Изображение
Автоматический контроль: на рабочей позиции	(3) x_4^1	0,31	0,40	
на отдельной позиции	(5) x_4^2	0,56	0,48	
Комбинированный	(6) x_4^3	0,13	0,12	

KEY:

- | | |
|---|-------------------------|
| 1. Principle of organization of automatic checking system | 4. At work position |
| 2. Representation | 5. At separate position |
| 3. Automatic checking | 6. Combination |

Table 5. Principle of Organization of Automated Tool Support System of Flexible Manufacturing System

(1) Принцип организации	(2) Обозначение переменной	(3) Значение коэффициентов применяемости
(4) Специальные автоматизированные системы инструментального обеспечения	ЦИС—станок (5)	x_5^1 0,25
	ЦИС—ИУ—станок (6)	x_5^2 0,12
(7) Организация инструментального обеспечения на базе АТСС ГПС	ЦИС—станок	x_5^3 0,32
	ЦИС—ИУ—станок	x_5^4 0,24
(8) Подача инструмента вручную на тележках	ЦИС—станок	x_5^5 0,10
	ЦИС—ИУ—станок	x_5^6 0,07

(Key on following page)

KEY:

1. Principle of organization
2. Notation of variable
3. Value of applicability factors
4. Special automated tool support systems
5. Central tool storage-machine tool
6. Central tool storage-tool section-machine tool
7. Organization of tool support based on automated transport warehouse system of flexible manufacturing system
8. Delivery of tool manually on carts

Table 6. Principle of Organization of Automated Waste Removal System of Flexible Manufacturing System

Принцип организации (1)	(2) Обозначение переменной	Значение (3) коэффициентов при- меняемости
Специальные автоматизированные системы удаления отходов (4)	x_6^1	0,41
Удаление отходов через АТСС ГПС (5)	x_6^2	0,19
Удаление емкостей с отходами с помощью кран-балок и ручных тележек (6)	x_6^3	0,40

KEY:

1. Principle of organization
2. Notation of variable
3. Value of applicability factors
4. Special automated waste removal systems
5. Removal of wastes through automated transport warehousing system of flexible manufacturing system
6. Removal of tanks containing wastes using boom cranes and hand carts

Bibliography

1. "Gibkiye proizvodstvennyye sistemy Yaponii" [The Flexible Manufacturing Systems of Japan], translated from Japanese by A. L. Semenov, edited by L. Yu. Lishchinskiy, Moscow, Izdatelstvo "Mashinostroyeniye", 1987.
- 2 Zherarden, L. "Morphological Analysis--A Method of Creativity," "Rukovodstvo po nauchnotekhnicheskому прогнозированию" [Handbook on Scientific and Technical Prediction], Moscow, Izdatelstvo "Progress", 1977.

3. Ordin, V. M. "Morfologicheskiy analiz sistem: morfologicheskiye metody poiska" [Morphological Analysis of Systems: Morphological Search Methods], Kiev, 1986 (Preprint No 5 of Ukrainian SSR Academy of Sciences. Institute of Cybernetics imeni V. M. Glushkov).
4. Mikhalevich, V. S., Volkovich, V. L. "Vychislitelnyye metody issledovaniya i proyektirovaniya slozhnykh sistem" [Computer Methods of Study and Design of Complex Systems], Moscow, Izdatelstvo "Nauka", 1982.
5. Ordin, V. M. "Morfologicheskiy sintez sistem: postanovka zadachi, klassifikatsiya metodov, morfologicheskiye metody 'konstruirovaniya'" [Morphological Synthesis of Systems: Postulation of Problem, Classification of Methods, Morphological Methods of "Design"], Kiev, 1986 (Preprint No 3, Ukrainian SSR Academy of Sciences. Institute of Cybernetics imeni V. M. Glushkov).
6. Polovinkin, A. I., Bobkov, N. K., Bush, G. Ya. "Avtomatizatsiya poskovogo konstruirovaniya" [Automation of Search Design], Moscow, Izdatelstvo "Radio i svyaz", 1981.
7. "Tekhniko-ekonomicheskiye kharakteristiki i strukturno-komponovochnyye resheniya zarubezhnykh gibkikh proizvodstvennykh sistem dlya mekhanoobrabotki" [Technical and Economic Characteristics and Structural-Configuration Solutions of Foreign Flexible Manufacturing Systems for Machining], Moscow, NIIMash, 1984.
8. "Tipovyye kompleksno-avtomatizirovannyye uchastki tipa ASV iz oborudovaniya s ChPU s primeneniem EVM: Metod. rekomendatsii" [Typical Integrated Automated Sections of the ASV Type and Equipment With Numerical Program Control Using Computers: Methodical Recommendations], Moscow, ENIMS, 1983.

COPYRIGHT: "IZVESTIYA VUZOV SSSR - PRIBOROSTROYENIYE", 1990

UDC 658.52.011:681.51

MODIFIED NET METHODS IN PROBLEMS OF CONTROL AND AUTOMATED SIMULATION OF ASSEMBLY MANUFACTURING SYSTEMS

917F0203A Leningrad IZVESTIYA VYSSHIKH UCHEBNYKH ZAVEDENIY:
PRIBOROSTROYENIYE in Russian No 10, 1990 (manuscript received 28 Feb 90)
pp 16-19

[Article by A. V. Borusan, A. A. Lavrov, K. B. Ostapchenko et al., Kiev Polytechnical Institute]

[Text] Methods are proposed for synthesis of correction algorithms for control of assembly processes and parametric correction of simulation models of flexible manufacturing systems, based on hierarchical Petri nets. Problems related to development of effective methods of control of assembly processes and to analysis of them by simulation are considered.

The assembly process as an object of automation is characterized by cyclicity, hierarchy of representation of production processes, asynchronism and parallelism in operation of assembly equipment. This multiplan layout and complexity of assembly manufacturing determines the need to use methods of simulation in problems of analysis, design and control. The most effective means of solving problems of simulation of objects of a given class is the apparatus of Petri nets (SP). Practical application of Petri nets requires specific modification of their classical apparatus. In the given case, this modification is directed toward solution of the following problems: adequate description of the simulated object, the possibility of designing automated procedures of synthesis of control models of assembly processes, and implementation of automated control of simulation experiments.

Problem 1. It is suggested that a modification of the Petri net--a hierarchical painted net (IR-net), which has the properties of animation and safety--be used as a model of the discrete assembly process. The positions of the net in this model are compared to the operations of the process, transfers are compared to events of a change of operations, and the colors of marks are related to elements of material and information flows. The characteristic feature of the proposed modification is

construction of a known correct (animated and safe) net with as large a number of elements as desired from some simple nets, which show the properties of the object of simulation, the correctness of which has been established. Let us call the IR-net a structure consisting of a finite set of correctly formulated net structures (blocks) $N = \{N_i\}$, where

$$N_i = (P_i, T_i, F_i, H_i,$$

$$\Omega_i, \lambda_i, \psi_i, \mu_0^i),$$

$$T_i = T_i^* \cup T_{iu} \cup T_{is},$$

$$T_{iu} = \{t_u | \forall p \in P_i : F_i(p, t_u) = 0\}, \quad T_{is} = \{t_s | \forall p \in P_i : H_i(t_s, p) = 0\},$$

on which the operation of substitution of the net block is determined. This set is partially ordered and graphically represented by a tree, to the root of which corresponds an elementary net or correctly formulated block. The elementary net is a strongly connected automatic net of two positions and two transitions with initial distribution of all colors of the marks in one of the positions. The substitution operation is an operation of superposition of the net structure of the block on a fragment of the net with a doubler position, substitution of its input and output transitions-sources t_u and discharges t_s of the block and removal of the doubler position from the received net. The block is considered correctly formulated if substitution of it instead of the position of the elementary net generates an animated and safe Petri net. It is shown that any Petri net, belonging to a class of correct IR-nets, is animated and safe.

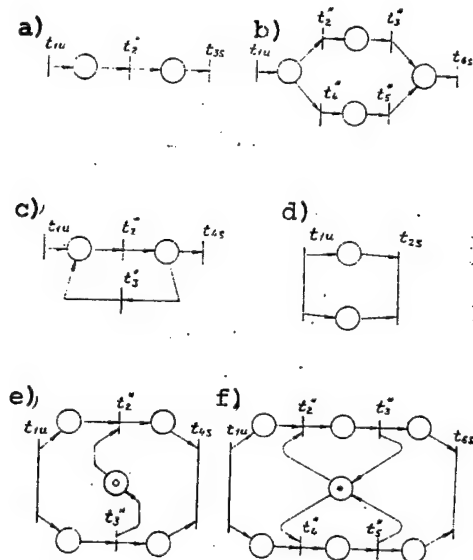


Figure 1

The form of representation of correct IR-nets is determined. It is suggested that six typical blocks that give the main ratios of the relationship of operations of the manufacturing process be used, an automatic block (Figure 1, a); an alternative block (Figure 1, b); a cyclical block (Figure 1, c); a parallel block with the absence of interactions (Figure 1, d); a parallel block with synchronization by event (Figure 1, e); and a parallel block with competition (Figure 1, f). The type of net structure of the root of the vertex of the tree of the IR-net predetermines the class of the simulated processes. The elementary net of the root vertex corresponds to cyclical processes, while a net structure, represented by an automatic, alternative or cyclic block with introduced inhibitor arcs that guarantee its safety corresponds to a conveyer net.

Problem 2. Management of the manufacturing system in terms of a Petri net reduces to the need to manage transitions of the net as a function of the markings of its positions. The problem of synthesizing the control model consists in assigning the representation (PR), which determines the order of response of competing transitions, on a set of transitions T of a model of the process N. The control algorithm is given in the form of a control net $N_y = (N, X, \varphi, Y, f, PR)$, where X is the set of states of the control object, Y is the set of control actions, $\varphi: T \rightarrow 2^X$ is a function of clear agreement of the set of transitions and subset of states, $f: \mu \rightarrow Y$ is a function of the clear conformity of marking of the net and the set of controls, and $PR: (P \times Q) \times T \rightarrow \{0, 1, \dots\}$ is the priority function of response of transitions of the net.

Problem 3. Automated simulation (AIM) in control and design problems of assembly plants is related to implementation of direction runs of the simulation model (IM) to find a combination in the given range of variation of input parameters that provides the best value of some index of quality (performance, cost and so on). The conditional structure of the AIM is represented by the simulation model itself and by the experiment control device--the search model (PM) (Figure 2).

Hierarchical representation of the simulation model based on the proposed net structures guarantees direct interaction with algorithms of the search model and the possibility of parametric correction of the model.

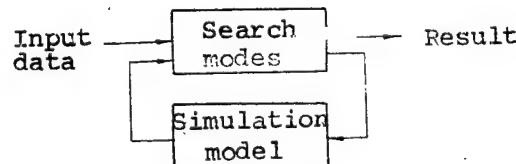


Figure 2

The search model algorithm realizes some optimization method. Its specifics consists in calculating the index of quality on the basis of the results of the run of the simulation model. The relationship of the parameters represented in the simulation model, the length of the run of the model and other characteristics require correct and effective organization of management of the series of experiments. The correctness of interaction of the search and simulation models is maintained by specially developed control procedures. Based on decomposition and analysis of the structure of the discrete optimization algorithms realized in the search model, methods of improving the efficiency of automated decision-making during control of experiments were worked out.

The proposed modifications of net methods and approaches to use of them permit an increase of the effectiveness of solving complex object control problems, and also design and automated simulation of assembly plants.

COPYRIGHT: "IZVESTIYA VUZOV SSSR - PRIBOROSTROYENIYE", 1990

UDC 681.3;621.865.8

IMPLEMENTATION OF CONTOUR CONTROL IN NP SYSTEMS OF MULTILINK ARTICULATED MANIPULATORS

917F0203A Leningrad IZVESTIYA VYSSHIKH UCHEBNYKH ZAVEDENIY:
PRIBOROSTROYENIYE in Russian No 10, 1990 (manuscript received 22 Mar 90)
pp 19-24

[Article by S. V. Goryachev and M. Ya. Ostrovskiy, Leningrad Polytechnical Institute imeni M. I. Kalinin]

[Text] Implementation of contour control in multilink articulated manipulators based on solution of the inverse kinematic problem is considered. Algorithms are proposed for solving kinematic controls based on combination use of a modified "number by number" method. The characteristics of hardware and microprogram support of contour control based on a functionally oriented processor in the SChPU 4S-02 are described.

When developing NP systems for contour control of industrial robots (PR), main attention is devoted to algorithms for solving trajectory problems, which determine to a significant degree the accuracy of reproduction of the trajectory and the speed of the industrial robot [1, 2]. A distinguishing feature of NP systems of multilink manipulators is the need to solve two main problems during control of motion: the problem of interpolation that calculates the position of the industrial robot grab in Cartesian coordinates and the inverse kinematic problem (OKZ), which calculates the angular coordinates of the industrial robot according to the given Cartesian coordinates of the grab. Whereas the interpolation algorithms are now well known and are widely used in machine tool NP systems [1, 2], algorithms for solving the inverse kinematic problem in real time have been very weakly developed.

Numerous gradient and other iterative algorithms for solving the OKZ [3] contain a large number of operations of multiplication, division and computing the trigonometric functions and, therefore, are used only for simulation of the motions of the industrial robot. In this regard, preference is given to analytical solution of the OKZ [4] with subsequent tabular implementation of the main trigonometric functions in

NP systems of 5-6-degree manipulators. A disadvantage of this approach is the large volume of tables and at the same time the long cycle time of solving the OKZ (up to 75-125 ms).

Thus, working out analytical or tabular-analytical methods of solving the kinematic equations of multilink manipulators, which reduce the volume of tables and the time of solving the OKZ, and also those adapted for effective implementation on functionally oriented processors (FOP), performed within the NP system, is promising.

Mathematical postulation of the problem is dependent on the design of the industrial robot. Let us consider as an example a system of equations that describe the kinematics of one of the relatively simple robots of the TUR-10 type (Figure 1):

$$\left. \begin{array}{l} X = [L_2 \cos(Q_2) - L_3 \cos(Q_2 + Q_3) + L_4 \cos(Q_2 + Q_3 + Q_4)] \cos(Q_1); \\ Y = [L_2 \cos(Q_2) - L_3 \cos(Q_2 + Q_3) + L_4 \cos(Q_2 + Q_3 + Q_4)] \sin(Q_1); \\ Z = L_1 + L_2 \sin(Q_2) - L_3 \sin(Q_2 + Q_3) + L_4 \sin(Q_2 + Q_3 + Q_4); \\ A = Q_2 + Q_3 + Q_4; \\ O = Q_1; \\ T = Q_5, \end{array} \right\} \quad (1)$$

where X, Y, and Z are the Cartesian coordinates of the grab, A, O, and T are the orientation angles (Euler angles), L_j ($j = \overline{1, 4}$) are the lengths of the links, and Q_i ($i = \overline{1, 5}$) are the angles between the links.

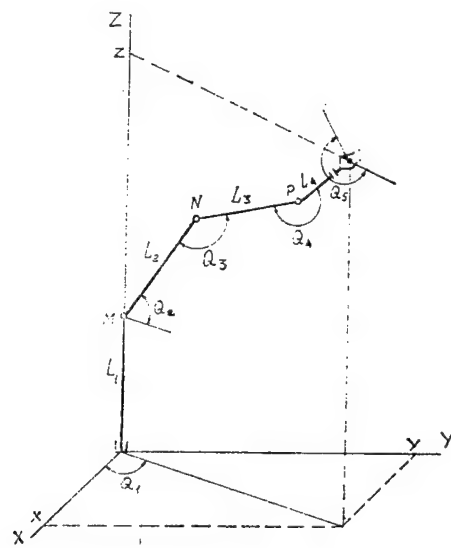


Figure 1. Kinematic Layout of TUR-10 Robot

The expressions look so simple for the orientation angles due to the simplicity of the design of the robot.

Analysis of relations (1) shows that the fraction of trigonometric operations and multiplication operations is high both when solving the direct kinematic problem (PKZ) (the Cartesian coordinates are determined by the angles of rotation of the links) and when solving the inverse kinematic problem. Thus, the number of "long" operations when solving the OKZ, depending on the method of solution and on the design of the industrial robot, fluctuates in the range of 12-16 transcendental functions, and 30-40 multiplication and division operations and extracting the square root for different types of six-link manipulators [3, 4].

Ordinarily, trigonometric transformations are determined as standard transformations, and different methods are used to implement them [5]. At the same time, as follows from analysis of relations (1), more complex operations of transformation and rotation of the coordinate system can be distinguished as typical (POLDEK--transformation from a polar to a Cartesian coordinate system, DEKPOL--transformation from a Cartesian to a polar coordinate system, and ROTATE--rotation of a Cartesian coordinate system). The algorithm for solving the inverse kinematic problem can be represented with regard to the introduced operations in the form presented in Figure 2.

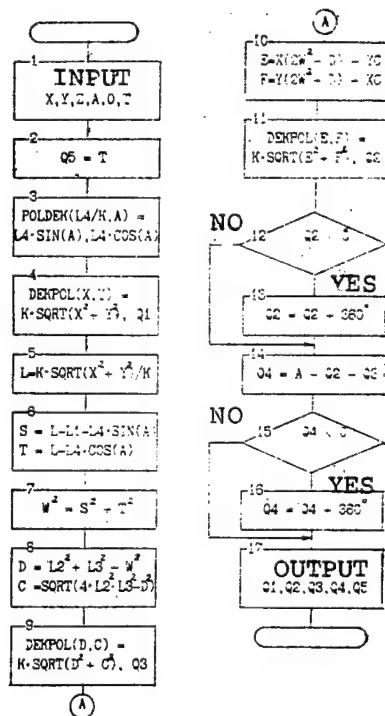


Figure 2. Algorithm for Solving Inverse Kinematic Problem

The use of POLDEK and DEKPOL commands reduces the number of "long" operations, which results in a reduction of the time of fulfilling the algorithm. The use of the "number by number" method [2, 5], specifically, Volder and Medjit methods, is promising for fulfillment of these operations. Although the given methods have a disadvantage in speed to some other methods of calculation of trigonometric functions, a significant advantage is achieved in the given case due to multiple use of all the functional capabilities of the operations. For example, the POLDEK operation is "equivalent" to simultaneous fulfillment: sin, cos and two multiplications.

The NP systems of industrial robots are now constructed on the basis of universal 16-bit microprocessors, the architecture of which is insufficiently effective for solving a class of trajectory problems [1]. This is caused by the small word length and rigid fixed list of commands. An effective method of solving the performance of general-purpose microcomputers is connection of functionally oriented processors. The use of functionally oriented processors, oriented toward solution of only trigonometric problems, is undesirable in universal terminal control systems (TSU) of modules of flexible manufacturing systems, which include not only robots, but machine tools and other auxiliary equipment.

The 4S-02 terminal control system has been developed at the Leningrad Polytechnical Institute for control of the modules of a flexible manufacturing system that includes the SChPU Elektronika NMS-12402 control module (based on the K1801VM1 microprocessor) and a functionally oriented processor-active memory module (MAP) [6]. The distinguishing features of active memory modules are the increased word length of the operations block (48), the memory capacity--4K 48-bit words, hardware support of realization of complex logic transformations, and dynamic microprogramming that introduces specialized commands.

The indicated commands--POLDEK, DEKPOL and ROTATE--are realized at the microprogram level for effective solution of trajectory problems in the active memory module. The iteration procedures that realize these commands are reflected in the table. The given relations are variants of known Volder and Medjit algorithms [5], modified for more complete consideration of the architectural features of the active memory module: 48-bit words, 2-bit shifts and other features of the operations block. The most significant characteristics of the algorithms are enumerated below. A specially developed microprogramming automation system SYMON was used for microprogram realization of typical commands [7]. Inclusion of the given operations into the command system of the active memory module enhances the level of its internal language, while microprogram realization reduces the time of fulfillment of trigonometric operations by a factor of 2-2.5, compared to program realization.

Operation	Recursion relation	Initial condition	Result
DÉKPOL(A, B)	$Z_{i+1} = 2(Z_i + U_i X_i)$ $X_{i+1} = X_i - U_i Z_i \cdot 2^{-2i}$ $U_i = -\text{sgn}(Z_i)$ $\Phi_{i+1} = 2[\Phi_i - U_i \arctg(2^{-1})]$	$(A) = X_0 = X$ $(B) = Z_0 = Y$ $\Phi_0 = 0$	$(A) = X_n = K\sqrt{X^2 + Y^2}$ $(B) = \Phi_n = \arctg(Y/X)$
POLDEK(A, B)	$\Phi_{i+1} = \Phi_i - U_i \arctg(2^{-1})$ $U_i = \text{sgn}(\Phi_i)$ $Z_{i+1} = 2(Z_i + U_i X_i)$ $X_{i+1} = X_i - U_i Z_i \cdot 2^{-2i}$ $Y_n = Z_n \cdot 2^{-n}$	$(A) = X_0 = R$ $Z_0 = 0$ $(B) = \Phi_0 = \Phi$	$(A) = X_n = KR \cos(\Phi)$ $(B) = Y_n = KR \sin(\Phi)$
ROTATE(A, B)	$\Phi_{i+1} = \Phi_i - U_i \arctg(2^{-i})$ $U_i = \text{sgn}(\Phi_i)$ $Z_{i+1} = 2(Z_i + U_i X_i)$ $X_{i+1} = X_i - U_i Z_i \cdot 2^{-2i}$ $Y_n = Z_n \cdot 2^{-n}$	$(A) = X_0 = X$ $RG = Y_0 = Y$ $(B) = \Phi_0 = \Phi$	$(A) = X_n =$ $K[X \cos(\Phi) -$ $-Y \sin(\Phi)]$ $(B) = Y_n =$ $= K[Y \sin(\Phi) +$ $+ X \sin(\Phi)]$

Note. K is a Volder constant ($K \approx 1.65$); A, B--addresses of operands participating in commands, third independent variable that participates in ROTATE command, is transmitted through one of the RONs [not further identified] of the active memory module.

The characteristic features realizing the above operations in the active memory module reduce to the following:

1. The algorithm mainly corresponds to a Medjit algorithm, which, compared to a Volder algorithm, guarantees greater accuracy and speed of computations, and also has hardware support in the active memory module in the form of shift microoperations by two bits simultaneously.
2. Unlike the Medjit algorithm, one cycle was organized for the POLDEK and ROTATE operations: the rotations are performed, beginning with the largest angles (as for the Volder algorithm). Upon completion of the cycle, the result is shifted by N bits to the right. There are no losses of accuracy, since additional bits can be stored due to the long word length of the active memory module in calculation with accuracy up to 24 bits.
3. The angles of rotation can be given in degrees, radians or other units (sensor codes) by switching by program to one or another table of constants. This permits one in many cases to do away with additional scaling of operands when shaping drive control signals and "saves" five-six multiplication operations. There are no restrictions on the value of the angles of rotation. The constants correspond to the Volder algorithm. A longer word length permits one to select the number of additional bits, necessary for the required accuracy.

4. Program adjustment for the accuracy of the calculations is possible and a proportional increase of the time of fulfillment due to accuracy is provided.

5. There is a K-bit shift to the value $K = P$, where P is ordinarily selected equal to $N/2$, but it can be changed by program as a function of the required accuracy.

We note that a long word length of the active memory module permits one to store the values of coordinates, squares and fourth powers of coordinates in one cell, necessary for realization of operations in blocks 8 and 10 of the algorithm for the inverse kinematic problem without a loss of accuracy (see Figure 2). A total of three-four memory cells would be required to store the intermediate values when realizing the algorithm on a general-purpose microcomputer, which would considerably reduce the speed of performing the operations.

Problems, similar to robot control problems, are also encountered for multicoordinate machine tools having rotary coordinates. Whereas accuracy for performing 16-bit operations is ordinarily sufficient for robots, 20-24 bits are required for a machine tool. There is a nonproportional increase of the completion time with an increase of accuracy when the given algorithms are realized on a microcomputer. Thus, the completion time is $T_g(16) = 2.07$ ms with accuracy of 16 bits and $T_g(24) = 4.1$ ms with accuracy of 24 bits for the Elektronika-60 computer with realization according to Medjit [2, 5]. The corresponding times are equal to $T_M(16) = 0.5$ ms and $T_M(24) = 0.8$ ms for an active memory module. The total time of solving trajectory problems for a manipulator of the type given in Figure 1 comprises: 2.6 ms for the direct kinematic problem and 4 ms for the inverse kinematic problem (with accuracy of 16 bits). The characteristics for the Elektronika-NMS 12402 microcomputer are similar: 10 ms for the direct kinematic problem and 16 ms for the inverse kinematic problem.

As indicated earlier, speed is increased due to the use of an algorithm (see Figure 2) containing a fewer number of "long" operations than ordinarily used algorithms, as a result of using complex POLDEK and DEKPOL commands, as a result of using modifications of the Volder and Medjit algorithms that permit a reduction of the time of fulfilling the algorithm due to the long word length of the active memory module and also due to transition of the algorithms to the microprogram level when solving the direct and inverse kinematic problems.

Thus, realization of contour control is feasible on the basis of complex operations of transformation of coordinates, realized at the microprogram level in a functionally oriented processor, and which considerably increase the performance of a general-purpose microcomputer.

Bibliography

1. "Mnogotselevyye sistemy ChPU gibkoy mekhanoobrabortkoy" [Multipurpose NP System for Flexible Machining], edited by V. G. Kolosov, Leningrad, Izdatelstvo "Mashinostroyeniye", 1984.
2. Baykov, V. D., Vashkevich, S. N. "Resheniye trayektornykh zadach v mikroprotsessornykh sistemakh ChPU" [Solution of Trajectory Problems in Microprocessor NP Systems], edited by V. B. Smolov, Leningrad, Izdatelstvo "Mashinostroyeniye", 1986.
3. Petrov, A. A. "Software of Information Control Systems of Adaptive Robots. Motion Shaping Algorithms. Results of Science and Technology. Part 2," IZVESTIYA AKADEMII NAUK SSSR. SERIYA TEKHNICHESKAYA KIBERNETIKA, Vol 18, 1983.
4. Ranky, P. G., Ho, G. Y. "Robot Modeling. Control and Application With Software," IFS LTD, 1985.
5. Baykov, V. D., Smolov, V. B. "Spetsializirovannyye protsessory: iteratsionnyye algoritmy i struktury" [Specialized Processors: Iteration Algorithms and Structures], Moscow, Izdatelstvo "Radio i svyaz", 1985.
6. Alekseyev, V. N., Konovalov, A. M., Kolosov, V. G. et al. "Mikroprotsessornyye sredstva proizvodstvennykh sistem" [Microprocessor Devices of Manufacturing Systems], edited by V. G. Kolosov, Leningrad, Izdatelstvo "Mashinostroyeniye", 1988.
7. Yevlannikov, D. L., Petrenko, A. A. "Sistem for Automation of Microprogramming of Terminal Control System Coprocessor 4S-02 GPS," "Opyt sozdaniya i vnedreniya sistem upravleniya dlya GPS: Sbornik" [Experience of Development and Introduction of Control Systems for Flexible Manufacturing Systems: A Collection], Leningrad, LDNTP, 1989.

COPYRIGHT: "IZVESTIYA VUZOV SSSR - PRIBOROSTROYENIYE", 1990

UDC 62.50

PROGRAM-ADAPTIVE ALGORITHMS FOR POSITIONAL AND CONTOUR CONTROL OF ROBOT

917F0203A Leningrad IZVESTIYA VYSSHIKH UCHEBNYKH ZAVEDENIY:
PRIBOROSTROYENIYE in Russian No 10, 1990 (manuscript received 28 Feb 90)
pp 24-31

[Article by A. V. Timofeyev and A. B. Godun, Leningrad Institute of Aviation Instrument Building]

[Text] Algorithms for adaptive control of a robot, based on correction of programmed motions at fixed parameters of the control law, are considered. The calculating relations and experimental results of simulation of the developed algorithms are presented.

The efficiency and reliability of traditional robot program control systems are reduced significantly under indeterminant production conditions of operating them. This is manifested in a decrease of accuracy, occurrence of vibrations, soft failures and hard failures. One of the effective methods of increasing the reliability and quality of functioning of a robot is the use of adaptation devices in their control system, which provide automatic adaptation to various types of disturbances and noise. Known methods of adaptation are based on the use of algorithms for identification of unknown factors or on self-adjustment of the parameters of the control laws. However, they are complicated, which makes it difficult to implement them in a robot control system.

New adaptive control algorithms, based on correction of the programmed motions (PD) of the robot as a function of the nature and level of perturbations and noise occurring under real operating conditions of the robot, are proposed in this article.

Postulation of problem of program-adaptive control of robot. The dynamics of a wide range of robots is described by a system of differential equations of type

$$A(q, \xi)q^{(r)} + b(q, \dot{q}, \dots, q^{(r-1)}, \xi) = u + \pi, \quad (1)$$

where $q = q(t)$ is an m -dimensional vector function of the generalized coordinates, $q^{(j)}$ is its j -th derivative by time t , $j = 2 \dots r$, $\xi = \xi(t)$ is the p -dimensional vector function of the robot parameters, $u = u(t)$ is an m -dimensional vector function of control actions, $A(q, \xi)$, $b(q \dots q^{(r-1)}, \xi)$ are given $m \times m$ and m functions, respectively, $\pi = \pi(t)$ is an m -dimensional vector function of constant external perturbations, about which it is known only that $\|\pi(t)\| \leq c\pi$, where $c\pi$ is some positive value. The order of r vector differential equations (1) is dependent on the type of motors used in the robot. In the case of torque motors, $r = 2$; when using DC motors, $r = 3$.

Let it be required to switch the robot during time $T = t_T - t_0$ from a given initial state to the desired final state, determined by the following boundary conditions

$$q(t_0) = q_0 \dots q^{(r-1)}(t_0) = q_0^{(r-1)}; \quad q(t_T) = q_T \dots q^{(r-1)}(t_T) = q_T^{(r-1)} \quad (2)$$

with given accuracy ϵ . In this case, the purpose of control is given by

$$\|E(t_T)\| \leq \epsilon, \quad (3)$$

here $E(t) = \{e^{(i)}(t)\}_{i=0}^{r-1}$; $e(t) = q(t) - q_p(t)$. In practice, only part of the combination of boundary conditions rather than all of them, usually boundary and specific conditions, are frequently given

$$q(t_0) = q_0, \quad q(t_T) = q_T, \quad (4)$$

$$\|e(t_T)\| \leq \epsilon \quad (5)$$

or

$$q(t_0) = q_0, \quad \dot{q}(t_0) = \dot{q}_0; \quad q(t_T) = q_T, \quad \dot{q}(t_T) = \dot{q}_T, \quad (6)$$

$$\|e(t_T)\| \leq \epsilon, \quad \|\dot{e}(t_T)\| \leq \epsilon. \quad (7)$$

Solution of this problem is naturally divided into two steps. The programmed motion $q_p(t)$, $t \in [t_0, t_T]$, which satisfies boundary conditions of type (2), (4), and (6), is synthesized in analytical form. In the second step, the control law that guarantees fulfillment of specific conditions of type (3), (5), and (7) is synthesized. The control laws that solve the formulated problems will be called terminal laws. They are primarily oriented toward use in robot position control systems.

The specific condition in contour control systems generally has the form

$$\|E(t)\| \leq \varepsilon; \quad t \in [t_0, t_T]. \quad (8)$$

If truncated boundary conditions (4) and (6) are given, the specific condition has the form

$$\|e(t)\| \leq \varepsilon; \quad t \in [t_0, t_T] \quad (9)$$

or

$$\|e(t)\| \leq \varepsilon, \quad \|\dot{e}(t)\| \leq \varepsilon; \quad t \in [t_0, t_T]. \quad (10)$$

This means that the contour control laws guarantee tracking of a given programmed motion $q_p(t)$ and possibly of its derivatives in the sense of (8), (9), and (10) with given accuracy over the entire range of motion $[t_0, t_T]$.

Solution of terminal (position) and contour control problems is complicated by the fact that in practice there may be initial, parametric or constantly acting perturbations. They have an unfavorable influence on the quality of control, and result in a decrease of accuracy, in autooscillations or even in a loss of stability. Adaptation devices are necessary to compensate for the indicated perturbations. Effective methods of adaptation, based on identification of unknown perturbing factors or on self-adjustment of the parameters of the control laws, are suggested in [1-3].

A new method of adaptation in positioning and contour control systems, the characteristic feature of which includes the fact that the programmed motion is corrected instead of the parameters of the control law, is studied in the article. This permits one to use ordinary positioning and contour control systems with standardized regulators of actuating drives, supplementing them only by programmed motion correction programs, which implement the program-adaptive control

algorithms suggested below. For definiteness, robots with DC motors whose dynamics is described by differential equation (1) at $r = 3$ and specific conditions of type (5), (7) and (9), (10) are considered.

Program-adaptive position control algorithms. Let us take as an example the problem of position (terminal) control with a specific condition of type (5) or (7). The parametric optimization method of programmed motions, proposed in [2, 3], can be used for analytical synthesis of programmed motions with regard to given boundary conditions (4) or (6). However, it requires solution of the variational problem, which complicates analytical synthesis of programmed motion. Therefore, let us consider simpler algorithms for analytical synthesis of programmed motion. The desired programmed motion for boundary conditions (4) is described by a linear function of type

$$q_p(t) = q_0 + (q_T - q_0)(t - t_0)/T \quad (11)$$

at $t \in [t_0, t_T]$ and by a third-power polynomial for boundary conditions (6)

$$q_p(t) = q_0 + \alpha_1(t - t_0) + \alpha_2(t - t_0)^2/2 + \alpha_3(t - t_0)^3/6. \quad (12)$$

Here $t \in [t_0, t_T]$, $\dot{\alpha}_1 = \ddot{q}_0$, $\alpha_2 = \frac{6}{T^2}(q_T - q_0) - \frac{2}{T}(\dot{q}_T + 2\dot{q}_0)$, $\alpha_3 = -\frac{12}{T^3} \times$
 $\times (q_T - q_0) + \frac{6}{T^2}(\dot{q}_T + \dot{q}_0)$.

Let us consider the stabilizing control law

$$u = A(q, \xi)[\ddot{q}_p + \Gamma_1(\ddot{q} - \ddot{q}_p) + \Gamma_2(\dot{q} - \dot{q}_p) + \Gamma_3(q - q_p)] + b(q, \dot{q}, \ddot{q}, \xi), \quad (13)$$

in which Γ_1 , Γ_2 , and Γ_3 are $m \times m$ matrix amplification factors in the feedback channels, selected from the condition of providing the desired nature of the transition process (PP). It is sufficient to take matrices Γ_1 , Γ_2 , and Γ_3 as diagonal to compensate for cross-connections in a closed system. By substituting (13) into (1) at $r = 3$, we find the equation of the transition process in a closed system

$$\dot{E} = \Gamma E + A^{-1}(q, \xi)\pi,$$

where $E = \{e^{(i)}(t)\}_{i=0}^2$, $e = q - q_p$, $\Gamma = \begin{pmatrix} 0 & I & 0 \\ 0 & 0 & I \\ \Gamma_3 & \Gamma_2 & \Gamma_1 \end{pmatrix}$.

The following estimate in component form is valid:

$$\left\| \begin{array}{l} e(t) \\ \dot{e}(t) \\ \ddot{e}(t) \end{array} \right\| \leq c \left\| \begin{array}{l} e(t_0) \\ \dot{e}(t_0) \\ \ddot{e}(t_0) \end{array} \right\| \exp(-\gamma(t-t_0)) + c\gamma^{-1}\mu^{-1}c\pi.$$

Here $t \geq t_0$, γ is the module of the most essential part of eigennumbers of matrix Γ , c is a positive constant, dependent only on Γ , and μ is a positive number, $\mu \leq \min_i \lambda_i(A)$, where $\lambda_i(A)$ are the eigennumbers of matrix $A(q, \xi)$.

If the initial perturbations are equal to zero, i.e., if $e(t_0) = \dot{e}(t_0) = \ddot{e}(t_0)$, selection of the amplification factors Γ_1 , Γ_2 , and Γ_3 from the condition

$$\gamma \geq c\mu^{-1}c\pi\varepsilon^{-1} \quad (14)$$

ensures fulfillment of specific condition (5) for programmed motion (11) and of specific condition (7) for programmed motion (12).

Let us consider the case when the initial perturbations are distinct from zero and that their level $\|E(t_0)\| \leq \varepsilon_0$, where ε_0 is some positive integer. Let us assume that the constantly effective perturbations are $\pi(t) = 0$. Let us then select amplification factors Γ_1 , Γ_2 , and Γ_3 , at which the following inequality will be fulfilled, for the given times of motion T , accuracy ε and for the level of initial perturbations ε_0

$$\gamma \geq \frac{1}{T} \ln \frac{c\varepsilon_0}{\varepsilon}. \quad (15)$$

Control law (13) ensures fulfillment of specific condition (5) for programmed motion (11) and of specific condition (7) for programmed motion (12).

Let $\pi(t) \neq 0$. Then for given T , ε , and ε_0 , selection of the amplification factors from the condition (found on the assumption that $\exp(\gamma T) > 1 + \gamma T$)

$$\gamma \geq (c\varepsilon_0 + c\mu^{-1}c\pi T - \varepsilon + \sqrt{(c\varepsilon_0 + c\mu^{-1}c\pi T)^2 + 4\mu^{-1}cc\pi T\varepsilon})/2T\varepsilon \quad (16)$$

guarantees fulfillment of (5) for programmed motion (11) and of (7) for programmed motion (12). It may happen in practice that the real level of initial perturbations (for example, due to the inaccurate initial setting of the robot) will be greater than given ϵ_0 . Specific conditions (5) and (7) are then violated and adaptation of the control system is necessary. In this case, one could use the self-adjusting method of the control law by correction of parameters Γ_1 , Γ_2 , and Γ_3 or of vector ξ . But this method of adaptation with a large level of initial and external constantly acting perturbations may result in violation of the restrictions on control. Because of this, the control law may be unrealizable.

A simpler and more effective adaptation algorithm in these cases may be one based on correction of the programmed motion at fixed structure and parameters of control law (13). The essence of this algorithm includes the fact that the programmed motion is adjusted by formulas (11) or (12), into which their true values determined by the position and speed sensor are substituted instead of q_0 and \dot{q}_0 , at initial moment of time t_0 . This single correction of the programmed motion is sufficient to guarantee fulfillment of specific condition (5) or (6) at the level of constantly effective perturbations

$$c\gamma^{-1}\mu^{-1}c\pi \leq \epsilon. \quad (17)$$

Let us denote by t_k some moment of violation of specific condition (5) or (7) with respect to programmed motion (11) or (12), respectively, constructed as a result of the first correction of the programmed motion. This violation may occur, for example, due to too high a level of constantly acting perturbations, which results in violation of inequality (17). There can be an adaptation to these unmonitored perturbations due to correction of the programmed motion. To do this, the programmed motion must be constructed according to formulas (11) or (12), having substituted the values $q(t_k)$ and $\dot{q}(t_k)$, recorded by the position and speed sensor at moment of time t_k , instead of q_0 and \dot{q}_0 , and dimensionality $t_T - t_k$ instead of T . One can show that specific conditions (5) and (7) will be fulfilled after the final number of corrections of programmed motion.

Program-adaptive contour control algorithms. Let us now consider the problem of contour control of a robot with specific condition (9) or (10). The necessary condition for fulfillment of (9) and (10) is the low level of initial perturbations compared to the given machining accuracy of the programmed motion. It is necessary that $\|e(t_0)\| \leq \epsilon_0 \leq \epsilon$ in the case of specific condition (9). Let us select the program motion in the form of (11) and let us use control law (13). Specific condition (9) will be fulfilled if the levels of constantly active and initial perturbations satisfy the requirement

$$ce_0 + c\gamma^{-1}\mu^{-1}cn \leq \varepsilon.$$

Otherwise, it may be violated at some moment of time t_k . In this case, one must construct an auxiliary (corrected) programmed motion by formula (11), having substituted in it the values of $q(t_k)$ and $t_T - t_k$,

respectively, instead of q_0 and T . The programmed motion corrected in this manner is substituted into control law (13) and we check fulfillment of (9) with respect to the initial programmed motion (11). If it is violated, the auxiliary programmed motion, subsequently used in control law (13), is again corrected. One can show that the number of these corrections will be finite. The experimental results of simulation, considered subsequently, also indicate this.

The program-adaptive contour control algorithm is constructed in similar fashion, but programmed motion of type (12) is used and corrected in control law (13).

Results of simulation of program-adaptive robot control algorithms. The proposed program-adaptive control algorithms, based on correction of programmed motion, were simulated in the problem of control of an industrial robot of type (TUR-2.5) with actuating drives based on DC motors to perform manufacturing operations of laser machining of materials and the operation of grinding the edge of a blank during manufacture of footwear [4]. The adaptation was performed both with respect to errors of the initial setting of the manipulator and with respect to constant perturbations. Not only control law (13), but the programmed control law of the following type were simulated

$$u_p = A(q_p, \xi)\ddot{q}_p + b(q_p, \dot{q}_p, \ddot{q}_p, \xi), \quad (18)$$

and the programmed control law with linear feedback was simulated by position and speed of the following type

$$u = u_p + \Gamma_2(\dot{q} - \dot{q}_p) + \Gamma_3(q - q_p). \quad (19)$$

Control of the TUR-2.5 robot includes control of the manipulator directly according to degrees of mobility q_1 and q_2 and control of the working member (linear displacement and rotation of the grab). The first case is of the greatest applied interest. Let us present an explicit form of matrix function $A(q, \xi)$ and vector function $b(q, \dot{q}, \ddot{q}, \xi)$, used in control laws (13), (18) and (19), to make it more specific. With regard to the dynamics of DC motors, we find

$$\begin{aligned}
A(q, \dot{\xi}) &= L_R K_{\Delta}^{-1} (Jp + p^{-1} \eta^{-1} A_m(q, \xi_m)), \\
b(q, \dot{q}, \ddot{q}, \xi) &= (L_R K_{\Delta}^{-1} p^{-1} \eta^{-1} \dot{A}_m(q, \xi_m) + \\
&+ R_R K_{\Delta}^{-1} (Jp + p^{-1} \eta^{-1} A_m(q, \xi_m))) \ddot{q} + \\
&+ L_R K_{\Delta}^{-1} (K_T p \ddot{q} + p^{-1} \eta^{-1} \dot{b}_m(q, \dot{q}, \xi_m)) + \\
&+ R_R K_{\Delta}^{-1} (K_T p \dot{q} + p^{-1} \eta^{-1} b_m(q, \dot{q}, \xi_m)) + K_I p q,
\end{aligned}$$

where

$$\begin{aligned}
A_m(q, \xi_m) &= \begin{bmatrix} a_{11} & a_{12} \cos(q_1 - q_2) \\ a_{21} \cos(q_1 - q_2) & a_{22} \end{bmatrix}; \\
b_m(q, \dot{q}, \xi_m) &= \begin{bmatrix} a_{12} \sin(q_1 - q_2) \dot{q}_2^2 + b_1 \sin q_1 + K_{T1} \dot{q}_1 \\ -a_{12} \sin(q_1 - q_2) \dot{q}_1^2 + b_2 \sin q_2 + K_{T2} \dot{q}_2 \end{bmatrix}; \\
a_{11} &= m_1 r_1^2 + (m_2 + m_0) l_1^2; \quad a_{12} = a_{21} = m_2 l_1 r_2 + m_0 l_1 l_2; \quad a_{22} = m_2 r_2^2 + m_0 l_2^2, \\
b_1 &= (m_2 r_2 + m_1 l_1 + m_0 l_1) g; \quad b_2 = (m_2 r_2 + m_0 l_2) g; \\
\xi_m &= \{m_1, m_2, r_1, r_2, l_1, l_2, g, m_0, K_{T1}, K_{T2}\}.
\end{aligned}$$

Here m_1 , l_1 , m_2 , and l_2 are the mass and length of the first and second links of the manipulator, respectively, r_1 and r_2 are the distances from the centers of gravity to the rotational axes of the first and second links, m_0 is the mass of the weight, g is the acceleration of gravity, and J , K_T , p , η , L_R , R_R , K_1 and K_{Δ} are the constant diagonal 2×2 matrices of the robot parameters. After the values of γ that satisfy conditions (14), (15) or (16) as a function of the postulated problem have been selected, the amplification factors $\Gamma_j = \text{diag}(\gamma_{ii}^{(j)})$ can be calculated by the given eigenvalues $\gamma_T(\Gamma) \leq -\gamma$, $r = 1-6$ and by the formulas

$$\begin{aligned}
\gamma_{ii}^{(1)} &= \sum_{k=1}^3 \lambda_{3i-k+1}(\Gamma), \\
\gamma_{ii}^{(2)} &= -\lambda_{3i-2}(\Gamma) \lambda_{3i-1}(\Gamma) - \lambda_{3i-2}(\Gamma) \lambda_{3i}(\Gamma) - \lambda_{3i-1}(\Gamma) \lambda_{3i}(\Gamma), \\
\gamma_{ii}^{(3)} &= \lambda_{3i-2}(\Gamma) \lambda_{3i-1}(\Gamma) \lambda_{3i}(\Gamma)
\end{aligned}$$

at $i = 1, 2$.

Let us consider the results of typical experiments in the problem of position control with specific condition (5). Programmed motion was

synthesized in the form of (11), where $q(t_0) = (1, 1; 1, 1)$, $q(t_T) = (1, 0; 1, 0)$, $T = 1$ s, and the required positioning accuracy is $\epsilon = 0.01$ rad. The values of $\Gamma_1 = -15I$, $\Gamma_2 = 75I$, $\Gamma_3 = -125I$ (I is a 2×2 unit matrix), corresponding to $\gamma_T(\Gamma) = -5$, $r = 1 \dots 6$, were taken as the amplification factors in (13).

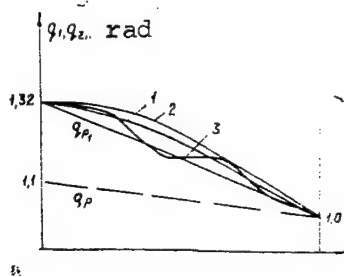


Figure 1

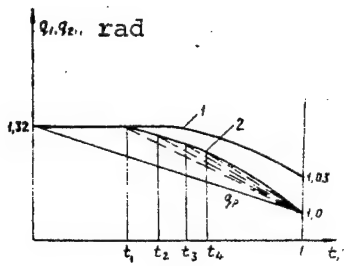


Figure 2

Graphs of the variation of generalized coordinates for three types of control law: stabilizing, programmed and programmed with linear feedback (trajectories 1, 2, 3, respectively)--are presented in Figure 1. The level of the initial perturbations $e(t_0) = (0.22; 0.22)$ considerably exceeded ϵ due to the errors of the initial setting of the manipulator. the real motion $q(t)$ lies entirely in the ϵ -neighborhood of the corrected programmed motion after one correction and, accordingly, (5) is fulfilled. Similar results were found in simulation of program-adaptive contour control of a robot with specific condition (9) and programmed motion (11).

The graphs of variation of generalized coordinates for a stabilized control law without corrections of programmed motions and with correction of programmed motion (trajectories 1 and 2, respectively) in the presence of constant perturbations π , the level $c\pi$ of which exceeded the permissible level (17), are shown in Figure 2. The programmed motion (11) was corrected at moments of perturbation (9), and after this

(four corrections), the specific condition (9) was fulfilled all the time. The use of control law (13) without corrections of programmed motion resulted in violation of (9) with $\epsilon = 0.01$ rad, which indicates the need to correct programmed motions at a high level of constant perturbations.

Bibliography

1. Timofeyev, A. V. "Postroyeniye adaptivnykh sistem upravleniya programmnym dvizheniyem" [Construction of Adaptive Programmed Motion Control Systems], Leningrad, Izdatelstvo "Energiya", 1980.
2. Timofeyev, A. V. "Upravleniye robotami" [Control of Robots], Leningrad, Izdatelstvo LGU, 1986.
3. Timofeyev, A. V. "Adaptivnyye robototekhnicheskiye kompleksy" [Adaptive Robotic Complexes], Leningrad, Izdatelstvo "Mashinostroyeniye", 1988.
4. Volokhov, M. A., Godun, A. B., Dolidze, R. T. "Methods of Sensitization and Programming of Robots for Laser Machining," "Robototekhnogolicheskiye i rotorno-konveyernyye linii v pererabotke plastmass: Sbornik" [Robot Production and Rotary Conveyer Lines in processing of Plastics: A Collection], Leningrad, LDNTP, 1989.

COPYRIGHT: "IZVESTIYA VUZOV SSSR - PRIBOROSTROYENIYE", 1990

UDC 621.856.8

SELF-ADJUSTING TWO-WAY SYSTEM WITH ADJUSTMENT BY VARIABLE PARAMETERS OF MANIPULATOR

917F0203A Leningrad IZVESTIYA VYSSHIKH UCHEBNYKH ZAVEDENIY:
PRIBOROSTROYENIYE in Russian No 10, 1990 (manuscript received 28 Feb 90)
pp 31-39

[Article by V. F. Filaretov and A. F. Polyanskiy, Far Eastern Polytechnical Institute imeni V. V. Kuybyshev]

[Text] The problems of designing a two-way copying manipulator system with active reflection of force, self-adjusting upon variation of load parameters, are considered. The regulator is designed according to the quadratic criterion of quality.

A human operator performs the decision-making and planning functions of the motion trajectories of the actuating member (IO) in copying manipulators (KM), and motions are distributed by separate degrees of freedom directly during operation. Two-way systems (SDD), located in each degree of freedom of the copying manipulator and which are systems of the actuating level of control, should provide precise tracking of the assigned trajectories of motion, and also reproduction of forces on the given member, developed in the degrees of freedom of the actuating member. The dynamic effects of the mutual influence between the degrees of freedom of the manipulator have a strong influence on the quality of operation of the two-way system during motion.

A two-way system was designed in [1] with regard to variation of the load parameters. It was assumed that the variable moments of inertia and also the moments of gravitational forces have the main influence on the dynamics of the two-way system. However, besides inertial and gravitational forces, Coriolis and centrifugal forces, which can not be disregarded at high speeds (more than 0.5 m/s) of the motion of the grab of the copying manipulator [2], also affects the links of the manipulator.

The problem of designing self-adjusting (SN) two-way systems is posed and solved in this paper with regard to the total dynamics of the actuating members of the copying manipulator. It is assumed that the

given member is light and its influence on the dynamics on any two-way system is determined only by the constant moment of inertia.

The moment effect of any degree of freedom of the copying manipulator on a two-way system is generally determined by the expression

$$Q = H'(q_1 \dots q_N) \ddot{a}_H(t) + h(q_1 \dots q_N; \dot{q}_1 \dots \dot{q}_N; \ddot{q}_1 \dots \ddot{q}_{i-1}, \ddot{q}_{i+1} \dots \ddot{q}_N), \quad (1)$$

where $H'(q_1 \dots q_N)$ is the moment of inertia of the kinematic circuit of the actuating member with load with respect to the considered degrees of freedom, $h(q_1 \dots q_N)$ is a term determined by the effect of gravitational, Coriolis and centrifugal forces, and also by the components of forces of inertia, which were not included in the first term, $q_1 \dots q_N$ are generalized coordinates of the kinematic circuit of the actuating member, $a_H(t) = q_i$, i is the number of the considered degree of freedom, and N is the number of degrees of freedom of the manipulator.

Let us consider a two-way system, the actuating elements of which are DC motors with independent excitation. The dynamics of these motors in the direction of the operator and load, respectively, is described by the following differential equations:

$$\begin{aligned} u_1(t) &= (R_1 + L_1 p) i_{\alpha 1}(t) + K_{\omega 1} i_1 \dot{a}_{\alpha 1}(t), \\ M_{\Delta B 1}(t) &= K_{M 1} i_{\alpha 1}(t) = J_1 i_1 \ddot{a}_{\alpha 1}(t) + M_{\tau 1}(\dot{a}_{\alpha 1}) - M_{\alpha 1}(t)/i_1; \end{aligned} \quad (2)$$

$$\begin{aligned} u_2(t) &= (R_2 + L_2 p) i_{\alpha 2}(t) + K_{\omega 2} i_2 \dot{a}_H(t), \\ M_{\Delta B 2}(t) &= K_{M 2} i_{\alpha 2}(t) = J_2 i_2 \ddot{a}_H(t) + M_{\tau 2}(\dot{a}_H) + Q/i_2, \end{aligned} \quad (3)$$

where R_1 and R_2 are the effective resistance of the armature circuits of the motors, L_1 and L_2 are the inductance of the armature circuits, $K_{M 1}$ and $K_{M 2}$ are the torque factors, $K_{\omega 1}$ and $K_{\omega 2}$ are the coefficients of the counter, emf, J_1 and J_2 are the moments of inertia of the rotors of the motors, of the rotating parts of the kinematic gears and of the corresponding links, i_1 and i_2 are the gear ratios of the reduction gears, $M_{\tau 1}(\dot{a}_{\alpha 1})$, $M_{\tau 2}(\dot{a}_H)$ are the dry friction moments, $u_1(t)$ and $u_2(t)$ are the control voltages, $i_{\alpha 1}(t)$, and $i_{\alpha 2}(t)$ are the currents of the motor armatures, $M_{\Delta B 1}(t)$ and $M_{\Delta B 2}(t)$ are the moments developed by the

motors, $a_{on}(t)$ and $a_H(t)$ are the coordinates of the operator and load shafts, $M_{on}(t)$ is a moment developed by the operator and p is a differentiation symbol.

According to the methods suggested in [1], let us assume that a_{on} , \dot{a}_{on} , \ddot{a}_{on} and \dddot{a}_{on} are independent input variables in the mode of induced motion of the operator shaft of the two-way system. Taking this into account and also taking into account relations (1)-(3), one can describe the dynamics of the two-way system in the mentioned mode with respect to phase coordinates (FK) $x_1 = a_H(t)$, $x_2 = \dot{a}_H(t)$, $x_3 = a_{on}(t)$, $x_4 = M_{on}(t)$ by the following system of differential equations:

$$\left. \begin{aligned} \dot{x}_1 &= x_2, \\ \dot{x}_2 &= x_3, \\ \dot{x}_3 &= -\frac{K_{M2}K_{\omega 2}}{L_2(J_2+H)}x_2 - \frac{R_2(J_2+H)+L_2\dot{H}}{L_2(J_2+H)} + \frac{K_{M2}}{i_2L_2(J_2+H)}u_2 - \\ &\quad - \frac{R_2/L_2+p}{i_2(J_2+H)}M_{r2} - \frac{R_2/L_2-p}{i_2^2(J_2+H)}\hat{h}, \\ \dot{x}_4 &= -\frac{R_1}{L_1}x_4 - i_1\frac{K_{M1}}{L_1}u_1 + i_1^2\frac{K_{M1}K_{\omega 1}}{L_1}\dot{x}_{on} + i_1^2J_1\frac{R_1}{L_1}\ddot{x}_{on} + \\ &\quad + i_1^2J_1\ddot{a}_{on} + i_1(R_1/L_1+p)M_{r1}, \end{aligned} \right\} \quad (4)$$

where $H' = H'/i_2^2$.

Since the load shaft of the two-way system should accurately reproduce all motions of the operator shaft, the desired values for phase coordinates x_1 , x_2 , and x_3 are given in the following manner: $x_1^* = a_{on}(t)$, $x_2^* = \dot{a}_{on}(t)$, $x_3^* = \ddot{a}_{on}(t)$. When giving the desired value for x_4 , one should proceed from the fact that the operator should sense the moment Q_0 , which is determined only by the object of manipulation. Therefore, let us assume that $x_4^* = nQ_0 = n[J_0\ddot{a}_H(t) + \tilde{h}_0]$, where $Q_0 = Q - Q_M$, Q_M is a component of moment Q , determined by the parameters of the links of the actuating member, J_0 and \tilde{h}_0 are the components of elements H' and \tilde{h} , respectively, determined by the parameters of the manipulation object, and n is a scaling factor.

Since $q_i = \alpha_H$, $\dot{q}_i = \dot{\alpha}_H$, then $\tilde{h} = \tilde{h}(\alpha_H, \dot{\alpha}_H)$. Assuming that the two-way system operates sufficiently accurately, i.e., variables α_H and $\dot{\alpha}_H$ hardly differ from α_{on} and $\dot{\alpha}_{on}$, respectively, function $\tilde{h}(\alpha_H, \dot{\alpha}_H)$ can be expanded into a Taylor series [3]

$$\begin{aligned}\tilde{h}(\alpha_H, \dot{\alpha}_H) &= h(\alpha_{on}, \dot{\alpha}_{on})(\alpha_H - \alpha_{on}) + \lambda(\alpha_{on}, \dot{\alpha}_{on})(\dot{\alpha}_H - \dot{\alpha}_{on}) + G = \\ &= h(\alpha_{on}, \dot{\alpha}_{on})\varepsilon_2 + \lambda(\alpha_{on}, \dot{\alpha}_{on})\varepsilon_1 + G,\end{aligned}\quad (5)$$

where

$$\begin{aligned}h(\alpha_{on}, \dot{\alpha}_{on}) &= \frac{\partial \tilde{h}}{\partial \alpha_H} \Big|_{\alpha_H = \alpha_{on}, \dot{\alpha}_H = \dot{\alpha}_{on}}, \quad \lambda(\alpha_{on}, \dot{\alpha}_{on}) = \frac{\partial \tilde{h}}{\partial \dot{\alpha}_H} \Big|_{\alpha_H = \alpha_{on}, \dot{\alpha}_H = \dot{\alpha}_{on}}, \\ G &= \tilde{h}(\alpha_H, \dot{\alpha}_H) - h(\alpha_{on}, \dot{\alpha}_{on})\varepsilon_2 - \lambda(\alpha_{on}, \dot{\alpha}_{on})\varepsilon_1.\end{aligned}$$

the term $h_0(\alpha_H, \dot{\alpha}_H)$ can also be expanded into components similar to (5):

$$\tilde{h}_0(\alpha_H, \dot{\alpha}_H) = h_0(\alpha_{on}, \dot{\alpha}_{on})\varepsilon_2 + \lambda_0(\alpha_{on}, \dot{\alpha}_{on})\varepsilon_1 + G_0, \quad (6)$$

where

$$\begin{aligned}h_0(\alpha_{on}, \dot{\alpha}_{on}) &= \frac{\partial \tilde{h}_0}{\partial \alpha_H} \Big|_{\alpha_H = \alpha_{on}, \dot{\alpha}_H = \dot{\alpha}_{on}}, \quad \lambda_0(\alpha_{on}, \dot{\alpha}_{on}) = \frac{\partial \tilde{h}_0}{\partial \dot{\alpha}_H} \Big|_{\alpha_H = \alpha_{on}, \dot{\alpha}_H = \dot{\alpha}_{on}}, \\ G_0 &= \tilde{h}_0(\alpha_H, \dot{\alpha}_H) - h_0(\alpha_{on}, \dot{\alpha}_{on})\varepsilon_2 - \lambda_0(\alpha_{on}, \dot{\alpha}_{on})\varepsilon_1.\end{aligned}$$

System (4), written with respect to errors of the phase coordinates, assumes the following form with regard to the type of desired values of the phase coordinates and expressions (5) and (6):

$$\left. \begin{aligned}\varepsilon_1 &= a_{12}\varepsilon_2, \\ \varepsilon_2 &= a_{23}\varepsilon_3, \\ \varepsilon_3 &= a_{31}\varepsilon_1 + a_{32}\varepsilon_2 + a_{33}\varepsilon_3 + b_{32}u_2 + f_3 + \omega_3, \\ \varepsilon_4 &= a_{41}\varepsilon_1 + a_{42}\varepsilon_2 + a_{43}\varepsilon_3 + a_{44}\varepsilon_4 + b_{41}u_1 + b_{42}u_2 + f_4 + \omega_4,\end{aligned}\right\} \quad (7)$$

where

$$\begin{aligned}
 a_{12} = a_{23} &= 1, \quad a_{31} = -\frac{R_2 \lambda + L_2 \dot{\lambda}}{i_2^2 L_2 (J_2 + H)}, \quad a_{32} = -\frac{K_{M2} K_{\omega 2} + [R_2 h + L_2 (\dot{h} + \dot{\lambda})]/i_2^2}{L_2 (J_2 - H)}, \\
 a_{33} &= -\left(\frac{R_2}{L_2} + \frac{\dot{H} + h/i_2^2}{J_2 + H}\right), \quad a_{41} = -n \left(J_0 a_{31} + \frac{R_1}{L_1} \lambda_0 + \dot{\lambda}_0\right), \\
 a_{42} &= -n \left(J_0 a_{32} + \frac{R_1}{L_1} h_0 - \dot{h}_0 + \dot{\lambda}_0\right), \quad a_{43} = -n \left[J_0 \left(a_{33} + \frac{R_1}{L_1}\right) + \dot{J}_0 + h_0\right], \\
 a_{44} &= -\frac{R_1}{L_1}, \quad b_{32} = \frac{K_{M2}}{i_2^2 L_2 (J_2 + H)}, \quad b_{41} = -\frac{i_1 K_{M1}}{L_1}, \quad b_{42} = -n J_0 b_{32}, \\
 f_3 &= g_{32} M_{12}, \quad f_4 = g_{42} M_{12}, \quad g_{32} = -\frac{R_2/L_2 + p}{i_2^2 (J_2 + H)}, \quad g_{42} = -n J_0 g_{32}, \\
 \omega_3 &= d_{31} \ddot{a}_{on} + d_{32} \ddot{a}_{on} + d_{33} \ddot{a}_{on} + m_{31} G + m_{32} \dot{G}, \\
 d_{31} &= -\frac{K_{M2} K_{\omega 2}}{L_2 (J_2 + H)}, \quad d_{32} = -\left(\frac{R_2}{L_2} + \frac{\dot{H}}{J_2 + H}\right), \quad d_{33} = -1, \\
 m_{31} &= -\frac{R_2/L_2}{i_2^2 (J_2 - H)}, \quad m_{32} = -\frac{1}{i_2^2 (J_2 - H)}, \\
 \omega_4 &= d_{41} \ddot{a}_{on} + d_{42} \ddot{a}_{on} + d_{43} \ddot{a}_{on} + d_{44} M_{11} + m_{41} G + m_{42} \dot{G} + m_{43} G_0 + m_{44} \dot{G}_0, \\
 d_{41} &= i_1^2 \frac{K_{M1} K_{\omega 1}}{L_1} - n J_0 d_{31}, \quad d_{42} = i_1^2 \frac{R_1}{L_1} J_1 - n \left[J_0 \left(d_{32} + \frac{R_1}{L_1}\right) + \dot{J}_0\right], \\
 d_{43} &= i_1^2 J_1, \quad d_{44} = i_1 (R_1/L_1 + p), \quad m_{41} = -n J_0 m_{31}, \quad m_{42} = n J_0 m_{32}, \\
 m_{43} &= -n R_1/L_1, \quad m_{44} = -n.
 \end{aligned}$$

It is obvious that system (7) is nonstationary, since parameters H , J_0 , h , h_0 , λ , λ_0 , \dot{H} , \dot{J}_0 , \dot{h} , \dot{h}_0 , $\dot{\lambda}$, $\dot{\lambda}_0$ are essentially variables.

Let us assume that the rates of variation of these parameters are much less than the rates of the transient processes in the system, i.e., let us assume that the parameters of the two-way system are quasi-steady, and the coefficients of the equations of system (7) then remain constant at small time intervals. In this case, system (7) will have the following form in vector form at each of the indicated intervals from the entire time range of operation of the two-way system:

$$\dot{E}(t) = AE(t) + BU(t) + f(E) + W(q, \dot{q}, \ddot{q}), \quad E(t_0) = X(t_0) - X^*(t_0), \quad (8)$$

here $E(t) = X(t) - X^*(t)$, $E(t) \in \mathbb{R}^4$ is a vector of the errors of the phase coordinates, $X(t) \in \mathbb{R}^4$ is a vector of the phase coordinates of the system, $X^*(t) \in \mathbb{R}^4$ is the vector of the desired values, $U(t) \in \mathbb{R}^2$ is a vector of the control actions, $B \in \mathbb{R}^{4 \times 2}$ is a matrix of the amplification

factors during control actions, $A \in R^{4 \times 4}$ is a matrix of the dynamic properties of the two-way system, $f(E) \in R^4$ is a nonlinear vector function, and $W(q, \dot{q}, \ddot{q}) \in R^4$ is a vector of external effects.

Let us assume that matrices A and B vary discretely upon transition from one time interval to another.

One can use the method proposed in [4] to design a regulator of a two-way system on any of the indicated time intervals in view of the steady nature of the parameters of equation (8). According to this method, quasi-optimal control for stationary system (8), which minimizes the quadratic criterion of quality, is

$$J = 0.5 \int_{t_0}^{t_1} [E^\top(t) \Phi E(t) + U^\top(t) \Psi U(t)] dt,$$

t_0 and t_1 are the initial and final integration time, Φ is a positive semidefinite matrix, and Ψ is a positive definite matrix

$$U(t) = -D^\top E(t) - D^H f(E) - D^B W, \quad (9)$$

where $D^\top = \Psi^{-1} B^\top K$, $D^H = D^B = -\Psi^{-1} B^\top (A^\top - KB\Psi^{-1}B^\top)K$.

Matrix K is determined from a Riccati equation

$$KA + A^\top K - KB\Psi^{-1}B^\top K + \Phi = 0.$$

In scalar form, equation (9) can be rewritten in the form

$$\begin{aligned} u_l &= K_{l1}\delta_a + K_{l2}\dot{a}_H + K_{l3}\ddot{a}_{on} + K_{l4}\ddot{a}_H + K_{l5}\ddot{a}_{on} + K_{l6}\delta_m + \\ &+ K_{l7}\ddot{h} + K_{l8}\ddot{\dot{h}} + K_{l9}\ddot{\dot{h}}_0 + K_{l10}\ddot{\dot{h}}_0 + K_{l11}\operatorname{sgn} \dot{a}_H + K_{l12}\operatorname{sgn} \ddot{a}_{on} + K_{l13}\ddot{\dot{a}}_{on}, \end{aligned} \quad (10)$$

where $\delta_a = -\varepsilon_1 = a_{on} - a_H$; $\delta_m = \varepsilon_4 = M_{on} - nQ_0$,

$$\begin{aligned} K_{l1} &= D_{l1}^\top + D_{l3}^H(m_{31}\lambda + m_{32}\dot{\lambda}) + D_{l4}^H(m_{41}\lambda + m_{42}\dot{\lambda} + m_{43}\dot{\lambda}_0 + m_{44}\dot{\lambda}_0); \\ K_{l2} &= -D_{l2}^\top + D_{l3}^H[m_{31}h + m_{32}(h + \dot{\lambda})] + D_{l4}^H[m_{41}h + m_{42}(h + \dot{\lambda}) + \\ &+ m_{43}h_0 + m_{44}(h_0 + \lambda_0)], \quad K_{l3} = -K_{l2} - D_{l3}^H d_{31} - D_{l4}^H d_{41}, \\ K_{l4} &= -D_{l3}^\top + D_{l3}^H m_{32}h + D_{l4}^H(m_{42}h + m_{44}h_0), \quad K_{l5} = -K_{l4} - D_{l3}^H d_{32} - D_{l4}^H d_{42}, \\ K_{l6} &= -D_{l4}^\top, \quad K_{l7} = -D_{l3}^H m_{31} - D_{l4}^H m_{41}, \quad K_{l8} = -D_{l3}^H m_{32} - D_{l4}^H m_{42}, \end{aligned}$$

$$K_{l9} = -D_{i4}^H m_{43}, \quad K_{l10} = -D_{i4}^H m_{44}, \quad K_{l11} = (-D_{i3}^H g_{32} - D_{i4}^H g_{42}) M'_{T2},$$

$$K_{l12} = -D_{i4}^H d_{44} M'_{T1}, \quad K_{l13} = -D_{i3}^H d_{33} - D_{i4}^H d_{44},$$

M'_{T1} and M'_{T2} are the steady frictional moments of motion, and $l = 1, 2$.

When realizing equation (10), the terms containing differentiation in g_{32} , g_{42} , and d_{44} can be disregarded, since they have no influence on the dynamic properties of the two-way system after the beginning of motion of the system [4]. Moreover, terms proportional to $\ddot{\alpha}_{on}$ must be disregarded, since the value of $\ddot{\alpha}_{on}$ can not be measured for use in control.

Having designed a stationary regulator for each of the considered time intervals of operation of the two-way system, knowing the corresponding intervals of the values of the variable parameters, one can calculate

the dependence of coefficient K_{lm} ($l = 1, 2, m = \overline{1, 13}$) of the regulator of a two-way system on these variable parameters. The functions described in this manner are written to the computer memory and are then used to organize adjustment of coefficient K_{lm} of the regulator of the self-adjusting two-way system as a function of the current values of the indicated variable parameters of the manipulator.

However, it is rather complicated to design and then to realize a self-adjusting two-way system with a large number of variable parameters, by which K_{lm} should be adjusted. All the enumerated parameters are functions of the generalized coordinates of the actuating member q_j , of their derivatives \dot{q}_j , \ddot{q}_j (j is the number of the degree of freedom, $j = \overline{1, N}$, $j \neq i$) and of the mass of the object of manipulation m_0 . Therefore, the dependence of coefficients K_{lm} of the synthesized regulator of a two-way system on the earlier indicated 12 variables can be transformed as a function of coordinates q_j , \dot{q}_j , \ddot{q}_j and m_0 . If only three transferable degrees of freedom, which mainly determine variation of the load parameters of the two-way system [5], are taken into account, the values of K_{lm} will be dependent on a maximum of 7 variable parameters rather than on 12, since $j = \overline{1, 3}$, $j \neq i$. Since the mass m_0 during operation of a copying manipulator ordinarily remains fixed, after calculation of it, for example, by the relations found in [6] on the initial step of motion of the manipulator, continuous adjustment of the amplification factors K_{lm} to functions of only six variables q_j , \dot{q}_j , and \ddot{q}_j is required.

Studies of the effectiveness of the proposed approach were conducted on the example of a two-way system of the first degree of freedom of a copying manipulator, the kinematic layout of the actuating member of which is presented in Figure 1. The considered actuating member has the following parameters: lengths of links $l_1 = l_2 = 0.5$ m, mass of links $m_1 = 10$ kg and $m_2 = 5$ kg, moments of inertia of the links with respect to the axes of the joints $J_1 = 0.85 \text{ kg}\cdot\text{m}^2$, $J_2 = 0.42 \text{ kg}\cdot\text{m}^2$, and $m_0 = 1 \text{ kg}$. The numerical values of the parameters of the fixed part of the two-way system are presented in the table.

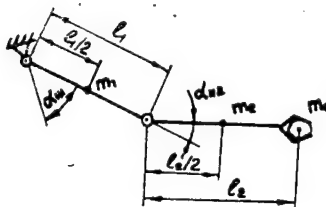


Figure 1

i	$K_{st,i}$ $\text{N}\cdot\text{m}/\text{A}$	$K_{\omega i}$ $\text{V}\cdot\text{s}$	J_i $\text{kg}\cdot\text{m}^2$	R_i , Ohm	L_i , H	i_i	M'_{Ti} , $\text{N}\cdot\text{m}$	n
1	$1,13 \cdot 10^{-2}$	$1,13 \cdot 10^{-2}$	$8,96 \cdot 10^{-6}$	3,8	$7,6 \cdot 10^{-2}$	180	$2 \cdot 10^{-3}$	0,2
2	$1,59 \cdot 10^{-2}$	$1,59 \cdot 10^{-2}$	$4,05 \cdot 10^{-5}$	0,0	$1,8 \cdot 10^{-2}$	150	$2 \cdot 10^{-2}$	

The mode of stimulated motion of the operator shaft of the first degree of freedom according to the law $a_{on}=1(t)/(0,167p+1)^3$ at different modes of motion of the second degree of freedom of the copying manipulator was considered during studies of a two-way system. Curves, corresponding to variation of the angle of rotation of the second degree of freedom by the law $a_{H2}=1,5[1+\sin(\pi t+\pi/2)]$, are presented in Figure 2, while curves corresponding to variation of the angle of rotation by the law $a_{H2}=1,5[1+\sin(\pi t-\pi/2)]$ are presented in Figure 3. The number 1 denotes curves for the case when a self-adjusting two-way system is accomplished only by the variable inertial parameters similar to [1]. The centrifugal and Coriolis forces during shaping of the control signal (control law) were disregarded. The curves denoted by the number 2 correspond to the case when the parameters of the regulator of the two-way system are adjusted as a function of variation of all the load

parameters (with regard to the moments of high-speed forces) according to the approach considered in this paper.

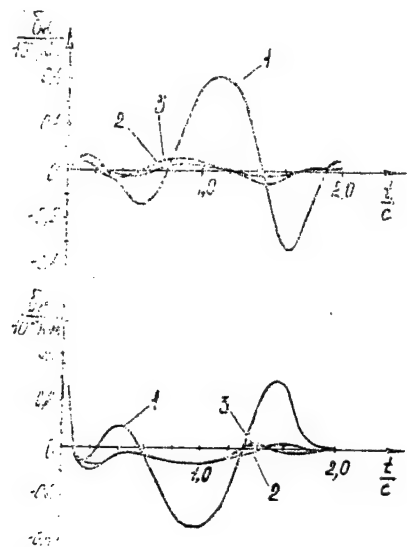


Figure 2

Analysis of the graphs presented in Figures 2 and 3 permits one to conclude that the method of synthesis and design of a self-adjusting two-way system, proposed in this paper and that takes into account the total dynamics of the actuating member of the copying manipulator, provides a significant improvement of the quality of operation of the system with significant and rapid variation of all the load parameters. However, the synthesized regulators are rather complex to realize and practice. Therefore, one can attempt to simplify self-adjusting regulators without significant deterioration of the quality of the main operating modes of two-way systems.

The results of the studies showed that parameters \tilde{h} and \tilde{h}_0 can be disregarded during formation of control law (10) at speeds of motion of the working member of the manipulator up to $5 \text{ m} \cdot \text{s}$. Moreover, coefficients K_{1m} can be adjusted only by the values of H and J_0 , but \tilde{h} and \tilde{h}_0 must be included in control law (10). The errors of the synthesized two-way system are denoted by the number 3 upon introduction of the indicated simplifications in Figures 2 and 3. It is obvious from these figures that curves 3 hardly differ from curves 2 for the considered operating modes, which correspond to a two-way system with accurate and complete self-adjustment for all variable load parameters.

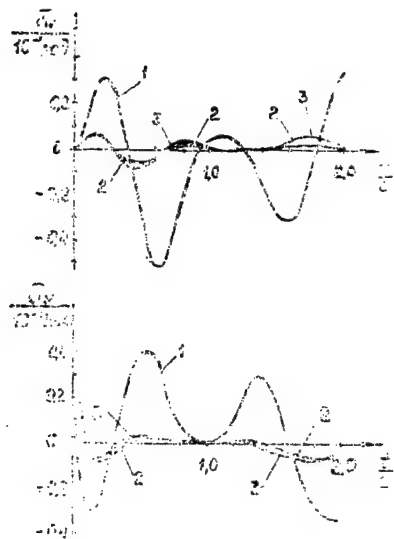


Figure 3

Of course, introduction of the indicated simplifications does not guarantee high-quality operation of two-way systems in all operating modes of copying manipulators; therefore, the efficiency must be checked at all possible motions of the actuating member when using the simplified regulator. However, studies and analysis of curves 2 and 3 permit one to hope that the coefficients of the regulator can sometimes be adjusted by only two parameters H and J_0 . This considerably simplifies practical realization of self-adjusting two-way systems without significant deterioration of the indicators of its operating quality.

Bibliography

1. Filaretov, V. F., Polyanskiy, A. F. "Self-Adjusting Two-Way System of Copying Manipulator With Active Reflection of Force," IZVESTIYA VUZOV SSSR. PRIBOROSTROYENIYE, No 1, 1989.
2. Dovbnya, N. M., Novachenko, S. I. "Methods of Designing Robot Control Systems by the Criterion of Dynamic Accuracy," "Upravleniye robotekhnicheskimi sistemami i ikh ochuvstvleniye" [Control of Robotic Systems and Sensitization of Them], Moscow, Izdatelstvo "Nauka", 1983.
3. Besekerskiy, V. A., Popov, Ye. P. "Teoriya sistem avtomaticheskogo upravleniya" [The Theory of Automatic Control Systems], Moscow, Izdatelstvo "Nauka", 1975.

4. Popov, Ye. P., Vereshchagin, A. F., Filaretov, V. F. "Design of Quasi-Optimal Nonlinear Reversible Manipulator Control System," IZVESTIYA AKADEMII NAUK SSSR. SERIYA TEKHNICHESKAYA KIBERNETIKA, No 4, 1975.

5. Vukobratovich, M., Stokich, D., Kurchanski, N. "Neadaptivnoye i adaptivnoye upravleniye manipulyatsionnymi robotami" [Nonadaptive and Adaptive Control of Manipulation Robots], Moscow, Izdatelstvo "Mir", 1989.

6. Filaretov, V. F., Polyanskiy, A. F. "Automation of Static Relief of Actuating Members of Manipulation Robots," IZVESTIYA VUZOV SSSR. MASHINOSTROYENIYE, No 11, 1985.

COPYRIGHT: "IZVESTIYA VUZOV SSSR - PRIBOROSTROYENIYE", 1990

UDC 621.865.8.005:681.586

EXPERIMENTAL ADAPTIVE ROBOTIC COMPLEX

917F0203A Leningrad IZVESTIYA VYSSHIKH UCHEBNYKH ZAVEDENIY:
PRIBOROSTROYENIYE in Russian No 10, 1990 (manuscript received 28 Feb 90)
pp 40-44

[Article by S. A. Vorotnikov, A. Yu. Korneyev, S. V. Runkov et al.,
Moscow State Technical University imeni N. E. Bauman]

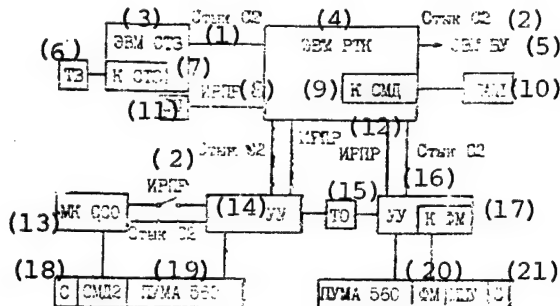
[Text] An adaptive robotic complex with robotic vision and force-moment sensitization systems has been developed for theoretical and experimental studies of the problems of using sensory information in control of industrial robots.

Modern experience of practical use of industrial robots (PR) showed the need to develop robotic complexes (RTK), oriented toward fulfillment of specific manufacturing operations and built into the hierarchical structure of the management system of a flexible automated plant. Special attention is devoted to giving these complexes adaptive properties to reduce expenditures for organization of the working environment and to readjust the manufacturing equipment.

A number of problems such as interaction of the robotic complex with the upper level control system, synchronization of simultaneous operation of several robots, processing and utilization of various sensory information for control of robots, depiction of the operating environment in the form of a model of the external world, planning the motions of robots with regard to variations of this model, teaching robots and so on must be solved in development of adaptive robotic complexes. An experimental adaptive robotic complex was developed to conduct theoretical and experimental studies in this field. The complex is oriented toward completion of mechanical assembly operations, machining, painting and soldering. The work is being conducted in several directions. The basic direction is related to development of the algorithms and software of robots, sensory systems and the control computer of the robotic complex. Much attention is devoted to design of multicomponent force-moment sensors and of passive centering devices for assembly of mechanical connections.

The developed robotic complex includes: a control computer, two industrial robots of type RM-01 (PUMA 560), television and photoarray robotic vision systems, two force-moment sensitization systems, a number of passive centering devices and a lighting system. When studying individual manufacturing operations, the robotic complex is delivered with additional fittings and tools.

The central part of the developed robotic complex is an Elektronika 15 VUMS-28 computer. Connection between separate subsystems of the complex is provided by using a serial interface of the Styk S2 type and a parallel interface of the IRPR type (see figure). The software of the robotic complex supports the following main functions: coordination of the joint operation of two manipulators, synchronization of the operation of individual subsystems, compilation of industrial robot control programs in ARPS language, and loading of them into the industrial robot controller (UU) Sfera-36, and transfer of data files and control commands of subsystems.



Block Diagram of Experimental Adaptive Robotic Complex:
 UU--Sfera-36 controller of RM-01 industrial robot;
 TV--television camera; K STZ--robotic vision system
 controller; FM--photomaster camera; K FM--photomaster
 controller; SMD1--force-moment sensor in base of assembly
 table; SMD2--force-moment sensor in wrist of industrial
 robot; KSMD--force-moment sensor controller; MK SSO--
 force-moment sensitization system microprocessor controller;
 MTsU--mechanical centering device; S--industrial robot grab;
 SO--lighting system; TO--manufacturing equipment; EVM VU--
 upper-level control computer

(Key on following page)

KEY:

- | | |
|-------------------------------------|---|
| 1. Styk S2 interface | 11. Lighting system |
| 2. Styk S2 interface | 12. IRPR interface |
| 3. Robotic vision system computer | 13. Force-moment sensitization system microprocessor controller |
| 4. Robotic complex computer | 14. Sfera-36 controller |
| 5. Upper-level control computer | 15. Manufacturing equipment |
| 6. Television camera | 16. Controller |
| 7. Robotic vision system controller | 17. Photopattern controller |
| 8. IRPR interface | 18. Industrial robot grab |
| 9. Force-moment sensor controller | 19. PUMA 560 industrial robot |
| 10. Force-moment sensor | 20. Photopattern |
| | 21. Mechanical centering device |

The complex is controlled through special commands, written in a separate file or introduced by the operator from the keyboard of the robotic complex computer in the form of symbolic lines. The commands are executed in the interpretation mode. Studies are now under way to develop a robotic complex control language.

Robotic vision systems (STZ). Two robotic vision systems are used in the developed robotic complex: a television and photopattern system. The television robotic vision system is designed to identify parts, to determine their position and orientation, and also for visual inspection of products. It includes a fixed television camera with standard television signal, an Elektronika NMS-1201.02 microcomputer, and an interface module for the computer to communicate with the camera. The interface module enters a frame of the image measuring 256×256 elements and writes it to the computer RAM in a format of 1 bit/element. The image is converted to the binary system according to a program-assigned threshold having 64 levels.

The photopattern camera is mounted on the industrial robot grab and is used to organize the external feedback according to the position of the grab with respect to the object. The pointing function is realized for a given moment. Besides a camera, the photopattern robotic vision system includes a photopattern controller with integration module with the Q-bus of the Sfera-36 controller. An image frame measuring 32×32 elements with 64 levels of brightness is written to the RAM of the controller.

The robotic vision system is programmed to perform a specific operation using tool software (PO). The latter consists of universal and specialized devices and functions under control of the RAFOS operating system.

The specialized part, which is the core of the image processing software in the robotic vision system of an assembly robotic complex, includes image analysis and synthesis systems, functioning modes of the robotic

vision system and communication modes. The basis of each system is a set of libraries that guarantee development and study of visual analysis procedures, and also creation of applications software. The analysis system includes image shaping libraries (formed by image input and output modules), description libraries (modules for construction of models, initialization of data structures, analysis of connectedness, description of components, formation of a list and image of the model) and image interpretation. The image synthesis library includes input, primitive, filling and image modules; the communication libraries including loading, dialogue and systems subroutine modules; and the teaching libraries include mode, statistics and image modules.

The program modules of the libraries process the images, shaped by both television and photopattern cameras. The operating mode of the modules is determined by the values of the parameters assigned during generation of the robotic vision system software.

To implement the functions of the robotic vision system, the image to be analyzed is represented in the form of an oriented root tree of components, i.e., of image domains, corresponding to individual parts or fragments of them. Each vertex of the tree representing a component is characterized by a set of parameters that determine the absolute and relative position and orientation of the component and that guarantees identification of it. The "encompassing-embedded component" ratios are given between the vertices of the tree. The image is described within some window of rectangular or arbitrary shape, and the position and dimensions of the window are assigned earlier when teaching the system or are determined directly during the manufacturing process.

The developed a priori glossary of component parameters includes those calculated on the set of component elements, contour elements and local characteristics, and also a number of relative values, and permits one to describe objects of different shape. The developed algorithms permit one to use various types of representation of contours and is adapted to the shape of the objects, which results in an increase of the speed of the system. The algorithms for analysis of the connectedness and description of components, used in the system, guarantee processing of images of scenes of the assembly processes in real time (1-3 s).

The main restrictions imposed on the composition of the software of industrial robotic vision systems are the low main memory capacity of the computer and the need to solve problems in real time with regard to the characteristics of the manufacturing process.

To automate the process of developing the robotic vision system software, it is suggested that a hierarchical system be used, the task of which includes a flexible interface with operator, information support of the decision search process, evaluation of the software as a whole and evaluation of individual modules according to the used criteria, storage and generalization of the operator's action and a number of auxiliary functions. Each program module is evaluated by the

quantitative and qualitative parameters such as processing time, capacity of the memory occupied, degree of universality, quality of processing and so on. It is suggested that expert analyses be used with regard to the possibility of total formalization of parameters.

Linguistic variables (LP), designed on the basis of odd set theory, are considered for design of a system of expert evaluations. A context-free grammar of linguistic variables is worked out, which is a group of four

$$G = \langle N, T(N), U, S \rangle,$$

where N is the number of the linguistic variable, $T(N)$ is the term or term-set of the values of the linguistic variable, U is the set of values of the basic variable, and S is the syntactical rule for formation of the linguistic variable.

The characteristic feature of the introduced grammar includes the universality of the image of both even and interval values and of qualitative estimates.

The criterion of the usefulness of the module within the robotic vision system software is an unevenly suspended discriminant function

$$NEC = \sum_{i=1}^k \omega_i e_i,$$

where ω_i is the coefficient of preference of the i -th parameter and e_i is expert analysis of the i -th parameter. As a result, the corresponding values of the preference factors were found for different types of robotic vision systems. Variants of the configuration of the robotic vision system software were selected and they were generated after ranking of the available program modules by the value of the utility factor.

Force-moment sensitization systems (SSO). The experimental robotic complex includes two force-moment sensitization systems. The sensor of the first system is located in the base of the assembly table and is used to measure the components of the main force and moment vector, occurring upon assembly of the unit, mounted on the table. Force-moment information is introduced and processed in the robotic complex computer and is used to check the assembly process and to control the robots.

The second system is made in the form of a separate design, located between the last link of the industrial robot and its grab. The controller built into the housing of the sensor guarantees input, processing and transmission of the force-moment information in the Sfera-36 controller for organization of external force feedback. The

1816 VE48 single-chip microcomputer with ROM having capacity of 4 kbytes is included in the controller, which permits implementation of specialized data processing programs. The indicated programs are designed to compensate for the temperature-time instability of the measuring circuits, to take into account the static components of forces and force moments, caused by the weight of the grab and tool, and also to present a system of forces from the center of measurement of the sensor to a point, connected to the end executive of the manipulator. Location of the controller inside the sensor housing permits one to use the concept "intelligent sensor," according to which force-moment information is processed autonomously. This frees to a considerable degree the computer resources of the control computer of the robot.

The force-moment sensors of both systems contain strain gage resistor sensitive elements and have diagonal stiffness matrices, which permits a level of cross-connections between channels in the range of 3-5 percent at speed of the force-moment sensitization system of not worse than 100 μ s.

Mechanical centering devices (MTsU). Along with force-moment sensitization devices, the experimental robotic complex includes passive force-moment adaptation devices, realized in the form of mechanical centering devices with remote stiffness center. The device is located in the wrists of the industrial robot and is designed to compensate for the mutual positioning errors of conjugate parts of the "shaft-bushing" type due to the effect of forces occurring during assembly. The presence of a remote stiffness center reduces the probability of jamming. The mechanical centering device is designed in the form of a combination of linear and angular pliancy modules, which permits one to provide small values of linear and angular stiffnesses simultaneously (up to 1,000 N/m and 6 N·m/rad), and, accordingly, to provide forces of interaction of parts at a significant distance of the stiffness center of the device (up to 200 mm) from its end flange. The high reliability of the device is achieved by using elastomeric structures of directed pliancy as the elastic elements, which are subjected to shearing and compression, and which do not experience tensile loads.

The utilized mechanical centering devices contain interchangeable modules, having different stiffness and geometric characteristics, which permits online adjustment of the robotic complex for assembly of other types of products.

COPYRIGHT: "IZVESTIYA VUZOV SSSR - PRIBOROSTROYENIYE", 1990

UDC 621.865.8

FORCE SENSITIZATION SYSTEM OF DEBURRING ROBOT

917F0203A Leningrad IZVESTIYA VYSSHIKH UCHEBNYKH ZAVEDENIY:
PRIBOROSTROYENIYE in Russian No 10, 1990 (manuscript received 28 Feb 90)
pp 45-49

[Article by A. Yu. Sumich, Moscow State Technical University imeni N. E. Bauman]

[Text] The operating characteristics of the force sensor of an industrial robot in a technological cleaning operation are considered. A mathematical model of the force sensor is presented, and the operating and working principles of individual functional modules of the force sensitization system are described.

Such technological operations as rough grinding, abrasive and milling cleaning can be combined into one group of operations of the "trimming" type. Regardless of the type of material to be machined, the characteristic features of this group of operations are the presence of random projection and use of a rotating milling tool, which determines the dynamics of interaction with the part to be machined. An abrasive disk or cutter is frequently used as the tool. Practical solutions are implemented slowly with the obvious importance of automating these human-hazardous technological operations, which is explained by the complexity of the technical task. We in the USSR already have several industrial robotic trimming robotic complexes, while industrial robots are used extensively in these operations abroad, judging by the publications and recent exhibitions. Power sensors are not yet used in trimming robotic complexes in the USSR. For example, thermosetting plastic parts are trimmed at the Elektrosila Association without a power adaptation; the trimming complexes manufactured by NPO [scientific production association] Granat are also not yet equipped with force sensors. The use of force feedback permits one to develop a trimming robot control system, having the highest machining performance, since the extent of the projection is indirectly estimated through measurement of the cutting forces, which permits one to regulate the rate of delivery of the tool along the contour of the part as a function of the real value of the projection. The use of adaptation according to the

cutting force also increases the safety of trimming and the quality of machining. A large number of designs of various force sensors for industrial robots are described in the Soviet and foreign literature [1, 2], but there are no descriptions of force sensitization systems (SSO) for trimming robots.

A force sensitization system has been developed and manufactured at MGTU [Moscow State Technical University] imeni N. E. Bauman, specially designed for trimming operations. The sensitization system has the following specifications:

Number of measured components (total force vector at any point of work zone of sensor)	3
Range of measured forces (for each component), N	±50
Accuracy by channels, percent	3, 5, 5
Maximum frequency of input signal, kHz	50

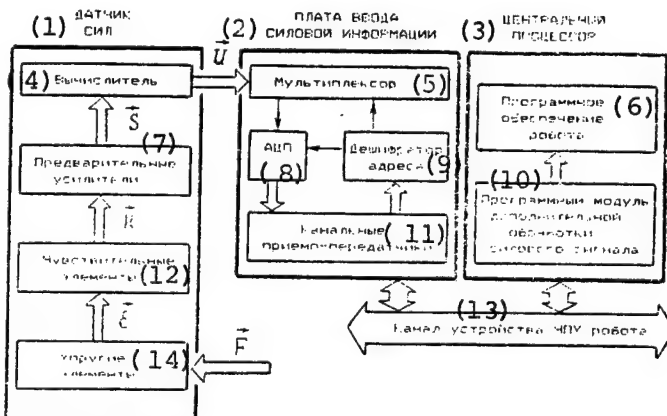
The specifics of the given force sensitization system includes the fact that the total cutting force vector in the region of contact of the tool and part can be measured at any point of the circumference of the tool. Since the force vector is measured at a specific spatial region (work zone) of the force sensor coordinate system rather than at a fixed point, no restrictions are imposed on the diameter of the tool, and the given force sensitization system can be used not only with small-diameter end mill cutters, but also with disk cutters, and with abrasive and diamond disks. During trimming, the contact zone of the tool and part can be shifted around the circumference of the tool and can significantly change its coordinates, which will not essentially affect the measurement of the force vector components.

A block diagram of the force sensitization system of a trimming robot is shown in the figure. According to this layout, several force sensitization systems have been manufactured at MGTU imeni N. E. Bauman for different types of robots. Let us consider in more detail a version of a force sensitization system for the RM-01 industrial robot with PUMA-NOKIA electromechanical actuating device. The force sensitization system consists of three functionally complete modules: a force sensor, a force data input card and a program module, which additionally processes the force signal.

The force sensor is a structurally complete product, included in the gap of the force circuit between the mounting flange of the robot and the working tool (a pneumatic turbine with cutter). The force sensor

measures the cutting force vector F , which occurs in the contact region of the tool and part, and emits in analog form three components of the cutting force in the coordinate system of the sensor. KF-5P foil strain gages with base of 2 mm and with rated resistance of 200 ohms are used as the sensitive elements. The principle of structural separation of force factors, similar to that presented in [3], is used in the considered sensor. But the force sensitization sensor, designed on the

basis of the sensor developed at MGTU imeni N. E. Bauman, also has new properties, manifested in measurement of forces exactly on trimming operations.



Block Diagram of Robot Force Sensitization System

KEY:

- | | |
|--------------------------------|--|
| 1. Force sensor | 9. Address decoder |
| 2. Force data input card | 10. Program module of additional force signal processing |
| 3. Central processor | 11. Channel transceivers |
| 4. Computer | 12. Sensitive elements |
| 5. Multiplexer | 13. Channel of robot NP device |
| 6. Robot software | 14. Flexible elements |
| 7. Preamplifiers | |
| 8. Analog-to-digital converter | |

The primary signal vector of the sensitive elements R, the dimension of which is determined by the selected number of measuring points, is introduced to analyze the conversion of data in the force sensor. Each

component of the vector R is an electric signal, taken from the measuring circuit of strain gages, glued to a specific region of the flexible element. The strain gages are ordinarily connected by the measuring bridge or semibridge layout, which affects only the level of the removed signal and does not affect the functional conversion of the signal; therefore, let us assume that a bridge or semibridge is one generalized sensitive element, which measures deformation at one point of the surface layer of the flexible element. Let us also introduce the

relative deformation vector E, the components of which are the relative deformations of the surface layers of flexible elements at the measuring point. With regard to the assumption that one generalized sensitive element measures deformation at one point of the surface layer of the

flexible element, let us take the dimension of vector \vec{E} , equal to that of vector \vec{R} . Vectors \vec{E} and \vec{R} can then be linked by the matrix of the transfer coefficients of sensitive elements B by the relation $\vec{R} = B\vec{E}$, where matrix B is a diagonal $B = \text{diag}[b_{11}, b_{22}, b_{33}, b_{44}, b_{55}, b_{66}]$, and its elements are constants, determined by the coefficients of the strain-sensitive strain gages, by their connection circuits, and also by the power supply voltage of the bridges. The sensor generally measures the total vector of force factors \vec{G} , consisting of the principal vector \vec{F} and of principle moment \vec{M} , reduced to the measuring center of the sensor:

$$\vec{G} = \begin{bmatrix} \vec{F} \\ \vec{M} \end{bmatrix}.$$

If the matrix of sensitivity of the flexible element of sensor A is introduced, the vector of relative deformation \vec{E} will be determined as $\vec{E} = A \cdot \vec{G}$.

One can assume for most trimming operations that the contact region of the tool and part is small and can be considered as a point. The main principle of the force sensor is that its measuring center is mobile and coincides with the contact point of the tool and part. The main moment of external forces is equal to zero with respect to this point and the

total vector of the external force factors \vec{G} , measured by the sensor, will consist only of the principal vector \vec{F} , i.e., its dimensionality will be equal to three. The dimensionality of the primary signal vector

of sensitive elements R and accordingly of the relative deformation

vector E in the sensor is equal to six, i.e., to the number of selected measuring points. This is determined by the need to measure, besides the three components of the force vector, three additional coordinates of the movable contact point of the tool and part. The sensitivity matrix of the flexible element of the sensor A is thus rectangular with dimensionality 6×3 . The primary signals of the sensitive elements are

amplified by the pre-amplifiers, i.e., vector R is transformed to signal vector $S = CR$, where C is the diagonal matrix of the force factors of

pre-amplifiers, and $C = \text{diag}[c_{11}, c_{22}, c_{33}, c_{44}, c_{55}, c_{66}]$. After the six-dimensional vector \vec{S} has been processed by the computer, a three-dimensional vector of the measured force $\vec{U} = \vec{DS}$ is found. Here D is a rectangular 3×6 matrix of the computer. Complete transformation of the data by the force sensor can be expressed by the relation $\vec{U} = \vec{HF}$, in which $H = DCBA$.

The considered sensor has a sensitivity matrix of the flexible element A

$$A = \begin{bmatrix} a_{11} & 0 & 0 \\ a_{21} & 0 & 0 \\ 0 & a_{32} & 0 \\ 0 & a_{42} & 0 \\ 0 & 0 & a_{53} \\ 0 & 0 & a_{63} \end{bmatrix} \quad (1)$$

and computer matrix D

$$D = \begin{bmatrix} d_{11} & d_{12} & 0 & 0 & 0 & 0 \\ 0 & 0 & d_{23} & d_{24} & 0 & 0 \\ 0 & 0 & 0 & 0 & d_{35} & d_{36} \end{bmatrix}. \quad (2)$$

Expressions (1) and (2) show an ideal type of matrices A and D , since realistically all the elements of the indicated matrices may not be zero matrices, which results in a mutual effect between the channels and an increase of the total measurement error. As the test results of the sensor showed, the measurement error with regard to the reciprocal influence of the channels does not exceed 5 percent in the temperature range of 15-30°C--this is sufficient to design an adaptive force control system of a trimming robot. The flexible element of the sensor is made of 40Cr steel, subjected to heat treatment, and consists of three assembly units, pinned during assembly. The flexible element can also be made a unit element, but this complicates the manufacture and subsequent gluing of the strain gages. The overall dimensions of the sensor ($60 \times 65 \times 80$) essentially do not limit the service angles of the actuating device. The developed design is technologically effective, but imposes high requirements on the accuracy of the production equipment and can be manufactured at any plant. The electronic part of the sensor consists of an additional internal stabilizer, pre-amplifiers, and a computer, realized on 153UD5 operational amplifiers.

The force data input card is made in the design of the Sfera-36 controller and is a specialized high-speed multichannel analog-to-digital converter. The input card is connected to the force sensor by a cable, through which power of ± 15 V is fed to the sensor and three analog signals, corresponding to the components of the measured cutting

force vector F , are received. As shown in the figure, the basis of the force data input card is an analog-to-digital converter, realized on a K1107PV1 integrated analog-to-digital converter. The high speed of the analog-to-digital converter and of the K590KN6 multiplexer guarantees switching of the required channel and subsequent analog-to-digital conversion within time less than $10 \mu s$, i.e., less than the maximum permissible delay of the "Response" signal of the passive device on the channel of the central processor. This permits one to do away with an internal data buffer, and the central processor immediately reads the code of the converted value from the analog-to-digital converter. The input card in the address space of the central processor has three addresses, and each address corresponds to its own channel (the component of the measured force vector). After decoding the address, the multiplexer switches the channel corresponding to this address and starts the analog-to-digital converter, which emits the received code to the data address bus through the channel receivers after completion of conversion.

Final processing of the force signal occurs in the program module for additional processing of the force signal (see figure), which solves the following tasks: it filters the low-frequency noise component, switches the force signal, compensates for the gravitational component of the force signal and determines the emergency situation. Commutation of the force signal guarantees that it will be disconnected for the time of completion of transport operations. Compensation of the gravitational component of the force signal eliminates the effect of the weight of the tool as a function of its orientation in space. The program module for additional processing of the force signal operates under control of modified ARPS language of the RM-01 robot.

The tests of the developed force sensitization completely confirmed the operating principles, embedded in all its functional modules. A set of technical documentation, which permits duplication of it for use in trimming complexes based on the RM-01 robot, has been developed for the sensitization system.

Bibliography

1. "Sistemy ochuvstvleniya i adaptivnyye promyshlennyye roboty" [Sensitization Systems and Adaptive Industrial Robots], edited by Ye. P. Popov and V. V. Klyuyev, Moscow, Izdatelstvo "Mashinostroyeniye", 1985.

2. Shneyder, A. Yu. "Silomomentnyye datchiki dlya robototekhnicheskikh sistem" [Force-Moment Sensors for Robotic Systems], Moscow, 1984 (Preprint Instituta problemy peredachi informatsii akademii nauk SSSR).

3. Wang, S. S. M., Will, P. M. "Sensors for Computer Controlled Mechanical Assembly," INDUSTRIAL ROBOT, Vol 5, No 1, 1978.

COPYRIGHT: "IZVESTIYA VUZOV SSSR - PRIBOROSTROYENIYE", 1990

UDC 62-50.531.3

RECOGNITION SYSTEM OF INDUSTRIAL ROBOTS

917F0203A Leningrad IZVESTIYA VYSSHIKH UCHEBNYKH ZAVEDENIY:
PRIBOROSTROYENIYE in Russian No 10, 1990 (manuscript received 28 Feb 90)
pp 50-57

[Article by Yu. D. Zhabotinskiy and V. A. Malyshev, Rybinskiy Aviation Production Institute]

[Text] The problem of synthesizing a system for recognition of the final number of images given by their brightness functions is considered. A procedure for determination of the location of the sensors and of designing a specialized computer for recognition of plane images is described. Examples of designing robotic vision systems, based on the given recognition system, are outlined.

One must solve diverse recognition problems when developing sensitized industrial robots. These problems are ordinarily solved by using integral [1-5] or contour [6, 7] methods. However, integral methods require reading of the entire image, while contour methods require reading the contour images, which leads in the first case to complex technical realizations and in the second case to low noise stability.

The proposed method is applicable for recognition of a finite number of images, given by their brightness functions. It permits one to synthesize $m \leq n$ sensors and a specialized computer, which, processing data from the sensors, performs the recognition, by the brightness functions of n images.

Operating principle of recognition system. Let on set X be given n mutually different functions $f_i: X \rightarrow \mathbb{R}$ ($i = 1 \dots n$), further called brightness functions. One of the brightness functions is represented. It is required to know which function.

Let us denote by x the point of set X and let us determine the image $F: X \rightarrow \mathbb{R}^n$ by the matrix equation

$$F(X) = \begin{bmatrix} f_1(x) \\ \dots \\ f_n(x) \end{bmatrix}.$$

Let us call system of points $x^1 \dots x^m$ of set X the separating system, if the rows of matrix $[F(x^1) \dots F(x^m)]$ are mutually different.

Let us synthesize a recognition system, formed of sensors and a specialized computer, in the next point by matrix $[F(x^1) \dots F(x^m)]$, and let us describe the operating principle of this system.

Let us assume that $x^1 \dots x^m$ is the separating system and let us show how it is proposed to solve the postulated recognition problem. Let f be the imposed brightness function. Let us form a row $[f(x^1) \dots f(x^m)]$, corresponding to one of the rows of the matrix $[F(x^1) \dots F(x^m)]$, for example, with the i -th row. In this case $f = f_i$ and, accordingly, the brightness function is proved.

Let us show that there is a separating system, formed of $m \leq n$ points, in set X. If the vectors $F(x^1) \dots F(x^m)$ form the basis of the linear subspace, generated by all vectors of type $F(x)$ at points $x^1 \dots x^m$, the system of points $x^1 \dots x^m$ will be the separating system. Let us present the proof by the method of the opposite. Let us assume that rows with numbers i and j coincide in the matrix $A = [F(x^1) \dots F(x^m)]$. There is the vector $y \in R^m$ at which $F(x) = Ay$ for any $x \in X$ by specific points $x^1 \dots x^m$. Therefore, $f_i(x) = f_j(x)$ at all $x \in X$, and this can not be, since the brightness functions were assumed mutually different. This means that the system of points $x^1 \dots x^m$ is the separating system.

The inequality $m \leq n$ is obvious.

Technical realization of recognition system. The values of $f(x^1) \dots f(x^m)$ of brightness function f must be calculated at points $x^1 \dots x^m$ of the separating function to realize the described recognition method. This can be accomplished by using sensors that operate in the following mode:

$$\delta_i = \begin{cases} 0 & \text{at } i < \lambda_q, \\ 1 & \text{at } i \geq \lambda_q, \end{cases}$$

where $q = 1 \dots k$, λ is an input signal, $\lambda_1 < \lambda_2 < \dots < \lambda_k$ are the quantification levels, and $\delta_1 \dots \delta_k$ are output signals. The necessary sensors are designed by matrix columns $[F(x^1) \dots F(x^m)]$ and includes selection of quantification levels $\lambda_1' \dots \lambda_{k'}'$ and of their number k' ($j = 1 \dots m$).

Let $\mu_1^j < \mu_2^j < \dots < \mu_{k_j}^j < \mu_{k_j+1}^j$ be the different elements of column $F(x^j)$.

Let us assume that $\lambda_1^j = \mu_1^j, \dots, \lambda_{k_j}^j = \mu_{k_j}^j$, as the quantification levels of the j -th sensor. The number of k_j is a unit less than the number of different elements in column $F(x^j)$. Let us denote the input signal by λ^j and let us denote the output signals by $\delta_1^j, \dots, \delta_{k_j}^j$.

A block diagram of the recognition system is shown in Figure 1, where $D^1 \dots D^m$ are sensors and SV is a specialized computer.

The specialized computer performs the function of decoder: if signals $\lambda^1 = f_1(x^1), \dots, \lambda^m = f_m(x^m)$ are fed to the inputs of sensors $D^1 \dots D^m$, the i -th output signal of the computer is equal to one, and all remaining signals are equal to zero.

To design this computer, let us be given the constant

$$C_{ijq} = \begin{cases} 1 & \text{at } f_i(x^j) < \lambda_q^j, \\ 0 & \text{at } f_i(x^j) \geq \lambda_q^j, \end{cases}$$

and here $i = 1 \dots n$, $j = 1 \dots m$, and $q = 1 \dots k_j$.

The computer that realizes the output signals $r_1 \dots r_n$ by the formula

$$r_i = \prod_{j=1}^m \prod_{q=1}^{k_j} (\delta_{ij}^j \oplus C_{ijq}),$$

where $i = 1 \dots n$, while \oplus is addition modulo 2, operates in the required mode.

It should be noted that a perturbed function $f + g$, where g is noise, rather than an ideal brightness function f is fed to the inputs of the sensors in engineering problems. Therefore, the problem of protecting the recognition system against noise occurs. This problem can be solved by selecting the values of the quantification levels of the sensors.

Let us be given the number

$$\varepsilon = \frac{1}{2} \min_{1 \leq j \leq m} \min_{1 \leq q \leq k_j} (\mu_{q+1}^j - \mu_q^j)$$

and let us use as the quantification levels the values $\lambda_{jq} = \mu_{jq} + \varepsilon$, where $j = 1 \dots m$, and $q = 1 \dots k_j$. The recognition system is protected against noise that does not exceed the number ε in absolute value at these quantification levels.

Moreover, the brightness functions $f_1 \dots f_n$ are not equally probably manifested in engineering problems; therefore, the problem of providing the required probability of correct operation of the recognition system arises. This problem is solved by increasing the number of sensors and of modifying the specialized computer. Since the description of the general solution is rather cumbersome, it will be illustrated further on the example of a specific problems.

Examples of synthesis of recognition system [8]. The described recognition system was technically realized in different modifications for recognition of large parts of the K701 tractor, for determination of the orientation of nonmagnetic conducting parts, when designing the robotic diesel painting complex, to determine the position of the parts in the cold stamping section, and when designing the recognition systems and a nondestructive quality system. Photosensors, inductive and strain-gage sensors, and gamma-radiation sensors were used in developing these systems. Specialized computers were realized in all systems on microcircuits of series K153 and K155.

The proposed method will be illustrated on examples of design of flat part recognition systems.

Example 1. Flat part recognition systems. Let us determine the brightness function $f(x)$ of a flat image $G \subset R^2$. Let $D(x, r)$ be a circle with center at point x and with radius r , and let $\mu(A)$ be the area of section A . The brightness function f of image G is given on set $X = R^2$ and is determined by the formula

$$f(x) = \frac{\mu[G \cap D(x, r)]}{\pi r^2} .$$

Constant r is the radius of a circular section, from which the sensor perceives information. The brightness function f is similar to the characteristic function of set G , equal to one at G and equal to zero outside G , at small r .

The brightness function f is measured by sensors operating in the following mode:

$$\hat{f} = \begin{cases} 0 & \text{at } \lambda < \frac{1}{2}, \\ 1 & \text{at } \lambda \geq \frac{1}{2}. \end{cases}$$

Let us consider examples of synthesizing a system for recognition of the positions of a fixed part (variant 1), parts with one degree of freedom (variant 2), and parts with two degrees of freedom (variant 3). The part has the shape of an angle in all cases.

Variant 1. If the part 1 is transported by belt conveyer 2 (Figure 2, a), It begins to be rotated due to friction forces upon approach to stop 3. It is clamped by jaws 4 after completion of rotation for fixation of the part and occupies one of three positions, shown on Figure 3, a. In this figure, axis X proceeds along the stop, while axis Y proceeds along the left jaw of the grab. The superimposed contours of the positions of the part are shown in Figure 4, a.

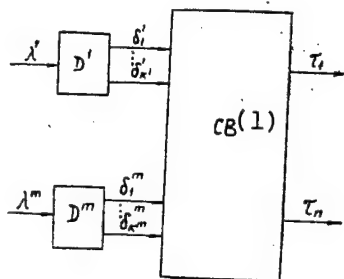


Figure 1

KEY:

1. Specialized computer

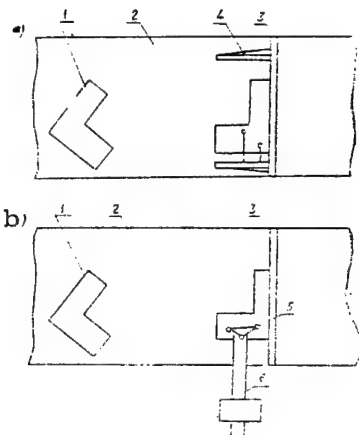


Figure 2

Let f_1 , f_2 and f_3 be brightness functions of plane images, shown in Figure 3, a. Let us assume that constant r is sufficiently small. In this case, points x^1 and x^2 , shown in Figure 4, a by the asterisks, form a separating system.

Matrix $[F(x^1), F(x^2)]$ will have the form

$$\begin{bmatrix} 1 & 1 \\ 0 & 1 \\ 1 & 0 \end{bmatrix}.$$

Accordingly, the specialized computer should realize the following output signals to recognize the positions of the part

$$\begin{aligned}\tau_1 &= \delta_1 \delta_2, \\ \tau_2 &= (\delta_1 \oplus 1) \delta_2, \\ \tau_3 &= \delta_1 (\delta_2 \oplus 1).\end{aligned}$$

If P is the probability of correct operation of the sensor, the probability of correct operation of the synthesized recognition system will be $P_1 = P^2$.

Let us place additional sensors at points x^3-x^6 , shown in Figure 4, a by the asterisks. The specialized computer that realizes the following output signals

$$\tau_i = \bigoplus_{k=1}^{11} \prod_{j=1}^6 (\delta_j \oplus C_{kj}),$$

where $i = 1, 2, 3$, while 11×6 matrices C^1 , C^2 , and C^3

$$\left[\begin{array}{cccccc} 0 & 0 & 0 & 1 & 1 & 1 \\ 1 & 0 & 0 & 1 & 1 & 1 \\ 0 & 1 & 1 & 1 & 1 & 1 \\ 0 & 1 & 0 & 1 & 1 & 1 \\ 0 & 1 & 0 & 1 & 1 & 0 \\ 0 & 0 & 1 & 1 & 1 & 1 \\ 0 & 0 & 1 & 0 & 1 & 1 \\ 0 & 0 & 0 & 1 & 1 & 0 \\ 0 & 0 & 0 & 1 & 0 & 1 \\ 0 & 0 & 0 & 0 & 1 & 1 \\ 0 & 0 & 0 & 0 & 1 & 0 \end{array} \right] \quad \left[\begin{array}{cccccc} 1 & 1 & 0 & 0 & 0 & 1 \\ 1 & 1 & 1 & 0 & 1 & 1 \\ 1 & 1 & 1 & 0 & 0 & 1 \\ 1 & 1 & 0 & 1 & 0 & 1 \\ 1 & 1 & 0 & 0 & 1 & 1 \\ 1 & 1 & 0 & 0 & 1 & 0 \\ 1 & 1 & 0 & 0 & 0 & 1 \\ 1 & 1 & 0 & 0 & 0 & 0 \end{array} \right] \quad \left[\begin{array}{cccccc} 1 & 1 & 1 & 1 & 1 & 0 \\ 1 & 1 & 1 & 1 & 0 & 0 \\ 1 & 0 & 1 & 1 & 1 & 0 \\ 1 & 0 & 1 & 1 & 0 & 1 \\ 1 & 0 & 1 & 1 & 0 & 0 \\ 1 & 0 & 1 & 0 & 1 & 1 \\ 1 & 0 & 1 & 0 & 1 & 0 \\ 1 & 0 & 1 & 0 & 0 & 0 \\ 1 & 0 & 0 & 1 & 0 & 0 \\ 0 & 1 & 1 & 1 & 0 & 0 \\ 0 & 0 & 1 & 1 & 0 & 0 \end{array} \right],$$

guarantees the probability of correct operation of the recognition system $P_2 = p^6 + 6p^5(1-p) + 4p^4(1-p)^2$. At $p \geq 0.54$, the probability $P_2 > P_1$. Therefore, the second recognition system operates more correctly.

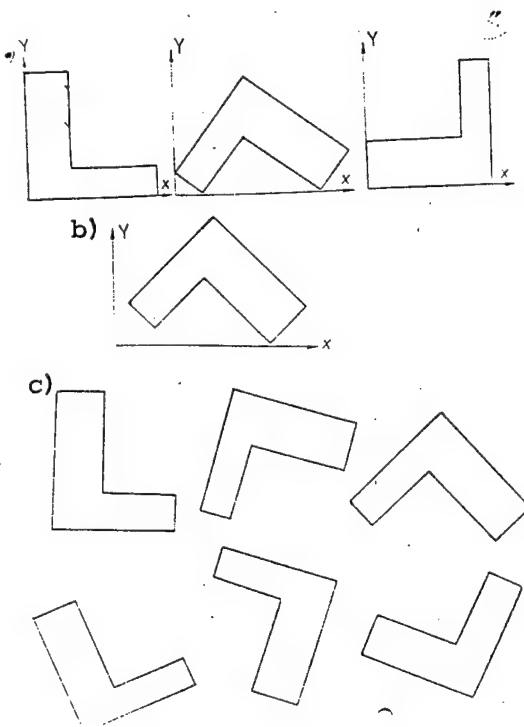


Figure 3

Variant 2. Let part 1, as in the first case, be transported by a belt conveyer 2 (Figure 2, b), but after rotation near stop 3 is not squeezed by the jaws. To determine the position of the part, let us place sensors 5 on push rod 6, having the possibility of forward displacement parallel to the stop 3. The mutual arrangement of points x^1 , x^2 , and x^3 of the sensors is shown in Figure 4, b. The matrix $[F(x^1), F(x^2), F(x^3)]$ has the form

$$\begin{bmatrix} 1 & 1 & 1 \\ 0 & 0 & 1 \\ 1 & 0 & 1 \end{bmatrix},$$

therefore, the output signals of the specialized computer are

$$\begin{aligned} \tau_1 &= \delta_1 \delta_2 \delta_3, \\ \tau_2 &= (\delta_1 \oplus 1) (\delta_2 \oplus 1) \delta_3, \\ \tau_3 &= \delta_1 (\delta_2 \oplus 1) \delta_3. \end{aligned}$$

We note that the sensors placed at points x^1 and x^2 determine the number of the position of the part, while the sensor located at point x^3 determines its displacement with respect to the stop.

Variant 3. Let the part be arbitrarily located on a plane. Let us link coordinate system XY to the plane (Figure 3, b). Let us measure the coordinates (X_1, Y_1) of the topmost and (X_2, Y_2) bottommost vertices of the part (the possible ambiguity is easily eliminated). This measurement can be made, for example, by using an integral photodetector array.

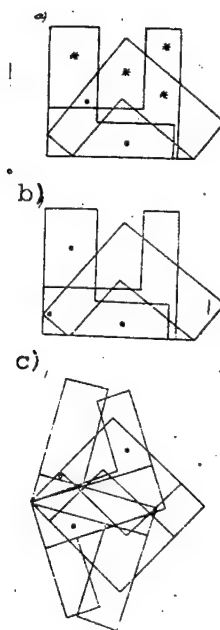


Figure 4

Six possible positions of the part, when its different vertices are the upper or lower, are shown in Figure 3, c.

Knowing coordinates (X_1, Y_1) and (X_2, Y_2) , let us transform the coordinate system so that the equalities $\tilde{X}_1 = \tilde{Y}_1 = \tilde{Y}_2 = 0$ are fulfilled in new coordinate system XY. The contours of all six images can then be combined in the new coordinate system, as shown in Figure 4, c.

The points of placement of sensors \tilde{x}^1 , \tilde{x}^2 , and \tilde{x}^3 are shown by the circles in Figure 4, c in coordinate system XY. Let us apply the inverse transform of coordinates to points \tilde{x}^1 , \tilde{x}^2 , and \tilde{x}^3 to determine the coordinates of cells x^1 , x^2 , and x^3 in the photodetector array, from

which the information must be read. Regardless of the transformation of coordinates, matrix $[F(x^1), F(x^2), F(x^3)]$ will have the form

$$\begin{bmatrix} 1 & 1 & 0 \\ 1 & 0 & 0 \\ 0 & 1 & 0 \\ 0 & 1 & 1 \\ 0 & 0 & 1 \\ 0 & 0 & 0 \end{bmatrix}.$$

Accordingly, the specialized computer should realize the following output signals

$$\begin{aligned} \tau_1 &= \delta_1 \delta_2 (\delta_3 \oplus 1), & \tau_2 &= \delta_1 (\delta_2 \oplus 1) (\delta_3 \oplus 1), \\ \tau_3 &= (\delta_1 \oplus 1) \delta_2 (\delta_3 \oplus 1), & \tau_4 &= (\delta_1 \oplus 1) \delta_2 \delta_3, \\ \tau_5 &= (\delta_1 \oplus 1) (\delta_2 \oplus 1) \delta_3, & \tau_6 &= (\delta_1 \oplus 1) (\delta_2 \oplus 1) (\delta_3 \oplus 1). \end{aligned}$$

Example 2. Recognition system for three-dimensional parts. Let us determine the brightness function f of a three-dimensional image $G \subset R^3$. Let $X = R^3 \times S^2$, where S^2 is a unit sphere. Points X of set $R^3 \times S^2$ are pairs (x_1, x_2) , where x_1 is an arbitrary vector and x_2 is an arbitrary unit vector, which controls the direction. Let $D(x, r)$ be a circle with center at point x_1 and with radius r , located in plane α , perpendicular to vector x_2 , and let $\pi(x_1, G)$ be the orthogonal projection of the body G onto plane α . The brightness function f of the image G is determined by the formula

$$f(x) = \frac{\mu[\pi(x_1, G) \cap D(x_1, r)]}{\pi r^2}.$$

The sensors that measure brightness function f operate in the previously described mode.

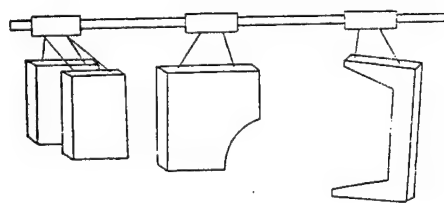


Figure 5

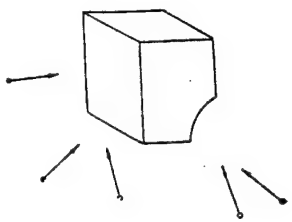


Figure 6

Let us present a system for recognition of 12 parts of the K701 tractor, moved by an overhead push conveyer. Some of these parts on the conveyer are shown in Figure 5. The points $x^1 = (x_1^1, x_2^1)$, $x^2 = (x_1^2, x_2^2)$, $x^3 = (x_1^3, x_2^3)$, $x^4 = (x_1^4, x_2^4)$, $x^5 = (x_1^5, x_2^5)$, which form the separating system, are shown in Figure 6 [8].

Bibliography

1. Zlobin, V. K. "Integral Algorithm for Normalization of Plane Images," "Avtomatizatsiya schityvaniya i raspoznavaniya grafikov: Sbornik" [Automation of Reading and Recognition of Graphs: A Collection], Minsk, 1979.
2. Katys, G. P. "Opticheskiye informatsionnyye sistemy robotov-manipulyatorov" [Optical Information Systems of Manipulator Robots], Moscow, Izdatelstvo "Mashinostroyeniye", 1977.
3. Yerosh, I. L. "Using Krestenson Transformations to Determine the Position Parameters of Objects by Plane Projections," IZVESTIYA AKADEMII NAUK SSSR. SERIYA TEKHNICHESKAYA KIBERNETIKA, No 3, 1981.
4. Young, J. P. "Robototekhnika" [Robotics], Leningrad, Izdatelstvo "Mashinostroyeniye", 1979.
5. Myasnikov, V. A., Ignatyev, M. B., Pokrovskiy, A. M. "Programmnoye upravleniye oborudovaniyem" [Program Control of Equipment], Leningrad, Izdatelstvo "Mashinostroyeniye", 1975.
6. Zlatkis, V. M. "Method of Determining the Angle of Inclination of Contour Figures," "Avtomatika i opoznavaniye obrazov" [Automation and Pattern Recognition], Issue 4, Izhevsk, 1969.
7. "Novaya sistema raspoznavaniya oriyentatsii detaley" [New System for Recognition of Orientation of Parts], EKSPRESS-INFORMATSIYA VINITI. SERIYA TEKHOLOGIYA I OBORUDOVANIYE MEKHANOSBOROCHNOGO PROIZVODSTVA, No 13, 1979.

8. Zhabotinskiy, Yu. D., Isayev, Yu. V. "Adaptivnyye promyshlennyye roboty i ikh primeneniye v mikroelektronike" [Adaptive Industrial Robots and Their Application in Microelectronics], Moscow, Izdatelstvo "Radio i svyaz", 1985.

COPYRIGHT: "IZVESTIYA VUZOV SSSR - PRIBOROSTROYENIYE", 1990

UDC 681.531.2

MATHEMATICAL MODEL OF POINTER STROBE TELEVISION SYSTEM UNDER NOISY CONDITIONS

917F0203A Leningrad IZVESTIYA VYSSHIKH UCHEBNYKH ZAVEDENIY:
PRIBOROSTROYENIYE in Russian No 10, 1990 (manuscript received 28 Feb 90)
pp 57-65

[Article by V. M. Artemyev and K. V. Glagolev, Moscow State Technical University imeni N. E. Bauman]

[Text] A mathematical model of a strobe pointer television system is proposed. The effective noise on the operation of the system in the steady mode is considered. The operation of a two-circuit system with connection between channels with a light-scattering layer in the working space was analyzed within the model by the statistical linearization method.

A strobe pointer system can be used in robotic visual sensitization problems as the sensor of information about the coordinates of the object under noise conditions, caused by the presence of a light-scattering layer in the working space of the system [1]. A narrow visual field permits one to reduce the effect of scattered emission and thus to enhance the contrast of the tracked object. The mathematical model of an optical angle coordinator, based on the strobe pointer principle, is proposed in the article for operating in the presence of a light-scattering layer in the working space of the coordinator. The system, shown in Figure 1, operates on the closed cycle and has two control circuits--an external circuit, closed by the television camera rotational drives, and an internal circuit, closed by the strobe generator. The problem of the internal circuit is to keep the strobe pointer on the image of the object.

The length of the image along the horizontal and vertical is denoted by θ_x and θ_y (Figure 2). In modern systems, the dimensions of the "window" are automatically adjusted to the dimensions of the image; therefore, let us further assume that the horizontal length of the window is equal to θ_x , while the vertical length is θ_y . The errors l_x and l_y between

the axes of the "window" and the axes of the image will be small, if the center of the image is located near the origin of the television screen.

The nature of the signal at the output of the television receiver within one line is shown in Figure 3. The signal from the source is perceived on some background, the mean level of which is denoted by U_ϕ . The amplitude, i.e., the maximum value of the signal with respect to U_ϕ , is denoted by A. Each signal in the line is normalized by a limiter, at the output of which a square-wave signal is formed with amplitude U_0 , the level of which is determined in the background level estimation circuit [2].

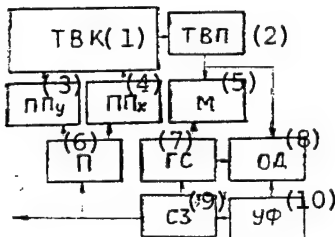


Figure 1. Structure of Television System:
 TVK--television camera; TVP--television receiver
 with image scanning; M--monitor; OD--optical
 discriminator; UF--amplifying and filtering elements;
 SZ--delay circuit; GS--strobe generator; P--delay time
 to voltage converter; PP_x and PP_y--drives for rotation
 of television camera through coordinates x and y

KEY:

- | | |
|--|------------------------------------|
| 1. Television camera | 5. Monitor |
| 2. Television receiver | 6. Delay time to voltage converter |
| 3. Drives for rotation of television camera through coordinate y | 7. Strobe generator |
| 4. Drive for rotation of television camera through coordinate x | 8. Optical discriminator |
| | 9. Delay circuit |
| | 10. Amplifying and filter elements |

Each of the four strobes shown in Figure 2 "cuts out" part of the image falling into this strobe. Four voltages U_{g1} , U_{g2} , U_{g3} , and U_{g4} , proportional to the mean values of the quantified signals impinging on the corresponding strobes, are formed at the end of the frame.

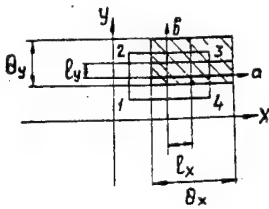


Figure 2. Screen of Television Monitor With Coordinate System x , y :
 a, b--coordinate system of strobe pointer;
 1-4--numbers of strobos

For example, let errors l_x and l_y lie in the limits $0 \leq |l_x| \leq 0.5\theta_x$ and $0 \leq |l_y| \leq 0.5\theta_y$. It is this case of the image that is in Figure 2. The averaged voltages in the strobos are then equal to

$$\left. \begin{array}{l} U_{g1} = (U_0/T_K) 0.5\theta_x \cdot 0.5n_y; \\ U_{g2} = (U_0/T_K) (0.5\theta_x - l_x) 0.5n_y; \\ U_{g3} = (U_0/T_K) (0.5\theta_x - l_x) (0.5n_y - f(l_y)); \\ U_{g4} = (U_0/T_K) 0.5\theta_x (0.5n_y - f(l_y)), \end{array} \right\} \quad (1)$$

where T_K and T_0 are the time of the frame and line scanning, respectively, $n_y = \theta_y/T_0$ is the number of lines in the "window," and $f(l_y)$ is the function l_y , which denotes the maximum integer, close to the ratio l_y/T_0 . The error voltages are generated by the laws

$$\begin{aligned} U_x &= (U_{g1} + U_{g4}) - (U_{g2} + U_{g3}), \\ U_y &= (U_{g1} + U_{g2}) - (U_{g3} + U_{g4}). \end{aligned} \quad (2)$$

Generalizing expressions similar to (1) and using (2), one can write the following formulas for the discrimination characteristics (DKh):

$$\begin{aligned} K_{gx}(l_x) &= \left\{ \begin{array}{l} (U_0/T_K) (n_y - |f(l_y)|) l_x; \quad 0 \leq |l_x| \leq 0.5\theta_x, \\ (U_0/T_K) (\theta_x - |l_x|) (n_y - |f(l_y)|) \operatorname{sgn} l_x; \\ \quad 0.5\theta_x \leq |l_x| \leq \theta_x; \end{array} \right\} \\ K_{gy}(l_y) &= \left\{ \begin{array}{l} (U_0/T_K) f(l_y) (\theta_x - |l_x|); \quad 0 \leq |l_y| \leq 0.5\theta_y, \\ (U_0/T_K) (\theta_y - |f(l_y)|) (\theta_x - |l_x|) \operatorname{sgn} f(l_y); \\ \quad 0.5\theta_y \leq |l_y| \leq \theta_y. \end{array} \right\} \end{aligned} \quad (3)$$

It is obvious that the continuous error function l_x is located along the horizontal (line) coordinate of the discrimination characteristic, while

the dependence of the discrimination characteristic on the error is a discrete step function along the vertical (frame) coordinate.

The conversion factors KP (the characteristic slope) of the channels of the discriminator are found from (3)

$$k_{gx} = \frac{U_0}{T_K} (n_y - |f(l_y)|); \quad k_{gy} = -\frac{U_0}{T_K T_0} (\theta_x - |l_x|) \quad (4)$$

It follows from (4) that there is a dependence between the channels of the discriminator through their conversion factor, which is manifested stronger, the greater the value of the errors.

Let us now consider the effect of noise on the operation of the system in the steady mode. The presence of the noise component of the signal at the input to the receiver is shown in Figure 3. Let the mean noise output (dispersion) by time with respect to the background level U_ϕ be equal to P_{III} . The effect of noise reduces to variation of the moments of response of the threshold device t_1 and t_2 . As a result of the internal noise of the receiver, the lengths of the pulsed signals in the strobes become random and random components appear in voltages $U_{g1}-U_{g4}$ that also lead to the appearance of fluctuating components at the input of the discriminator. Let us find the value of the spectral densities of these fluctuations at zero errors $l_x = l_y = 0$. Consideration of the instability of the response of the threshold circuit is described in [3]. The dispersion of the instability of the length of the pulse front is approximately equal to $D = P_{III}/a^2$, where a is the characteristic slope of the signal pulse in the region of threshold level U_0 [4]. This value can be taken into account in the following manner. With triangular shape of the signal with amplitude A , $a = 2A/\theta_x$. Variation of the characteristic slope with a different shape of the pulse is denoted by coefficient α : $a = 2\alpha A/\theta_x$. The dispersion of the instability of the pulse length will then be

$$D = \frac{P_{III}}{a^2} = \frac{P_{III} \theta_x^2}{4\alpha^2 A^2} .$$

Let us call the signal/noise ratio $q = A^2/P_{III}$. The dispersion is then

$$D = \theta_x^2 / 4\alpha^2 q .$$

Since there are $0.5n_y$ lines in each strobe and since the front of each pulse in the line fluctuates statistically regardless of other lines, the dispersion of each of the voltages U_{g1} - U_{g4} will be equal to

$$\frac{0.5n_y D U_0^2}{T_K} = \frac{\theta_x^2 U_0^2}{8\alpha^2 q T_K} n_y.$$

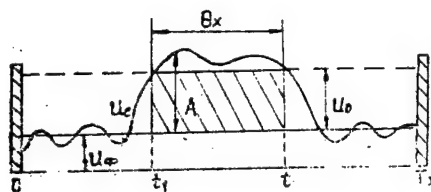


Figure 3. Signal at Output of Receiver Within One Line

When voltage U_x and U_y are formed, all four signals U_{gi} are added algebraically; therefore, the dispersion of the amplitude of each of the

voltages will be fourfold greater, i.e., $\frac{\theta_x^2 U_0^2 n_y}{2\alpha^2 q T_K}$. Since the error

voltages U_x and U_y are filled for the period T_K of scanning the next frame, the fluctuation component forms a sequence of square-wave pulses with statistically independent amplitudes (dispersions D).

For the subsequent narrowband actuating part of the system, this process can be considered white noise with the spectral density

$$N = D_m T_K = \frac{\theta_x^2 U_0^2 n_y}{2\alpha^2 q T_K}.$$

If the value of the conversion factor of the line channel is written in the form

$$k_{gx} = \frac{U_0 n_y}{T_K} \left(1 - \frac{|f(l_y)|}{n_y} \right)$$

and if the multiplier $U_0 n_y / T_K$ in the conversion factor of the actuating part of the system is taken into account, the parameters of the discrimination characteristic of the line channel will be equal to

$$k_{gx} = 1 - \frac{|f(l_y)|}{n_y}; \quad N_x = \frac{\theta_x^2 T_k}{2\alpha^2 q n_y}. \quad (5)$$

In similar fashion, for the frame channel

$$k_{gy} = 1 - \frac{|l_x|}{\theta_x}; \quad N_y = \frac{n_y T_k T_0^2}{2\alpha^2 q}. \quad (6)$$

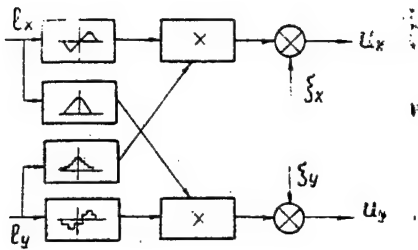


Figure 4. Block Diagram of Television Discriminator

The scattering layer in the working space of the system leads to a decrease of the optical signal at the input to the system and, therefore, to a decrease of the signal/noise ratio q . If this decrease is taken into account by introduction of coefficient $\beta = q/q_0$, where q_0 is the signal/noise ratio in the absence of a scattering layer, the spectral densities of the noise components in the line and frame channels will, according to formulas (5) and (6), be inversely proportional to coefficient β :

$$N_x = \frac{N_{x0}}{\beta}; \quad N_y = \frac{N_{y0}}{\beta}, \quad (7)$$

where N_{x0} and N_{y0} are the spectral densities of noise in the line and frame channels, respectively, are determined by formulas (5) and (6) at $q = q_0$.

Let us carry out further analysis, assuming that $\alpha = \text{const}$. If the useful signal is determined by a non-scattering component of source emission, the characteristic slope of the signal pulse will not be dependent on scattering and coefficient α can be considered constant. Of course, when the optical coordinator operates on the scattering component, coefficient α will vary as scattering increases in the located space due to variation of the intensity and due to an increase of the spreading surface of an image of a light spot. However, this

does not alter the methods of analysis of errors in the system, so that one can assume that variation of coefficient β includes not only variation of the signal/noise ratio, but also variation of the characteristic slope of the signal pulse due to scattering. Comparison of formulas (4) and (7) shows that an increase of the error is equivalent to a decrease of signal/noise ratio for a strobe pointer television system.

As one can see from expressions (5) and (6), there is a relationship between the discriminator channels through cofactors $(1 - |f(l_y)|/n_y)$ and $(1 - |l_x|/\theta_x)$. As a result, the block diagram of the television discriminator assumes the form shown in Figure 4, where ξ_x and ξ_y are white noise processes.

A two-circuit interconnected system can be analyzed in two steps. In the first step, the properties of only the internal circuits are studied with regard to the relationship between them, and in the second step, the system as a whole is studied. Let us consider the method of calculating the fluctuation errors in the system shown in Figure 4, under the following conditions: the work proceeds on linear sections of the discrimination characteristic, the number of television scanning lines, required for the dimensions of the image along the vertical, is greater than 20, which permits one to disregard quantization of the signal by the level in the frame channel of tracking and to assume that its characteristics are continuous functions. Let us use the statistical linearization method to analyze this system in the steady mode [5].

Since only the fluctuation effects $\xi_x(t)$ and $\xi_y(t)$ are taken into account in the form of white noise, tracking errors $l_x(t)$ and $l_y(t)$ will be random processes with zero mean value and variance D_{lx} and D_{ly} . Let us find the statistical linearization coefficients for a system with a block diagram shown in Figure 4 by the equations

$$\left. \begin{aligned} k_{0x} &= 1 - \sqrt{\frac{2D_{ly}}{\pi\theta_y^2}} = k_{0x}(D_{ly}); \\ k_{0y} &= 1 - \sqrt{\frac{2D_{lx}}{\pi\theta_x^2}} = k_{0y}(D_{lx}), \end{aligned} \right\} \quad (8)$$

in which it is taken into account that the mean values of the tracking errors are equal to zero in the expressions for normal probability densities.

Using the Parseval integral, let us write the variance of errors in the steady mode [6]:

$$D_{lx} = N_x I_x, \quad D_{ly} = N_y I_y, \quad (9)$$

where I_x and I_y are Parseval integrals for transfer functions of the errors of the line and frame channels, respectively. Relations (9) form a system of two equations, connected by coefficients k_{0x} and k_{0y} . Since the Parseval integrals I_x and I_y can be found in explicit form, (9) with regard to (8) forms a system of nonlinear algebraic equations, which is solved numerically or graphically.

Further analysis concerns study of a television-optical location system, developed by V. V. Vasiliyev [1] and having the following characteristics: transfer functions of the internal circuits

$$K_1(p) = k_1/p, \quad K_2(p) = k_2/p;$$

transfer functions of the external circuits, containing DC electric motors

$$K_3(p) = \frac{k_3}{p(1+pT_3)}, \quad K_4(p) = \frac{k_4}{p(1+pT_4)}.$$

As the experiments showed, the mean square values of the tracking errors are on the order of several angular minutes. This means that the signal to noise ratio under conditions of a clean atmosphere is $q_0 > 5$. Based on (8) and (9) for internal circuits, we arrive at the following system of algebraic equations:

$$\left. \begin{aligned} D_{tx} &= \frac{N_x k_1}{2k_{0x}} = \frac{D_{x0}}{\beta} \left(1 - \sqrt{\frac{2D_{ly}}{\pi\theta_y^2}} \right)^{-1}; \\ D_{ly} &= \frac{N_y k_2}{2k_{0y}} = \frac{D_{y0}}{\beta} \left(1 - \sqrt{\frac{2D_{tx}}{\pi\theta_x^2}} \right)^{-1}, \end{aligned} \right\} \quad (10)$$

here D_{x0} and D_{y0} are the variants of the errors in the channels of the system without regard to cross-correlation between channels and in the absence of a scattering layer.

Graphical solution of system of equations (10) is presented in Figure 5. We find solutions of them at the intersection points of A and B of curves 1 and 2. According to the condition of the problem, the desired point is point A, since the values of D_{tx} and D_{ly} increase only for this point as D_{x0} and D_{y0} increases. At some values of D_{x0} and D_{y0} , curves 1 and 2 cease to intersect, and this means that the system lost stability due to cross-correlation of the channels.

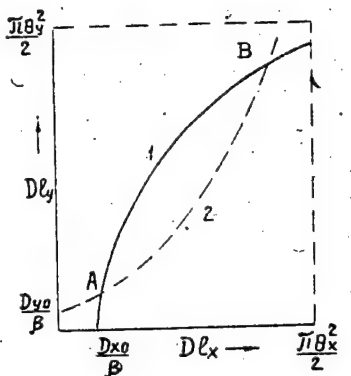


Figure 5. Graphical Solution of System (10):
1--graph of function $D_{lx} = f(D_{ly})$; 2--graph of
function $D_{ly} = f(D_{lx})$

It is more convenient for practical calculations to use the relative values of the variance of errors in formulas (10)

$$\left. \begin{aligned} \delta_x &= \frac{D_{lx}}{D_{x0}} = \frac{1}{\beta} \left(1 - \sqrt{\frac{2}{\pi} \Delta_y \delta_y} \right)^{-1}; \\ \delta_y &= \frac{D_{ly}}{D_{y0}} = \frac{1}{\beta} \left(1 - \sqrt{\frac{2}{\pi} \Delta_x \delta_x} \right)^{-1}, \end{aligned} \right\} \quad (11)$$

where

$$\Delta_x = D_{x0}/\theta_x^2, \quad \Delta_y = D_{y0}/\theta_y^2.$$

Let us present the analytical solution of equations (11) for the special case when the parameters of the channels are identical. It is obvious that here $\Delta_x = \Delta_y = \Delta_0$ and $\delta_x = \delta_y = \delta$. At some value of δ and at given parameter Δ_0 , we calculate

$$f = 1 - \sqrt{\frac{2}{\pi} \Delta_0 \delta}$$

and we find coefficient β as a function of the variance of the random component of the error in the channel:

$$\beta = (f\delta)^{-1}; \quad (12)$$

δ is determined by formula (11). The dependence of the variance of the error in the channel on coefficient β , calculated for different values of parameters Δ_0 , is shown in Figure 6. The errors in the system increase strongly at the same values of β as Δ_0 increases. Analysis of expression (12) shows that disruption of tracking in the channels of the internal circuit begins at variance of error in the channel of $\delta = 2\pi/9\Delta_2$. Therefore, curve $\delta(\beta)$ breaks off at $\Delta_0 = 0.1$ in Figure 6, when $\beta = 0.43$, i.e., at the moment of disruption of tracking, and an increase of the variance of the error begins even with an increase of the signal/noise ratio (the dashed curve in Figure 6).

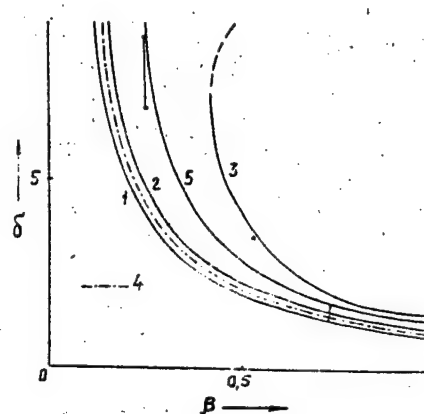


Figure 6. Dependence of Variance of Random Component of Error in Channel for One-Circuit (Curves 1-3) and Two-Circuit (Curves 4, 5) Systems on Coefficient β ; the Dashes Correspond to Experimental Results

The method described earlier is applicable for analysis of a two-circuit system--only the structure of the transfer function is complicated. The transfer function of the error of the first channel has the form

$$K_{lx}(p) = \frac{k_1 k_3}{k_{0x} k_1 k_3 + p k_{0x} k_1 + p^2 (1 + k_{0x} k_1 T_3) + p^3 T_3}.$$

Let us find the Parseval integral of this function and let us find the next expression for the variance of the error of the line channel:

$$D_{lx} = N_x \frac{k_3 (1 + k_{0x} k_1 T_3)}{2 k_{0x}^2 (k_{0x} k_1 T_3 - k_3 T_3 + 1)}.$$

The expression of the variance of the error for the frame channel is

$$D_{ly} = N_y \frac{k_4(1 + k_{0y}k_2T_4)}{2k_{0y}^2(k_{0y}k_2T_4 - k_4T_4 + 1)}.$$

These equations can be solved graphically. Let us carry out specific calculations, assuming that the parameters of the channels are identical; therefore, $D_{lx} = D_{ly}$.

If there is no light scattering ($\beta = 1$) and if there is no relationship between the channels ($k_{0x} = 1$), the variance is

$$D_{x0} = N_{x0} \frac{k_3(1 + k_1T_3)}{2(k_1T_3 - k_3T_3 + 1)}.$$

Taking (7) and (8) into account,

$$\delta_x = \frac{D_{lx}}{D_{x0}} = \frac{1}{\beta} \frac{(1 + k_{0x}k_1T_3)(k_1T_3 - k_3T_3 + 1)}{k_{0x}^2(k_{0x}k_1T_3 - k_3T_3 + 1)(1 + k_3T_3)}; \quad (13)$$

$$k_{0x} = 1 - \sqrt{\frac{2}{\pi}\delta_x\Delta_x}, \quad (14)$$

where $\Delta_x = D_{x0} = /0_x^2$, the same as for a one-circuit system.

One can find a clear relationship between k_{0x} and δ_x from equation (14) at some parameter of Δ_x , and one can calculate $k_{0x}(\delta_x)$ for the selected value of δ_x , while one can calculate

$$f = \frac{(1 + k_{0x}k_1T_3)(k_1T_3 - k_3T_3 + 1)}{k_{0x}^2(k_{0x}k_1T_3 - k_3T_3 + 1)(1 + k_3T_3)} \quad (15)$$

--the dependence of the variance of the error on the coefficient of statistical linearization in the absence of a scattering layer at some parameters of k_1 , k_3 , and T_3 for the derived value of k_{0x} . According to (13),

$$\beta = f/\delta_x, \quad (16)$$

here δ_x is the earlier selected value of the relative variance of the error. Relation (16) establishes the dependence between the relative

variance of the error and the coefficient of variation of the signal/noise ratio and permits one to calculate function $\delta_x(\beta)$.

Let us perform specific calculations at $k_1 = 500 \text{ s}^{-1}$, $k_3 = 200 \text{ s}^{-1}$, $T_3 = 0.2 \text{ s}$, $\Delta_x = 10^{-3}$ and $\Delta_x = 10^{-2}$. The functions $\delta_x(\beta)$ for a two-circuit tracking system is shown in Figure 6 by the dash-dot lines. The nature of function $\delta_x(\beta)$ is the same as that for a one-circuit system; the variance of the error increases rapidly as Δ_x increases. The greater Δ_x , the earlier disruption of tracking begins and it is expressed in the form of an increase of the variance of the error as coefficient β decreases. The errors at the same values of β are greater for a two-circuit system than in a one-circuit system at $\Delta_x = \Delta_0$. Moreover, system of equations (14) and (15) generally has no solution that satisfies the physical meaning of the problem at $\Delta_x = 10^{-1}$. The values of formula (16) are greater than unity in this case.

It is shown in Figure 6 that the values of δ_1 are small at $\beta = 1$, i.e., the relationship between channels in the system is weak in the absence of a scattering layer. For example, if $\Delta_x = 10^{-3}$, then $k_{0x}(\beta = 1) = 1.06$. Thus, the relationship of the channels upon transition from a one- to a two-circuit system is intensified.

The mathematical model of a tracking window television system was checked experimentally on a laboratory unit. 6-3N and 8-3N neutral light filters, initially calibrated on a spectrograph, were used to attenuate the light signal. The fluctuation component of voltage was taken by using an oscilloscope at the output of the discriminator. The resulting experimental values (the dashes in Figure 6) are easily described by a model function at $\Delta_x = 1.4 \cdot 10^{-2}$. We note that the probability of disruption of tracking, observed in experiment, was 0.5 at $\beta = 0.28$ (8-3N light filter).

Bibliography

1. Artemyev, V. M., Vasilev, V. V. "Television Tracking Identifying System," "Tezisy dokladov vtorogo Vsesoyuznogo nauchno-tehnicheskogo seminara 'Otsenka kharakteristik kachestva slozhnykh sistem i sistemnyy analiz'" [Report Topics of the Second All-Union Scientific and Technical Seminar "Evaluation of the Characteristics of Quality of Complex Systems and Systems Analysis"], Moscow, 1980.
2. Bakut, M. A., Bolshakov, I. A., Gerasimov, B. M. et al. "Voprosy statisticheskoy teorii radiolokatsii" [Problems of the Statistical Theory of Radar], Moscow, Izdatelstvo "Sovetskoye radio", 1964.
3. Tikhonov, V. I., Mironov, M. A. "Markovskiye protsessy" [Markovian Processes], Moscow, Izdatelstvo "Sovetskoye radio", 1979.
4. Tikhonov, V. I. "Statisticheskaya radiotekhnika" [Statistical Radio Engineering], Moscow, Izdatelstvo "Sovetskoye radio", 1966.

5. Kazakov, I. Ye. "Statisticheskaya metody proyektirovaniya sistem upravleniya" [Statistical Methods of Designing Control Systems], Moscow, Izdatelstvo "Mashinostroyeniye", 1969.

6. Artemyev, V. M. "Spravochnoye posobiye po metodam issledovaniya radioelektronnykh sledyashchikh sistem" [Handbook on Methods of Studying Radio Electronic Tracking Systems], Minsk, Izdatelstvo "Vysheishaya shkola", 1984.

COPYRIGHT: "IZVESTIYA VUZOV SSSR - PRIBOROSTROYENIYE", 1990

UDC 621.685

SEGMENTATION OF MULTIGRADATION IMAGES USING ODD LINGUISTIC VARIABLES

917F0203A Leningrad IZVESTIYA VYSSHIKH UCHEBNYKH ZAVEDENIY:
PRIBOROSTROYENIYE in Russian No 10, 1990 (manuscript received 28 Feb 90)
pp 66-69

[Article by V. I. Solntsev, Moscow State Technical University imeni N.
E. Bauman]

[Text] Problems of pre-processing of multigradation images of typical assembly scenes are considered. A context-free grammar of a linguistic variable is used to formalize the concept "BRIGHTNESS." It is suggested on its basis that the brightness scales be converted and that the images be segmented.

Information about the course of the manufacturing process must be obtained and processed under conditions of a flexible automated plant. The type of information systems is selected as a function of technology. Analysis of typical robotized assembly operations showed that a robotic vision system (STZ) has the greatest information content. It permits one to determine the position, orientation and characteristic dimensions of the assembly unit and of individual parts, and also to transfer this information to the robot control system. The assembly process can be checked by using the STZ.

The type of assembly position has a number of characteristic features from the viewpoint of using a robotic vision system. The assembly unit ordinarily consists of uniformly painted parts. Assembly is performed at the work position (assembly table, revolving table and so on), having a relief surface due to the presence of clamping devices, fasteners and other hardware. It is complicated to provide special lighting of the parts under production conditions.

Thus, the image of the work position, obtained by using optical sensors (vidicons, CCD-arrays, and photoarrays), has the following characteristics:

low contrast of individual parts and of their elements;

low contrast of the images of the assembly unit and of the work position;

nonuniform distribution of illumination due to selection of the local and general lighting system;

fluctuation of the level of illumination over time;

the presence of contrast interference on the image (contamination, highlights and so on).

Moreover, the assembly unit has a complex structure, which leads to the appearance of structures from uniformly lighted regions embedded in each other on the image.

Binary robotic vision systems, which have become widespread (the number of brightness gradations is equal to two), do not permit processing of scenes of this complexity. The use of binarization methods (both with fixed and with adaptive thresholds) and the preliminary processing step of the images requires uniformity and stability of lighting and high contrast between the "object" and "background." The resulting silhouette images contain only an insignificant part of the information about the scene. Thus, despite the low cost and high speed of binary robotic vision systems, the sphere of their application for automation of the assembly process is limited.

This problem can be solved by using multigradation STZ (the number of brightness gradations is from 8-16 to 256 and above). A monochromatic half-tone image is subjected to various types of transformations (correction, improvement, filtration, segmentation and so on) at the preliminary processing step to intensify contrast, to compensate for noise and to distinguish its characteristic elements.

A large number of methods and algorithms for processing multigradation images has now been developed [1-3]. However, robotized assembly imposes a significant restriction on the speed of the robotic vision system. All the processing steps from input of the image of the scene to recognition of it should occur within 1-3 s [1]. Therefore, many algorithms used with STZ to check assembly operations require development of special high-speed hardware, which increases the cost of the system.

Making a histogram of the image frame by brightness is most frequently used in industrial robotic vision systems for adaptation to variable lighting conditions. The threshold or interval of binarization is determined by the type of histogram, and the image is further processed the same as in binary STZ with adaptive threshold. This method is applicable for high-contrast images. The brightness distribution histogram for images of standard assembly units ordinarily has no characteristic "dark" and "light" peaks, which does not permit one to determine with sufficient accuracy the binarization threshold.

Gradient methods yield good results in the case of an absence of noise on the image [2]. But the low contrast results in disruption of the contour, approximation and connection of segments of which require large computer expenditures. Moreover, information is lost after calculation of any gradient function (Sobel or Roberts operator or something else), i.e., it becomes more difficult to determine to which of the parts it corresponds when determining the only the contour of parts.

Studies of man's visual perception system [4] indicate the psychological nature of perception of the illumination and color distribution function. The concept "BRIGHTNESS" is constructed on the basis of subjective impressions of man and is dependent on the total level of illumination of a scene, attention to its individual parts, and on a number of other factors. Determination of regions on an image, uniform in illumination, is one of the preliminary processing problems of multigradation images for robotic vision systems. Segmentation of images can be regarded as a problem of making a decision on the affiliation of the element of the image of some region to the level of illumination, typical for it.

It is suggested that linguistic variables, constructed on the basis of odd set theory, be used to formalize the concept "BRIGHTNESS" [5]. From the mathematical viewpoint, the degree of the affiliation of the image $\mu_i \in [0, 1]$ to the following odd set corresponds to the i -th element of an image with brightness code b_i

$$\mu_i = \mu_{\text{III}}(b_i), \quad (1)$$

where $\mu_{\text{III}}(b)$ is a function of the affiliation of the odd set. The key aspect is determination of the type of affiliation functions. Basic linguistic variables "LIGHT," "GRAY," and "DARK" were selected for the concept "BRIGHTNESS." Based on analysis of expert estimates of brightness for separate areas of images of a number of assembly units and parts, it was determined that the affiliation functions have a nature close to quadratic (Figure 1). The concept "BRIGHTNESS" can be approximated by a context-free grammar, which is the set of four

$$G = \langle N, T(N), U, S \rangle, \quad (2)$$

where N is the name of the linguistic variable, $T(N)$ is the term-set of its values, U is the set of values of the basic variable, and S is the syntactic rule of formation of the linguistic variable. The structure of the grammar (2) is presented in Figure 2.

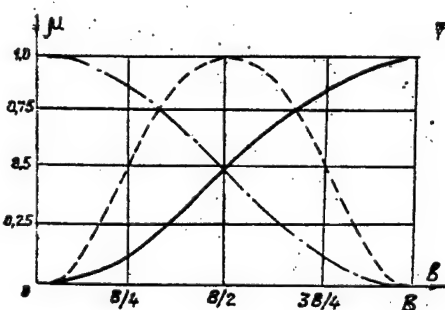


Figure 1. Functions of Affiliation of Basic Linguistic Variables:
 - · - - "LIGHT"; — — "DARK", - - - - "GRAY"

An alphabet of linguistic variables is formed by using the proposed grammar. The number of values of the variables is dependent on the postulated problem and should not exceed the Miller number 7 ± 2 , which expresses the maximum number of gradations of the parameter, simultaneously stored in the human memory [4]. Expression (1) can be considered as one of the methods of improving images by conversion of the brightness scale.

The result of conversion of the i -th element of the input image for the selected linguistic variable is determined by the formula

$$b_i^r = B\mu_{\text{III}}(b_i), \quad (3)$$

where B is the number of brightness gradations.

The "brightness cutoff" of the initial image is determined by using transformation (3). Adaptation to the dynamic range of brightness is made upon formation of the affiliation function $\mu_{\text{III}}(b)$ for one or several image frames. If the linguistic variable "DARK" is used, the result of the transformation will be a more contrasting image, and if the "LIGHT" variable is used, the result will be an inverted contrast image.

The image is segmented according to an alphabet of n linguistic variables. The k -th variable that corresponds to the maximum to it, for which the following condition is fulfilled

$$\mu_k = \max_j \mu_j(b_i), \text{ at } j=1, n. \quad (4)$$

is then selected for each i -th element of the image. This linguistic

variable is characterized by a brightness code B_k and is calculated by the centroid method as the abscissa of the center of gravity of the figure, limited by the affiliation function [5].

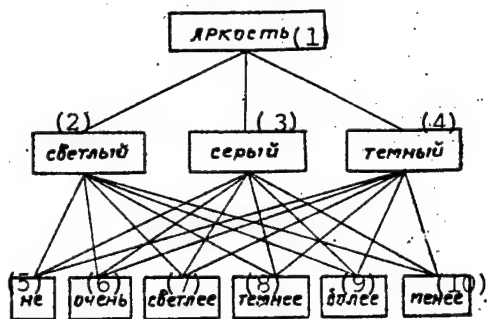


Figure 2. Structure of Grammar of Concept "BRIGHTNESS"

KEY:

- | | |
|---------------|------------|
| 1. Brightness | 6. Vary |
| 2. Light | 7. Lighter |
| 3. Gray | 8. Darker |
| 4. Dark | 9. More |
| 5. Not | 10. Less |

The proposed algorithm for segmentation of multigradation images using odd linguistic variables satisfies the principles of the completeness, connectedness, homogeneity and other requirements, imposed on the segmentation process [1]. It can be used in the case of low-contrast images with contrast noise, under conditions of fluctuation and irregular distribution of the level of illumination, along with other preliminary processing algorithms. Segmentation of images measuring 128×128 elements with 64 gradations of brightness yielded good results.

The advantages of the given algorithm, compared to other known algorithms, include the possibility of adaptation to variation of the conditions of illumination, greater information content of the resulting image, and high speed and simplicity of realization. The disadvantages may include some degree of subjectivism in selecting the type of affiliation functions and of the alphabet of linguistic variables as a function of the image. Studies of the possibility of automating this selection are now under way.

Bibliography

1. Kuaffe, F. "Vzaimodeystviye robota s vnishiyey sredoy" [Interaction of a Robot With the External Environment], Moscow, Izdatelstvo "Mir", 1985.

2. Pratt, W. "Tsifrovaya obrabotka izobrazheniy" [Digital Processing of Images], Moscow, Izdatelstvo "Mir", 1982.
3. Anisimov, B. V., Kurganov, V. D., Zlobin, V. K. "Raspoznavaniye i tsifrovaya obrabotka izobrazheniy" [Recognition and Digital Processing of Images], Moscow, Izdatelstvo "Vysshaya shkola", 1983.
4. Zinchenko, V. P., Munipov, V. M. "Osnovy ergonomiki" [The Fundamentals of Ergonomics], Moscow, Izdatelstvo MGU, 1979.
5. Borisov, A. N. et al. "Obrabotka nechetkoy informatsii v sistemakh prinyatiya resheniy" [Processing Odd Information in Decision-Making Systems], Moscow, Izdatelstvo "Radio i svyaz", 1989.

COPYRIGHT: "IZVESTIYA VUZOV SSSR - PRIBOROSTROYENIYE", 1990

UDC 007.52.535

USE OF ASSOCIATIVE PRINCIPLES FOR PROCESSING AND REPRESENTATION OF
VISUAL INFORMATION

917F0203A Leningrad IZVESTIYA VYSSHIKH UCHEBNYKH ZAVEDENIY:
PRIBOROSTROYENIYE in Russian No 10, 1990 (manuscript received 28 Feb 90)
pp 70-74

[Article by V. I. Volkov and R. M. Zharkoy, Moscow State Technical
University imeni N. E. Bauman]

[Text] Use of the principles of associative data processing in the area of computer vision is considered. A method of realizing associative concepts for pattern recognition is proposed, which includes selection of the method of encoding the image contours of objects, and formation of the basic dictionaries of the most typical elements of a silhouette image of an object.

Recognizing the images of objects is a process of analyzing them on the basis of selected features and working out decision rules, which permits one to relate each of the imaged objects to one of previously formulated classes according to a specific criterion. The theoretical methods of image recognition are based on two mathematical approaches: the discriminant and structure-linguistic [1].

Discriminant methods of recognition comprise the basis of the software of serially manufactured robotic vision systems (STZ), which are used successfully to analyze working scenes, containing isolated objects that have a limited number of stable equilibrium positions. Complication of the scenes and objects causes specific difficulties in the use of discriminant methods, since not only the numerical characteristics of the objects, but also information in terms of parts and relations that characterize their mutual location must be taken into account in these scenes. Structure-linguistic methods [2, 3], based on the structural relationships between "primitive" and their ordered combinations, correspond to the greatest extent to this situation.

However, despite a number of successful applications of structure-linguistic methods [1], practical realization of their potential

capabilities is now very low. This is explained by the following factor: specially developed methods of transforming physical objects to mathematical structures, convenient for using classification algorithms, do not yield a clear description of different objects [4]. In other words, different methods of structural description are required for different classes of objects.

Thus, a central problem in structure recognition is development of a universal method of describing the shape of objects (within the limits of two-dimensional projections of three-dimensional objects) using the principles of associative representation of information, realized by associative memories. The use of dynamic associative memories (DAZU), which store the dynamics of input events, is of greatest interest. The distinguishing feature of DAZU is the capability to structure the input data. Let us briefly present the main aspects [5, 6].

Presentation of information in associative memory. The DAZU can be described by a network of parallel-connected neuron-like elements (NE) with time summation of input signals. A neuron-like element of this type (Figure 1) is a device containing a multibit shift register, threshold converter and memory element, and all the cells of the register, having exciting or inhibiting input, are connected.

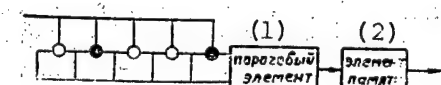


Figure 1

KEY:

1. Threshold element

2. Memory element

The first part of the NE operates as an address part. A sequence of pulses, which can be interpreted as the sequence $A = \{a_i : a_i \in \{0, 1\}\}$ (the 0 means the absence and 1 means the presence of pulses during some time cycle i), is fed to the input of the neuron-like element. Symbol a_i , arriving at moment i , is fed simultaneously to all cells of the shift register and is added to the contents of each cell with its own weight (+1 or -1). The contents of the cells of the register are then shifted by one position to the right (according to Figure 1). The maximum sum stored in the last element of the register may reach a value, equal to the sum of the ones in the address, and this occurs only if the input sequence repeats the distribution of signs at the inputs of the register.

The dynamic associative memory contains 2^n neuron-like elements, each of which simulates one of the vertices of an n -dimensional single hypertube in the signal space.

The binary sequence A, the input sequence for the dynamic associative memory, is transformed to the n-dimensional address space in the form of a sequence of points--trajectories $\hat{A} = F(A)$, from which the initial sequence $A = F^{-1}(\hat{A})$ can be restored. Transform F has the property of associative access to the information by association with respect to content (to n symbols of the input sequence). The trajectory is stored by introducing the memory function H at the vertices of the hypercube (the next symbol of the sequence is stored).

Allotment of function H by threshold properties permits one to realize statistical processing of the information stored in the dynamic associative memory, including formation of a dictionary of statistically reliable events $\{\beta\}$ at the input of the DAZU in the form of a set of sequences $\{A\}:\{\beta\} = F(\{A\})$.

Depending on the threshold of function H, the words $\{\beta\}$ will either be a combination of trajectories of realizations of events (all the information is stored), or will be a diffuse or point intersection of them (a more or less general part of the information is allocated). The coinciding sections of the sequences--events--are transformed to the same chain, and different sections are transformed to different chains, thus forming the graph word.

The information contained in dictionary $\{\beta\}$ is eliminated from the input sequence by introduction of transform F_C^{-1} ; only the connections of the words of the dictionary are retained in this case, and a syntactical sequence $C = F_C^{-1}[F(a), \{\beta\}]$ is formed. The mechanism of formation of the syntactical sequence permits one to use the dynamic associative memory for structured data processing within the framework of the hierarchical structure from the DAZU, since it becomes possible to combine several data flows.

Playback of the information using transform F^{-1} permits recognition of the input sequence by comparing it to the reproduced sequence.

Coding of input information sequence. The selected method of structured data processing is realized only by the presence of an active method of coding it, i.e., the input information should be described in the form of a sequence of codes. Thus, any information about the image, for example, contours that limit the zones of equal elimination or zones of identical texture, can be represented by this method. The external contour, a description of which is also selected for program realization of the proposed structured processing method, carries the basic information about the shape of the object.

Among the methods of contour coding, used in computer vision, differential Freeman codes are most suitable for solution of the given problem, since the information about the contour in them is already represented in the form of a closed series of symbols. However, this is

inadequate, since coding for a dynamic associative memory should be binary (the permissible symbols are only zero and one) and position-independent.

Fulfilling the first requirement permits considerable simplification of the methods of data processing in a dynamic associative memory, and fulfillment of the second requirement permits a significant increase of its operating reliability.

The binary method proposed by the authors describes a straight line in the form of a sequence of alternating zeros and ones, a turn to the left in the form of a combination of two zeros, and a turn to the right in the form of a combination of two ones, according to Freeman coding.

Formation of level-by-level dictionaries. The following sequence of writing information to the hierarchical structure of the dynamic associative memory has been suggested in the paper. Code sequences that describe a set of straight line segments are used as the elements of the lowest-level (first-level) dictionary. The arc of circles of different radius are included in the dictionary of the second level. The dictionary of the third level contains information about different angles. This representation is explained by the fact that the statistically more reliable elements of objects (straight-line fragments) are primarily allocated, then the less reliable (arcs of circles) and, finally, more variative (angles) are then allocated. The proposed representation can also be interpreted in terms of two-dimensional orthogonal transforms, where the process of detailing the description proceeds from the lower to the higher harmonics.

To study the processes occurring in the dynamic associative memory and the methods of structured processing of visual data, the authors developed a research complex that includes:

- a machine graphics program package for synthesis of the images;
- an image preprocessing program package that converts silhouette images of objects to contour descriptions (in the form of Freeman catenary codes);
- a program for recoding a catenary code to a binary code;
- a program model of the DAZU;
- a program for visualization of the trajectories written in the dynamic associative memory.

The complexity of transforming the trajectories in an n-dimensional signal space to a two-dimensional visualization plane was the reason for representing the graph of trajectory transitions in the DAZU in the form of a tree, in which branching of the trajectory in the signal space is depicted in the form of a fork, while the fusion of two trajectories

into one is depicted in form of the end of the branch of the tree. Continuation of the trajectory coincides with one of the points of the tree. The branching nature of the tree qualitatively reflects the degree of complexity of the graph. Thus, if the graph has no intersections (the degenerate case), its representation will be a straight line.

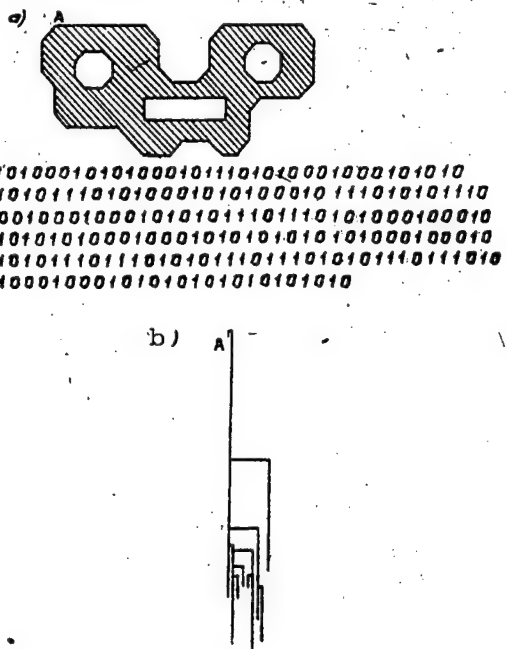


Figure 2

An example of teaching the DAZU is presented in Figure 2, where 2, a is a synthesized silhouette image of the object, and also its contour representation in binary code (A is the initial point), and 2, b is the internal representation in the form of a binary tree.

Bibliography

1. Fu, K. "Strukturnyye metody v raspoznavanii obrazov" [Structural Methods in Pattern Recognition], Moscow, Izdatelstvo "Mir", 1977.
 2. Pavlidis, T. Structural Pattern Recognition, New York, Springer-Verlag, 1977.
 3. Pavlidis, T. "Survey: A Review of Algorithms for Shape Analysis," COMPUTER GRAPHICS AND IMAGE PROCESSING, Vol 7, 1978.
 4. Pavlidis, T. "Hierarchical Method in Structural Pattern Recognition," TIIER, Vol 67, 1979.

5. Kharlamov, A. A. "Neuron-Like Elements With Time Summation of Input Signal and Associative Memory Modules Based on These Element," Voprosy kibernetiki. Ustroystva i sistemy" [Problems of Cybernetics. Devices and Systems], edited by N. N. Yevtikheyev, Moscow, MIREA, 1983.

6. Kharlamov, A. A. "The Associative Bionic Approach to Design of Central Speech Signal Processing Mechanism," Loc. cit., 1986.

COPYRIGHT: "IZVESTIYA VUZOV SSSR - PRIBOROSTROYENIYE", 1990

UDC 621.865.8.005:681.586

OPTICAL ROBOTIC VISION TELEVISION SYSTEM FOR CHECKING SHAPE OF
SEMICONDUCTOR CRYSTALS

917F0203A Leningrad IZVESTIYA VYSSHIKH UCHEBNYKH ZAVEDENIY:
PRIBOROSTROYENIYE in Russian No 10, 1990 (manuscript received 20 Feb 90)
pp 74-77

[Article by V. I. Syryamkin, V. S. Titov, A. A. Fomin et al., Tomsk
Institute of Automated Control Systems and Radio Electronics]

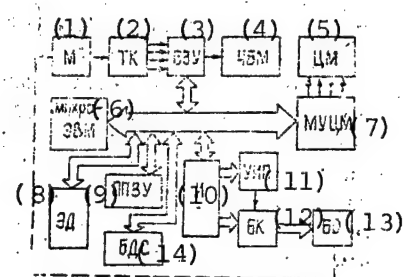
[Text] A robotic vision system has been proposed for
checking the shape of semiconductor crystals, realized
on the universal Elektronika-60 microcomputer. A
functional diagram of the visual system is described.
Algorithms for operation of the system and its
specifications are presented.

Much attention is now being devoted to development of robotic vision
systems (STZ), designed to automate product checking operations of the
electronics industry (semiconducting crystals and plates). One of the
methods of realizing STZ is to develop these systems on the basis of
universal microcomputers [1-3], the stock of which contains a large
number of various types of machines.

The robotic vision systems now developed on the basis of universal
microcomputers are either cumbersome and expensive (made in the CAMAC
design) [1], are inconvenient to service (there is no visual check of
the images to be analyzed) [3], or are incapable of remembering the
necessary number of reference images, and can not be connected to a
computer network [2].

The robotic vision system described in the article, designed for
automatic quality control of manufacture of semiconducting crystals
(check of the conformity of the shape (design) to a standard and of the
presence of mechanical damage (scratches)), does not have the indicated
deficiencies. An Elektronika-60 microcomputer is used as the control
computer in the robotic vision system. An Electronika MS0585 or
Elektronika MS1212 microcomputer can also be used in the STZ.

A functional diagram of the robotic vision system is presented in the Figure. The STZ consists of the following devices: an optical microscope (M), television camera (TK), buffer storage (BZU), programmable ROM (PPZU), electronic disk (ED), long-range communication module (BDS), an interface (I), a controlled power source (UIP), a key module (BK), lighting module (BO), color monitor control module (MUTsM), a color monitor (TsM), black-white monitor (ChBM) and a computer. The optical connections are shown on the diagram by dashed lines, while electric connections are shown by solid lines.



KEY:

- | | |
|---------------------------------|-------------------------------------|
| 1. Optical microscope | 8. Electronic disk |
| 2. Television camera | 9. PROM |
| 3. Buffer storage | 10. Interface |
| 4. Black-white monitor | 11. Controlled power supply |
| 5. Color monitor | 12. Key module |
| 6. Microcomputer | 13. Lighting module |
| 7. Color monitor control module | 14. Long-range communication module |

The total operating cycle of the STZ contains two steps: teaching (writing the image of the reference object to the memory) and operation (obtaining the necessary data on the object to be checked). The teaching step can be fulfilled either by writing the information to the memory of the STZ (to the electronic disk) by direct reading of the image of the reference object, or by recording the reference information (to the electronic disk or PROM) by program. The first method of teaching is used in the STZ, which begins with establishment of the necessary lighting, provided by the interface (a I-2 device), controlled power source, key module, and lighting module (assembled on light diodes of type AL107A) in the working zone of the microscope (of type PME-1 or MBS-9). The light module contains different numbers of light sources, the light intensity, operating frequency and frequency of switching-on of which are established from the computer. The light sources are arranged about the control object (crystal). An image of the crystal in the working zone of the microscope is perceived by the television camera, is read (written) to the buffer storage, which stores one frame of the image measuring 256×256 and 16 brightness gradations (64K four-bit words). The reference image is then copied to the electronic disk (with capacity of 2,000 kbits), which stores eight frames of the

images. The image is processed (filtered or segmented) when the reference information is written to the electronic disk according to the algorithms described below. This permits one to present a higher quality image and to enhance considerably the accuracy and operating speed of the STZ. The process of teaching the STZ terminates at this point. The STZ program, developed in Assembler language, is written to the programmable ROM. Communications are established through the common bus of the robotic vision system and central computer by using the long-range communication module (of the BDS-60 type), which permits one to provide problems of simulation of the operating algorithms of the STZ or program support of the STZ if necessary. A local data transfer net is used for this. The original devices of the STZ are the buffer storage and electronic disk.

The buffer storage operates in the following modes: writing the image frame from the television camera to the memory module (BP) with a simultaneous check of the image introduced to the black-white monitor, reading the information from the memory module to the computer, and writing the information from the computer to the memory module (to check the processed image) to the computer. The buffer storage is embedded in the design of the microcomputer and occupies one complete card. The memory module of the buffer storage is realized on 16 565RUZ microcircuits.

The electronic disk operates in the following modes: writing information from the microcomputer, regeneration, and reading the information to the microcomputer. In the write mode, the electronic disk generates all the necessary signals for storage of the line and column addresses in the internal registers of the memory microcircuits, and also for writing of data to the corresponding group of microcircuits. After the write cycle is completed, the electronic disk switches to the regeneration mode, which is achieved by accessing each of 256 lines of all frames at a speed of $2 \cdot 10^{-6}$ s. The read mode is similar to the write mode and is controlled from the computer. The electronic disk is structurally made in the microcomputer standard (one half-height card). The main memory of the electronic disk is assembled on 32 565RU5 microcircuits.

The software of the robotic vision system permits the operations of checking semiconducting crystals or plates: estimating the correctness of shape (arrangement of the structural components of the crystal), measurement of the geometric characteristics (area, linear dimensions, for example, length and width, and perimeter of the contour), and determination of the mechanical damage (the presence and dimensions of chips and scratches).

One operating cycle of the STZ consists of the following steps:

determination of the boundaries (the distance of the edges) of the image frame;

preliminary processing of the image;
removal of the necessary information.

The boundaries of the image are determined, achieved by eliminating the distortions on the edges of the image frame, in the first step of functioning of the robotic vision system. In the second step of operation of the STZ, the contours of the image are filtered and determined. The filtering operation is used to remove noise, interference and distortions of the images, which occur due to imperfection of the hardware and due to the process of formation of the image. This operation is achieved by one of three methods: by the threshold method, by low-frequency filtration or by median filtration [4]. The threshold method is based on measuring the brightness of all the elements of the image, on comparing this brightness to the mean brightness of adjacent elements of the image, and on replacing the measured brightness by the mean brightness. Low-frequency filtration is achieved by reducing the initial image file with the correcting file. Such methods of filtration as a window in three or five elements, a cross in five or nine elements, and the weighted mean (along the vertical or horizontal sequentially) in three or five elements are used with median filtration.

The operation of discrimination of contours is based on the use of one of the following methods [4, 5]: of a differential Roberts or Sobel operator, of a logarithmic Walsh detector, of formation of the contour by analysis of four or eight adjacent points of the image.

Selection of the filtration method and of discrimination of contours is determined by the geometric and light characteristics of the crystal, and by the required speed and operating accuracy of the robotic vision system.

All the necessary measurements of the visible upper plane of the crystal are made on the third operating step of the robotic vision system. The algorithms of the STZ, which realizes the method of comparison to a standard, consists of the following operations: "review" of the crystal plane, measurement of the length, width, perimeter, area and angles, determination of the correctness of the ratio of the design (for example, displacement of the contact surface from the center of the surface of the crystal), and estimation of the presence and value of the area of chips and scratches of the crystal. A reference file, formulated during teaching of the robotic vision system, is used to analyze the geometric characteristics. Estimation of crystal defects is based on the correlation method of comparison of images [5].

The following characteristics were obtained when testing the robotic vision system: resolution of 0.2 percent of the size of the image frame (for example, the resolution is no worse than 100 μm at frame size of $25 \times 25 \text{ mm}$, the accuracy of estimating the linear dimensions (total) is random (mean square deviation) and systematic, which comprise a

measurement error of 0.1 percent of the size of the image frame at checked size of the crystal $(0.3 \times 0.3)10^{-2}$ m, and the time of checking one crystal of 0.1-10 s as a function of the required measurements and complexity of the shape of the crystal. The described variant of the robotic vision system is being operated successfully at TIASUR [not further identified] and at other USSR enterprises. The cost of the STZ (including the computer) is approximately 13,000 rubles.

Thus, the described robotic vision system is less expensive and is distinguished from known systems [1-3] by better characteristics due to the capability of storing a sufficient number of reference images, due to connection of the STZ to a computer network, and due to convenience of servicing because of selecting the image on black-white or color monitors.

Bibliography

1. Pisarevskiy, A. N., Chernyayevskiy, A. F., Afanasyev, G. K. et al. "Sistemy tekhnicheskogo zreniya" [Robotic Vision Systems], Leningrad, Izdatelstvo "Mashinostroyeniye", 1988.
2. Matveyenko, V. I., Staroverov, Yu. G. "A Half-Tone Robotic Vision System," MIKROPROTSESSORNNYE SREDSTVA I SISTEMY, No 2, 1987.
3. "Tekhnicheskoye zreniye robotov" [Robotic Vision], translated from English by D. F. Mironov, edited by G. P. Katys, Leningrad, Izdatelstvo "Mashinostroyeniye", 1987.
4. Pratt, W. "Tsifrovaya obrabotka izobrazheniy" [Digital Processing of Images], translated from English, book 2, Moscow, Izdatelstvo "Mir", 1982.
5. Korikov, A. M., Syryamkin, V. I., Titov, V. S. "Korrelyatsionnyye zritelnyye sistemy robotov" [Correlation Robotic Vision Systems], Tomsk, Izdatelstvo "Radio i svyaz", 1990.

COPYRIGHT: "IZVESTIYA VUZOV SSSR - PRIBOROSTROYENIYE", 1990

UDC 621.865.8.008

CONTROLLED MODEL ON FIBER SORPTION ELECTRONIC MUSCLES

917F0203A Leningrad IZVESTIYA VYSSHIKH UCHEBNYKH ZAVEDENIY:
PRIBOROSTROYENIYE in Russian No 10, 1990 (manuscript received 28 Feb 90)
pp 78-86

[Article by S. G. Agranovskiy, Yu. N. Yegorov, I. V. Bolotin et al.,
Leningrad Polytechnical Institute imeni M. I. Kalinin]

[Text] The working and operating principle of a fiber sorption muscle and the structure of a one-step drive system are considered. The law of control of the drive is synthesized. Promising areas of using the module are indicated.

There are now two parallel creative processes. One is related to the evolutionary development of nature, unobtrusive in daily life, and is the original fiber universality of the muscular-receptor development of organisms. The other is more dynamic and is expressed in the results of the technical activity of man. The observed attenuation of the uniting mutually enriching bionic approach in the engineering of machines, mechanisms and, specifically, of robots and manipulators, is explained by the absence of satisfactory analogues of muscles, receptors and so on, which are possibly the key linking elements for the compatibility of the natural and technical approaches. The particularly theoretical papers on development of bionic approaches acquired the form of specific technical developments with synthesis of the world's first fiber sorption electronic muscle in the Soviet Union in 1988.

The main elements of a one-step controlled module are kinematic anthropomorphic links and an antagonistic pair of fiber sorption muscles. A layout of the working principle of the muscle is presented in Figure 1. It contains a cord of an anisotropic sheathing 1 in the form of a hollow cylindrical cord, inside which there is a closed elastomeric space 2. Adsorbent-adsorbent fillers 3 and 4 are located in this space. The adsorbent 3 is at the same time a thermocouple. Electric contacts 5 and 6 are hermetically led to the outside from the opposite ends of the sheathing 1. The surface of the adsorbent 3 is heated due to the effect of electric current delivered to contacts 5 and

6. As a result, the adsorbate 4 leaves the surface of the adsorbent 3, switching to a vaporous state. The pressure in the elastomeric space 2 is increased. The filaments in the internodes of the anisotropic sheathing 1 are rotated and the muscle is contracted. If the current is switched off, the adsorbent 3 is cooled by convection or preventively, and the adsorbate 4 is adsorbed due to reversibility. The pressure drops and the muscle does not prevent its own lengthening. Thus, the force developed by the muscle is determined in the final analysis by the pressure of the adsorbate.

Two main elements can be distinguished in the muscle unit: a micromechanism of a sheathing force converter and a sorption microengine. The sheathing transforms the internal energy of the muscle to force contraction.

Studies of the parameters of the cord 1 revealed a specific dependence of the maximum value of the relative longitudinal deformation on the nature of representation of braiding of the sheathing. Specifically, the following calculating function is valid for braided sheathing:

$$e_{n \max} = \left(1 - \frac{\cos \alpha_{\max}}{\cos \alpha_{\min}}\right) \left(1 + \frac{h_H}{c}\right)^{-1} \leq 0,21 \quad (1)$$

where e_n is the deformation of the braided cord of the muscle, α is the angle in the internodes of the braiding of rhombic elementary cells, c is the width of the initial filament, and h_H is the length of the side of the rhombus of the elementary cells of the cord.

For bound sheathing, the length of the edge seemingly increases by approximately the width of the filament which is oriented from above, while the value of the internodes becomes twofold greater than that in braided sheathing. On this basis, a similar function is

$$e_{b \max} = \left(1 - \frac{\cos \alpha_{\max}}{\cos \alpha_{\min}}\right) \left(\frac{c}{h_H} + 1\right) 0,5 \leq 0,54 \quad (2)$$

The maximum angles in the internodes of the rhombic cell of the cord layer of the muscle sheathing were established

$$54^\circ \geq \alpha \geq 24^\circ \quad (3)$$

The principles that link the pressure inside the muscle in the static mode to the deformations and forces developed by it in the absence of an external load are expressed by the formula

$$q = h_s = (\bar{x} - 1) \left(1 + \frac{h_s}{c}\right)^{-1} E \left\{ (r_2 - h_s) + (1 - \bar{x}) \left(1 + \frac{h_s}{c}\right)^{-1} \times \right. \\ \left. \times \left[(1 - \bar{x}) \left(1 + \frac{h_s}{c}\right)^{-1} - r_2 + 1 \right]^{-1} (r_2 - h_s) \right\}^{-1}, \quad (4)$$

where h_s is the thickness of the elastomeric volume of the muscle, \bar{x} is the relative variation of the length of the muscle (specific length), E is the modulus of elasticity of the material of the elastomeric volume of the muscle, and r_2 is the external radius of the elastomeric volume of the muscle.

The force developed by the muscles is related only to compressive strain. Therefore, the external load on it has physical meaning exclusively in the direction of the tension of its sheathing. The dependence of the steady internal pressure q_p on the external load P on the muscle is derived. The values of q and q_p , according to the principle of superposition, determined the total internal pressure

$$q_{\Sigma} = q + q_p, \quad (5)$$

where

$$q_p = P \sin^2 \alpha_{\min} [(1 - x^2 \cos^2 \alpha_{\min}) \pi r_1^2]^{-1}, \quad (6)$$

Here r_1 is the internal radius of the elastomeric volume of the muscle.

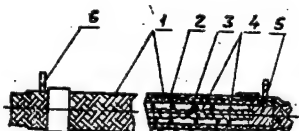


Figure 1. Working Principle of Electronic Muscle:
1--cord of anisotropic sheathing; 2--closed elastomeric volume; 3--adsorbent; 4--adsorbate; 5, 6--electric contacts

The mechanisms presented by formulas (1)-(6), which in combination permit numerical-step variation of the main parameters, specifically permitted calculation of the sheathing of the first electronic muscle.

Reversible sorption microengines in electronic muscles essentially perform the role of direct converter of electric energy to mechanical

energy. Adsorption-desorption equilibrium is in the given case the initial physical phenomenon. It is expressed in regulated concentration of materials on the surface or of solid micropores in the volume. Matter of the solid phase, on which the material to be absorbed is concentrated, is called the absorbent. The material to be absorbed, present in the gaseous phase outside the adsorbent, is called the adsorbive, while its part directly concentrated on this surface or in the pores is called the adsorbate. Construction of the sorption microengine is closely related to the concept on micropores as on the regions of space in a solid, comparable in dimensions to the adsorbed molecules. The field of the adsorption space includes three types of interactions in the given case. The main interaction is dispersion, manifested between nonpolar molecules. The electrons move in a complex manner about nuclei in atoms and molecules. The dipole moments of nonpolar molecules over average time are equal to zero, but the instantaneous value of the dipole moment may be distinct from zero. The instantaneous dipole creates an electric field, which polarizes adjacent molecules. As a result, there is interaction of the instantaneous dipoles. The energy of interaction of nonpolar molecules is the mean result of interaction of these instantaneous dipoles. In physics, forces of this class of interaction are called London forces. A common nature distinguishes them--they can occur between any atoms and molecules, by which their universality is also explained. An orientation effect, caused by dipole-dipole interaction due to the effect of Keesom forces, occurs in the presence of constant dipoles in the molecules of the adsorbate. Intermediate between the dispersion and dipole-dipole type of interaction is the induction effect, which is manifested between the polar and nonpolar molecules under the effect of Debye forces. London, Keesom and Debye forces are mutual attractive forces. Determination of the energy parameters of electronic muscles of fiber-sorption type is semi-empirical in nature. An adsorption isotherm is initially constructed for the selected type of adsorbate-adsorbate filler of the electronic muscle in the form

$$B=f(q) \text{ at } T=\text{const},$$

one of the experimental variants of which is presented in Figure 2.

The work of adsorption A , equal to the differential variation of the Gibbs adsorption energy, taken with opposite sign

$$A = -\Delta G = RT \ln(q_s q^{-1}), \quad (7)$$

where R is the universal gas constant, T is the absolute temperature, and q_s is the tabular value of the saturated vapor pressure above the liquid adsorbate, is then determined. The corresponding q_0 and T_0 , and also the differential molar work, which expresses the characteristic

adsorption energy B_0 , are found in the absence of adsorbent at temperature T . The maximum adsorption for temperature T_0 is determined by the equation

$$B_0 = B_{01} \exp[-\gamma(T - T_0)],$$

here γ is the thermal coefficient of maximum adsorption.

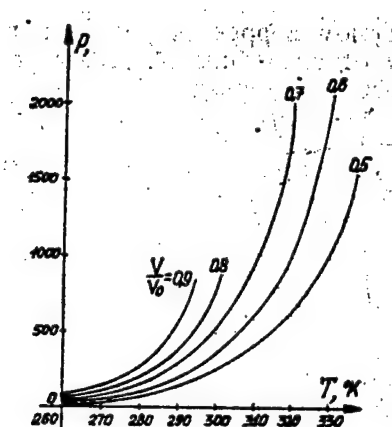


Figure 2. Experimental Isosteres for Different Fractions of Filling of Volume of Adsorbate-Adsorbent System of Electronic Muscle:
V--volume of pores of adsorbent; V_0 --total volume

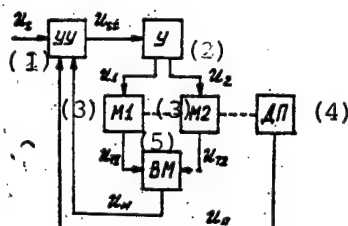


Figure 3. One-Step Drive System, Containing Antagonistic Pair of Electronic Muscles

KEY:

- | | |
|---------------|---|
| 1. Controller | 4. Position sensor of output element of drive |
| 2. Amplifier | 5. Computer of difference of mean and instantaneous power of heating of muscle adsorbents |
| 3. Muscle | |

Substituting the calculated values of B_0 and A_0 into the thermal equation of Dubinin-Astakhov adsorption

$$B = B_0 \exp \left[- \left(\frac{RT \ln (q_s q^{-1})}{A_0} \right)^2 \right],$$

the adsorption isotherms are calculated for a number of values T , lying in the temperature range of practical interest. The graphs of the adsorption isosteres are then constructed, i.e., functions of the following type are constructed

$$q = f_1(T) \quad \text{at } B_0 = \text{const.}$$

Adsorption increases as the pressure of the adsorbive increases. The differential work on a background of an increase of absorption with an increase of the pressure of the adsorbive decreases. The thermodynamic state of the electronic muscle is expressed by adsorption-desorption equilibrium between the adsorbate and adsorbive, which, as in the classical variant of a heat engine, is determined by three values: pressure, temperature and the volume of the working gas. The difference is only that the volume in the given case has adsorption properties 7. Differential variation of entropy can be expressed by finding the differential of ΔG by temperature:

$$\begin{aligned} \Delta S &= - \frac{\partial \Delta G}{\partial T} = - R \ln (q_s q^{-1}) - RT \left[\frac{\partial \ln (q_s q^{-1})}{\partial T} \right]_B = \\ &= - R \ln (q_s q^{-1}) - RT \left(\frac{\partial \ln q}{\partial T} \right)_B + RT \frac{d \ln q_s}{dT}. \end{aligned} \quad (8)$$

The direct derivative is correctly written in the last term, since q_s is independent of adsorption B . Let us find the differential variation of enthalpy, having substituted into the equation

$$\Delta H = \Delta G + T \Delta S$$

the corresponding expressions from equations (7) and (8):

$$\begin{aligned} \Delta H &= - RT \ln (q_s q^{-1}) - RT \ln (q_s q^{-1}) - RT \left[\frac{\partial \ln (q_s q^{-1})}{\partial T} \right] = \\ &= RT^2 \left(\frac{\partial \ln q}{\partial T} \right)_B - RT^2 \frac{d \ln q_s}{dT}. \end{aligned} \quad (9)$$

The first term of the right side of equation (9) expresses the differential heat of adsorption of the adsorbent, while the second term corresponds to the heat of condensation of the adsorbive. Thus, construction of isosteres is used to calculate the differential entropy and differential enthalpy of the sorption microengine of the electronic muscle.

If there is no external interactive force, the length of the muscle is dependent on its internal thermodynamic state. Without regard to thermal losses, it is characterized by the mean power of the heating of the adsorbent

$$N_c = \frac{1}{\tau_1} \int_0^{\tau_1} N d\tau_1, \quad (10)$$

where $N = I^2 r$ is the instantaneous heating power, I is the electric current in the adsorbent, r is the resistance to current, and τ_1 is time.

If the given contraction of the muscle was established, one can in the first approximation permit a link between length l_a and power:

$$l_a = K_3 N_c + l_0,$$

l_0 is the length of the muscle at $P_c = 0$ and K_3 is a coefficient determined experimentally. The steady force P_M , developed by the muscle, is represented by the formula

$$P_M = K_Z (l_a - l) = K_Z (K_3 N_c + l_0 - l),$$

in which l is the length of the muscle deformed from outside and K_Z is the longitudinal stiffness coefficient. With regard to (10), we find

$$P_M = K_Z \left(K_3 \frac{r}{\tau_1} \int_0^{\tau_1} I^2 d\tau_1 + l_0 - l \right).$$

The structure of a one-step drive system, containing an antagonistic pair of muscles, is shown in Figure 3: M_1 and M_2 are the muscles, U is an amplifier, UU is the controller, DP is the position sensor of the output element of the drive, and VM is a computer of the difference of

the mean and instantaneous power of heating of the adsorbents of the muscles.

For an antagonistic pair of muscles in the steady state, the forces developed by them are equal to

$$P_1 = K_Z \left(K_s \frac{r}{\tau_1} \int_0^{\tau_1} I_1^2 d\tau_1 + l_0 - l_1 \right);$$

$$P_2 = K_Z \left(K_s \frac{r}{\tau_1} \int_0^{\tau_1} I_2^2 d\tau_1 + l_0 - l_2 \right),$$

here I_1 and I_2 are currents of the first and second muscles and l_1 and l_2 are their lengths. Let us assume that $l_0 - l_1 = l_{II}$, $l_0 - l_2 = l_n$, $l_{II} \neq 0$ are the position of the output element of the drive. The values $l_{II} = 0$ and $l_1 = l_2 = l_0$ correspond to the off state of the pair of muscles.

The force of drive P is equal to the difference of forces P_1 and P_2 , acting oppositely. In the steady state

$$P = K_Z \left[K_s \frac{r}{\tau_1} \int_0^{\tau_1} (I_1^2 - I_2^2) d\tau_1 - 2l_n \right].$$

In the transient process from the initial (unheated) state of the muscle, P is calculated by the equation

$$P(\tau) = K_Z \left[K_s \frac{r}{\tau} \int_0^{\tau} (I_1^2 - I_2^2) d\tau_1 - 2l_n \right], \quad (11)$$

where $\tau = \tau_1 = \tau_0$ is the time, as a function of which force P developed by the drive with time delay varies, and τ_0 is the time delay in the appearance of force, corresponding to the difference of the mean heating power of the adsorbents of the muscles and to the position of the output element of the drive l_{II} at moment of time τ_1 .

In (11), $d\tau = d\tau_1$; $I_1 = I_1(\tau_1)$, $I_2 = I_2(\tau_1)$, $l_n = l_n(\tau)$. The forces of currents I_1 and I_2 are related to the value of signal U_{st} at the input of the amplifier

$$I_1 = K_y U_{st} \lambda_1; \quad I_2 = K_y U_{st} \lambda_2;$$

where K_y is the transfer coefficient of the direct channel of the drive, λ_1 is a coefficient equal to unity at $U_{st} > 0$ and equal to zero at $U_{st} \leq 0$; $\lambda_2 = 1 - \lambda_1$.

Let us substantiate the law of control U_{st} , realized in the controller (UU). The signal U_s (Figure 3) corresponds to a given position of the output element of the drive l_s , i.e., to the positions of the mechanical link $L_s = K_\Pi l_s$ at $K_\Pi = \text{const}$.

The different processes of the tasks $U_s(\tau)$ are found, having minimized by function $l_\Pi(\tau)$ the following functional, known in optimal control theory

$$J = \int_0^t [(l_s - l_n)^2 + K_s (l_s^{(1)} - l_n^{(1)})^2] d\tau, \quad (12)$$

Then varying the value of coefficient K_s . Here $l_s = l_s(\tau)$ and $l_s^{(1)}(\tau)$ are given functions, and $l_s^{(1)}(\tau) = dl_s/d\tau$, $l_n^{(1)}(\tau) = dl_n/d\tau$. If $\tau_k \rightarrow \infty$, $l_s - l_n \rightarrow 0$, $l_s^{(1)} - l_n^{(1)} \rightarrow 0$, the necessary condition of a minimum of (12) will be an Euler equation [2]

$$l_s - l_n + \sqrt{K_s} (l_s^{(1)} - l_n^{(1)}) = 0. \quad (13)$$

Let us find the relationship of the speed of the output element of the drive $l_\Pi^{(1)}$ to power N_Π and N_{nc} . To do this, let us first assume that there is no longitudinal deformation of the muscle by external force P_W . This means that the force of the drive P is equal to zero. Then

$$l_n(\tau) = \frac{K_s r}{2\pi} \int_0^\tau (I_1^2 - I_2^2) d\tau.$$

Having differentiated $l_\Pi(\tau)$ by variable τ , we find the desired function

$$l_n^{(1)}(\tau) = \frac{K_s (N_n - N_{nc})}{2\pi}, \quad (14)$$

in which $N_n = (I_1^2 - I_2^2)r$ is the instantaneous power and $N_{nc} = \frac{r}{\tau} \int_0^\tau (I_1^2 - I_2^2) d\tau$ is the mean power. For the position mode of development of the

task $U_s(\tau)$, let us assume that derivative $l_s^{(1)}(\tau)$ is equal to zero. After substitution of (14) into (13), we find

$$\tau(l_s - l_n) + \frac{\sqrt{K_a}}{2}(N_{nc} - N_n) = 0. \quad (15)$$

The relation $l_s - l_n$ is insignificant at small values of τ . If $\tau \rightarrow \infty$, the difference $N_{nc} - N_n$ can be disregarded.

The law of control of the drive is derived by combining (15) with the equation of motion of the output element of the drive

$$ml_n^{(2)} = P - P_w,$$

where m is the reduced mass of the structural elements, displaced by the drive, P_w is the force of resistance to the drive, and P is the force of the drive in the transient process. However, if the indicated equations are combined, we arrive at a control law U_{st} , to realize which is it possible only by having determined P_w and time derivatives of l_n . This is very difficult in practical realization.

The approach to control of the drive using only an Euler equation, valid at $P_w = 0$, appears more rational. In this case, the law of control is formulated so that the drive system approaches the state described by equation (15) at each moment of time τ . Let us assume that this equation is not exactly observed. Then either a positive or negative value is found in its right side. In both cases, the right side approaches zero, if the control signal is sufficiently large in absolute value $|U_{st}|$, and its polarity corresponds to the direction of development.

Let us introduce into consideration the control law

$$U_{st} = \int_0^{\tau} F(\sigma) d\sigma,$$

where $\sigma = \tau_n(l_s - l_n) + \frac{\sqrt{K_a}}{2}(N_{nc} - N_n)$, i.e., of the left side of equation (15); variable τ is replaced by $\tau_n = \text{const}$, τ_n is the time segment, on which the transient process of operation of the drive essentially ends with given accuracy, $F(\sigma) = U > 0$ at $\sigma > 0$, $F(\sigma) = U < 0$ at $\sigma < 0$, $F(\sigma) = 0$ at $\sigma = 0$, and $|U| = \text{const}$.

Replacing τ by constant τ_{II} means that increased sensitivity to the difference of lengths $l_s - l_{II}$ is given to the drive system.

Implementation of the integral control law $U_{st}(\tau)$ creates smoothness in development of the task by the drive system and contributes to elimination of autooscillations in the steady process. For direct adjustment of the drive, it is recommended that the proposed control law be used in the form

$$\left. \begin{array}{l} U_{st} = \int_0^\tau U d\tau \text{ at } \sigma = l_s - l_{II} + K(N_{nc} - N_{II}) > 0; \\ U_{st} = \int_0^\tau (-U) d\tau \text{ at } \sigma < 0; \\ U_{st} = \int_0^\tau 0 d\tau \text{ at } \sigma = 0, \\ U = \text{const} > 0. \end{array} \right\} \quad (16)$$

Adjustment of the drive reduces to finding coefficient K .

Let us assume that U_{st} , after integration, reaches saturation $U_H > 0$ at $\sigma > 0$ and $l_s - l_{II} < 0$ and that it satisfies the condition $N_{II} < N_{nc}$. K then increases due to the appearance of a large difference of the intensities of currents I_1 and I_2 . As a result, l_{II} , which approaches l_s , increases with a delay of τ . The difference $|N_{nc} - N_{II}|$ and $|l_s - l_{II}|$ decreases in absolute value and σ approaches zero. Initially $\sigma = 0$ at some small value of $|l'_s - l_{II}|$ and then $\sigma < 0$. The process of a decrease U_{st} begins, and a decrease of power N_{II} corresponds to this. Thus, power N_{nc} will increase on the final section of the transient process when $l_{II} \rightarrow l_s$, and N_{II} will decrease due to a decrease of U_{st} . As a result, $N_{nc} - N_{II} \rightarrow 0$, and $\sigma \rightarrow 0$. At the end of the process, in the stable system, $N_{nc} = N_{II}$, $U_{st} = \text{const}$, and $l_s = l_{II}$. The transient process should proceed in similar fashion if $\tau = 0$ and $\sigma < 0$ and $l_s - l_{II} < 0$.

One can judge the stability of the drive by equation (16). Let us assume that the mean power N_{nc} does not vary significantly during the transient process, a delay occurs after moment of time $\tau = t_0$.

The equation of dynamics

$$2K_z l_n + m l_n^{(2)} = K_y r K_s K_z U_{st}^2 - P_w$$

will then have the solution

$$l_n(\tau) = \left[\frac{P_w}{2K_z} - \frac{K_y^2 r K_s}{2} U_{st}^2 + l_n(0) \right] \tau \cos \sqrt{\frac{2K_z}{m}} + \\ + \frac{K_y^2 r K_s}{2} U_{st}^2 - \frac{P_w}{2K_z} . \quad (17)$$

It follows from (17) that the system is stable, but autooscillations are possible. The delay τ_0 almost disappears for adequately heated muscles. Each muscle approximates an aperiodic link. The controller changes U_{st} , maintaining the equality $l_{\Pi} = l_s$. The amplitude of the autooscillations of heated muscles reduces to a minimum or disappears by selecting coefficient K in formula (16).

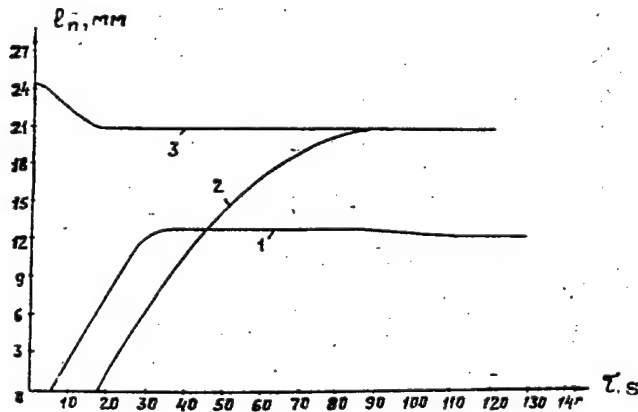


Figure 4. Experimental Curves of Transient Processes $l_{\Pi}(\tau)$ of Drive:

1--process of development of task at $P_w = 0.6$ N and at initial weakened state of muscles; 2--similar process at $P_w = 1$ N; 3--process of development of task by heated muscles at $P_w = 1$ N

The experimental curves of the transient processes $l_{\Pi}(\tau)$ of the drive are presented in Figure 4.

Drives based on fiber-sorption muscles with range of developed forces from 0 to 40 N have been manufactured since 1990. The efficiency of the first models of their drive is approximately 1 percent. The time constant of the drive for unheated muscles in the initial state, considered as an aperiodic link (without delay), is at the level of 30 s. Work is now under way to increase the speed of the muscles and of their efficiency.

Bibliography

1. Agranovskiy, S. G., Yegorov, Yu. N., B. I. I. Morozov, B. I. "USSR Inventor's Certificate 1,333,565. Robot Module," BYULLETIN IZOBREteniy, No 32, 1987.
2. Boychuk, L. M. "Optimalnyye sistemy avtomaticheskogo regulirovaniya" [Optimal Automatic Control Systems], Kiev, Izdatelstvo "Naukova dumka", 1965.
3. Timofeyev, D. P. "Kinetika adsorbsii" [The Kinetics of Adsorption], Moscow, Izdatelstvo AN SSSR, 1963.

COPYRIGHT: "IZVESTIYA VUZOV SSSR - PRIBOROSTROYENIYE", 1990

UDC 621.865.8;621.38(62-52)

MULTIOUTPUT ACTUATING MODULES FOR ROBOTS AND ROBOTIC COMPLEXES

917F0203A Leningrad IZVESTIYA VYSSHIKH UCHEBNYKH ZAVEDENIY:
PRIBOROSTROYENIYE in Russian No 10, 1990 (manuscript received 28 Feb 90)
pp 87-91

[Article by P. F. Khasanov, Kh. N. Nazarov, and Kh. Kh. Tadzhiev,
Tashkent Polytechnical Institute imeni A. R. Beruni]

[Text] The construction and design principles of multioutput actuating modules with several independent linear and angular motions are considered. A simulation model of a two-output actuating module, designed on the basis of Petri nets, is presented.

When developing industrial robots and manipulators, it is necessary to ensure simplicity of design and minimum values of mass-size indicators [1, 2]. One of the methods of solving this problem is the use of multioutput actuating modules (MIM) in the actuating subsystem of the robot, which permit one to produce a set of independent linear and angular motions at the output. MIM can be located directly in the joints of the structural layout of the robot or on a fixed base.

The design principle of the multioutput actuating module is based on supplying the moving parts of the motor with couplings, controlled separately from the controller [3]. A generalized block diagram of the MIM is presented in Figure 1. The MIM includes a controller, reciprocating motor, $2n$ ($n \geq 2$) working couplings, n fixing couplings, mechanically connected to the reciprocating motor, linking elements, made in the form of nonmagnetic rods and flexible cables, and transforming members, made in the form of pulleys connected to the moving links of the robots.

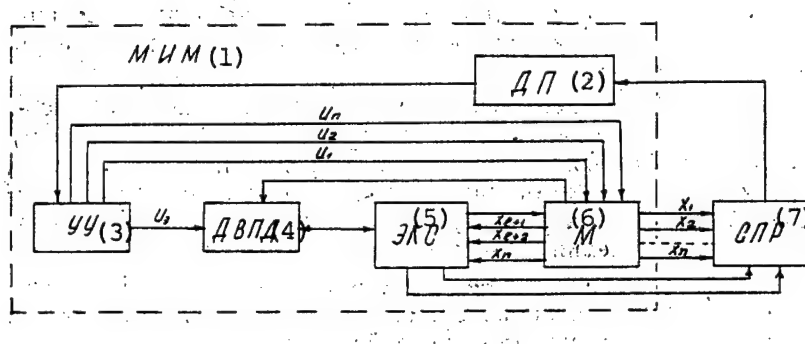


Figure 1. Generalized Block Diagram of Multioutput Actuating Module:
UU--controller; DVPD--reciprocating motor; EKS--fastening and joining elements; M--couplings; SPR--degrees of freedom of robot; PO--converting member; DP--position sensor

KEY:

- | | |
|---------------------------------|-----------------------------------|
| 1. Multioutput actuating module | 4. Fastening and joining elements |
| 2. Position sensor | 5. Couplings |
| 3. Controller | 6. Degrees of freedom of robot |

The controller controls the reciprocating motor, $2n$ working and n fixing couplings, and is connected to the robot's control system. The reciprocating motor can be based on electromagnets or pneumatic and hydraulic cylinders or other similar devices, and is used to ensure reciprocating motion of the working couplings. The working and fixing couplings are controlled separately from the controller and transmit reciprocating motions through the linking elements either directly or through transforming members to the movable links of the robot. The designs, shapes, dimensions and operating principles of the working and fixing couplings are dependent on the shapes, dimensions and materials of the linking elements, where the latter are used to transmit the motions of the couplings to the degrees of freedom of the robot and are different shafts, rods, and flexible elements (cables).

The linking elements and together with them the corresponding electromagnetic couplings can be located on the outside, inside, or a combination as a function of the kinematic layout of the MIM and the mutual spatial arrangement of the degrees of freedom of the robot.

The transforming member is used to convert the linear motions of the elements and is kinematically connected to the moving links of the robot manipulator.

The multioutput actuating module operates in the following manner. Producing several angular and linear motions is based on conversion of reciprocating motions of two moving parts, moving in the opposite direction in n ($n \geq 2$) independent linear and angular motions of the

rods and cables by alternately switching the groups of $2n$ working and n fixing couplings on and off, controlled separately for each independent motion. The functions of converting X to x_i ($i = \overline{1, n}$) are established by the laws of variation of the signals of the controller U_1, U_2, \dots, U_n over time.

As a result, the reciprocating motions of the reciprocating motor are transformed to a combination of linear (x_1, x_2, \dots, x_l), and angular ($\alpha_{1+1}, \alpha_{1+2}, \dots, \alpha_n$) motions, which are transmitted by transfer mechanisms to the moving links of the robot manipulator or of the robotic complex (RTK).

The controller of the MIM is based on a microprocessor complex of series K580 and generates control signals for the reciprocating motor and windings of the electromagnetic couplings according to a given algorithm. The control algorithm of the MIM is based on the phase engagement method, which permits uniform variation of the dynamic force. The controller of the multioutput actuating module is linked to the control system of the robot and generates control signals $\bar{U} = (U_1, U_2, \dots, U_n)$ according to deviation of the given values of vector \bar{q}_3 from the actual values of \bar{q}_ϕ .

Petri nets, which are distinguished by clearness of the model in combination with rather broad functional capabilities, have been used extensively of late among the set of simulation models, oriented toward solution of various problems of simulation, analysis and synthesis of processes of different physical nature.

The Petri net (SP) is formally determined as a set of five of type [4]

$$S = \langle P, T, I, O, \mu_0 \rangle \quad (1)$$

where P , T , I , and O are finite sets of transitions (events), positions, input positions, and output positions, respectively, μ_0 is the initial marking, and $\mu_3: P \rightarrow N$, $N = \{0, 1, 2, \dots\}$ is a set of natural numbers.

Problems of design of simulation models of multioutput actuating modules of robots and robotic systems are considered in the paper on the basis of the apparatus of expanded Petri nets, designed for description and analysis of the functioning of the latter.

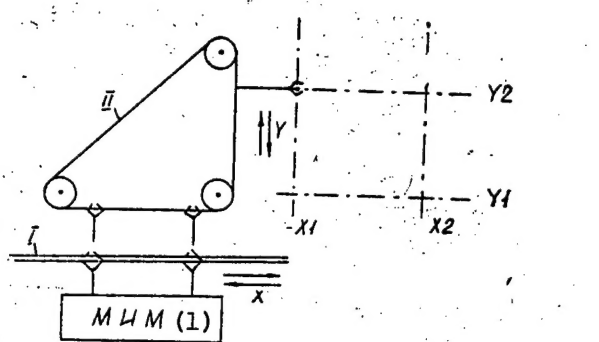


Figure 2. Multioutput Actuating Module With Two Degrees of Freedom

KEY:

1. Multioutput actuating module

A multioutput actuating module of the electromagnetic type, designed for horizontal and vertical motions in the structure of the robot or robotic system, is simulated. The MIM includes an electromagnetic module with movable elements, a coupling module, specifically electromagnetic couplings, which are divided into working and fixing, depending on the functional designation in the MIM, a controller and output rods.

Let us consider the design step of the interpreted Petri nets on the example of a multioutput actuating module with two degrees of freedom (Figure 2). One degree of freedom is realized by using a rod I, which performs horizontal displacement to the left (to the right), and the second degree of freedom is realized by using a flexible rod II (or cable), which performs vertical motions downward (upward).

The positions of the rods are fixed along the vertical and horizontal by using position sensors in coordinates Y1, Y2 and X1, X2, respectively. One of the variants of the model that describes the functioning of the multioutput actuating module is the Petri net, shown in Figure 3.

Positions 1 and 2 describe the starting conditions of the electromagnets of the MIM, 3, 4, and 5, 6 reflect the states of these electromagnets, 7, 8 and 9, 10 reflect the states of the couplings which are rigidly connected to the moving elements, 11 and 12 are introduced to simulate the processes of control of the electromagnetic couplings, 13 and 14 reflect the state of the output rod, 15-17 are used to simulate the processes of control of the motor with regard ot the information of the position sensor, and 18 simulates stopping of the rod. Transition t_1 reflects the process of variation of the state of the electromagnet, transition t_2 reflects the condition of connecting the coupling, t_3 means transition of the coupling from one state to another, and t_4 reflects transition of the rod from one position to another.

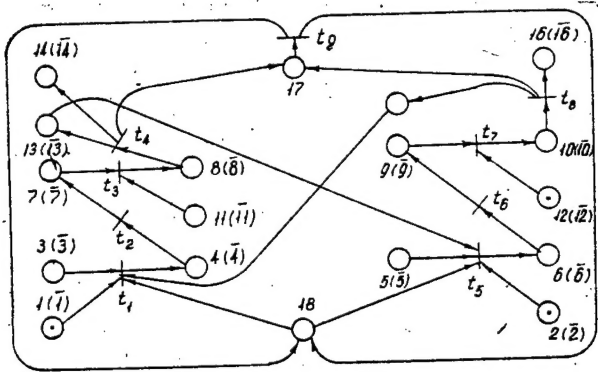


Figure 3. Simulation Model of Multioutput Actuating Module

The presence of markers at positions 13 and 14 denote the response of the sensor at position X1, and the presence of markers at positions 15 and 16 denote a response of the sensor at position X2. The marker at position 17 denotes response of the sensor at position of either X1 or X2, while a marker at positions 4 and 5 denotes motion to the left or to the right, respectively. The delay time of the marker, equal to the time of displacements between extreme positions, corresponds to these positions. Let the markers be located at positions 15-17. The electromagnets of the multioutput actuating module can be started only after a marker appears at position 1. Upon response of transition t_1 , a marker appears at position 4, which means motion of the movable element to the left. Markers arrive at positions 13, 14, and 17 after response of transitions t_2 , t_3 , and t_4 . The resulting marking is the initial marking for motion of the rod to the right.

The work of the second output of the multioutput actuating module can also be simulated by a Petri net, presented in Figure 3. In this case, positions $\bar{1}$, $\bar{3}$, $\bar{4}$, $\bar{7}$, $\bar{8}$, $\bar{13}$, and $\bar{14}$ simulate the motion of the output rod downward, while positions $\bar{2}$, $\bar{5}$, $\bar{6}$, $\bar{9}$, $\bar{10}$, $\bar{15}$, and $\bar{16}$ simulate motion of the output rod downward.

The resulting Petri net of the multioutput actuating module is formally described in the following manner:

$$\begin{aligned}
 P &= \{P_1, P_2, \dots, P_{18}\}, T = \{t_1, t_2, \dots, t_9\}; \\
 I(t_1) &= \{P_1, P_3, P_{15}, P_{18}\}, O(t_1) = \{P_4\}; \\
 I(t_2) &= \{P_4\}, O(t_2) = \{P_1\}, I(t_3) = \{P_1, P_{11}\}; \\
 O(t_3) &= \{P_8\}, I(t_4) = \{P_8\}, O(t_4) = \{P_{13}, P_{14}, P_{17}\}; \\
 I(t_5) &= \{P_2, P_5, P_{18}\}, O(t_5) = \{P_6\}, I(t_6) = \{P_6\}; \\
 I(t_7) &= \{P_9, P_{12}\}, O(t_7) = \{P_{10}\}; \\
 I(t_8) &= \{P_{10}\}, O(t_8) = \{P_{15}, P_{16}, P_{17}\}; \\
 I(t_9) &= \{P_{10}\}, O(t_9) = \{P_{18}\}.
 \end{aligned}$$

New designs of electromagnetic and pneumatic multioutput actuating modules, used as the actuating members of robots and robotic complexes, have been proposed on the basis of the generalized block diagram of MIM. The proposed designs are distinguished from existing robot drives by simplicity of design and minimal mass-size indicators.

The structural layouts of industrial robots, operating in different coordinate systems, have been worked out on the basis of multioutput actuating modules. The proposed designs of MIM can be used in construction of the actuating members of adaptive robots, robotic complexes, and of systems of different designation.

Bibliography

1. Afonin, A. A. "Elektromagnitnyy privod robototekhnicheskikh sistem" [Electromagnetic Drive of Robotic Systems], Kiev, Izdatelstvo "Naukova dumka", 1986.
2. Khasanov, P. F., Nazarov, Kh. N. "Mobilnyye robotekhnicheskiye sistemy: Uchebnoye posobiye" [Mobile Robotic Systems: A Textbook], Tashkent, Tashkenskiy politekhnicheskiy institut, 1987.
3. "USSR Inventor's Certificate 1,504,379. Pneumatic Step Drive," BYULLETIN IZOBREteniy, No 32, 1989.
4. Rozenblyum, L. Ya. "Petri Nets," IZVESTIYA AKADEMII NAUK SSSR. SERIYA TEKHNICHESKAYA KIBERNETIKA, No 5, 1983.

COPYRIGHT: "IZVESTIYA VUZOV SSSR - PRIBOROSTROYENIYE", 1990

- END -

NTIS
ATTN: PROCESS 103

2

5285 PORT ROYAL RD
SPRINGFIELD, VA

22161

This is a U.S. Government publication. Its contents in no way represent the policies, views, or attitudes of the U.S. Government. Users of this publication may cite FBIS or JPRS provided they do so in a manner clearly identifying them as the secondary source.

Foreign Broadcast Information Service (FBIS) and Joint Publications Research Service (JPRS) publications contain political, military, economic, environmental, and sociological news, commentary, and other information, as well as scientific and technical data and reports. All information has been obtained from foreign radio and television broadcasts, news agency transmissions, newspapers, books, and periodicals. Items generally are processed from the first or best available sources. It should not be inferred that they have been disseminated only in the medium, in the language, or to the area indicated. Items from foreign language sources are translated; those from English-language sources are transcribed. Except for excluding certain diacritics, FBIS renders personal and place-names in accordance with the romanization systems approved for U.S. Government publications by the U.S. Board of Geographic Names.

Headlines, editorial reports, and material enclosed in brackets [] are supplied by FBIS/JPRS. Processing indicators such as [Text] or [Excerpts] in the first line of each item indicate how the information was processed from the original. Unfamiliar names rendered phonetically are enclosed in parentheses. Words or names preceded by a question mark and enclosed in parentheses were not clear from the original source but have been supplied as appropriate to the context. Other unattributed parenthetical notes within the body of an item originate with the source. Times within items are as given by the source. Passages in boldface or italics are as published.

SUBSCRIPTION/PROCUREMENT INFORMATION

The FBIS DAILY REPORT contains current news and information and is published Monday through Friday in eight volumes: China, East Europe, Soviet Union, East Asia, Near East & South Asia, Sub-Saharan Africa, Latin America, and West Europe. Supplements to the DAILY REPORTS may also be available periodically and will be distributed to regular DAILY REPORT subscribers. JPRS publications, which include approximately 50 regional, worldwide, and topical reports, generally contain less time-sensitive information and are published periodically.

Current DAILY REPORTS and JPRS publications are listed in *Government Reports Announcements* issued semimonthly by the National Technical Information Service (NTIS), 5285 Port Royal Road, Springfield, Virginia 22161 and the *Monthly Catalog of U.S. Government Publications* issued by the Superintendent of Documents, U.S. Government Printing Office, Washington, D.C. 20402.

The public may subscribe to either hardcover or microfiche versions of the DAILY REPORTS and JPRS publications through NTIS at the above address or by calling (703) 487-4630. Subscription rates will be

provided by NTIS upon request. Subscriptions are available outside the United States from NTIS or appointed foreign dealers. New subscribers should expect a 30-day delay in receipt of the first issue.

U.S. Government offices may obtain subscriptions to the DAILY REPORTS or JPRS publications (hardcover or microfiche) at no charge through their sponsoring organizations. For additional information or assistance, call FBIS, (202) 338-6735, or write to P.O. Box 2604, Washington, D.C. 20013. Department of Defense consumers are required to submit requests through appropriate command validation channels to DIA, RTS-2C, Washington, D.C. 20301. (Telephone: (202) 373-3771, Autovon: 243-3771.)

Back issues or single copies of the DAILY REPORTS and JPRS publications are not available. Both the DAILY REPORTS and the JPRS publications are on file for public reference at the Library of Congress and at many Federal Depository Libraries. Reference copies may also be seen at many public and university libraries throughout the United States.